Production of light (anti-) nuclei and (anti-)hypernuclei with ALICE at the LHC

Ramona Lea

Physics Department, University and INFN Trieste

For the ALICE Collaboration

22 October 2019

Light nuclei in heavy-ion collisions

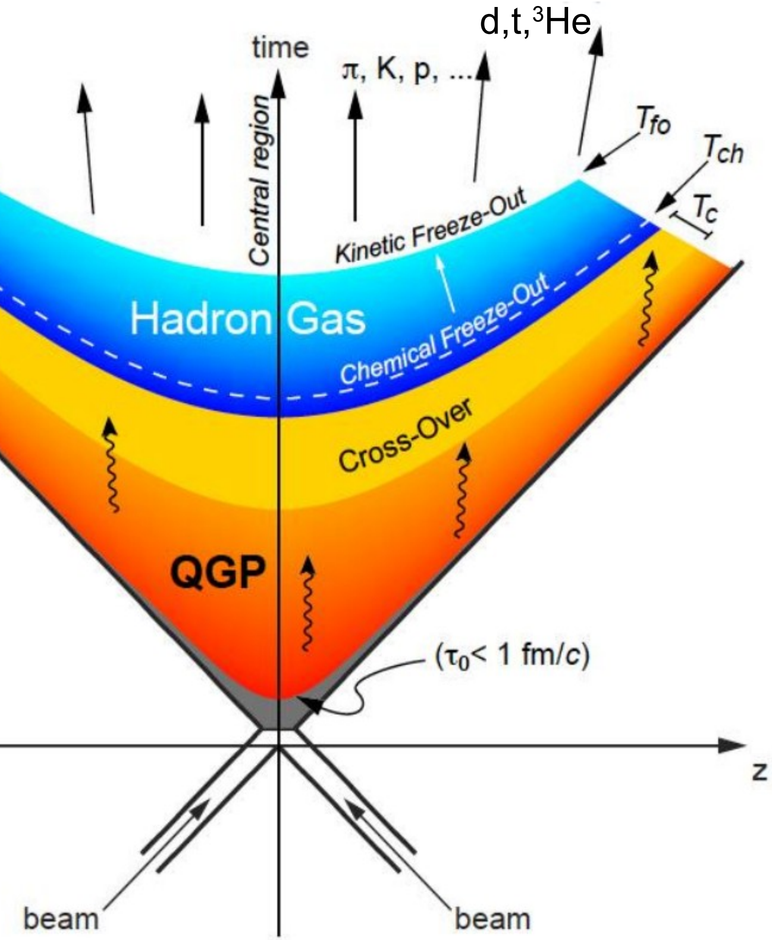

- The study of light (anti-)nuclei is very important:
  - Production mechanism is not well understood
    - How/when do they form?
      - "early" at chemical freeze-out (thermal production)
      - or "late" at kinetic freeze-out (coalescence)?
    - Do they suffer for the dissociation by rescattering?
  - Low binding energy (few MeV) "Snowballs in hell": nuclei formation is very sensitive to chemical freeze-out conditions and to the dynamics of the emitting source
  - Baseline for searches for exotic bound states
  - Light nuclei measurements in high energy physics can be used to estimate the background of secondary anti-nuclei in dark matter search

Particle production at LHC

- Particle production in pp, p-Pb, and Pb-Pb collisions shows an **equal abundance** of matter and anti-matter in the central rapidity region
- A large number of particles is produced: $dN_{ch}/d\eta \approx 2000$ (central Pb-Pb collisions)

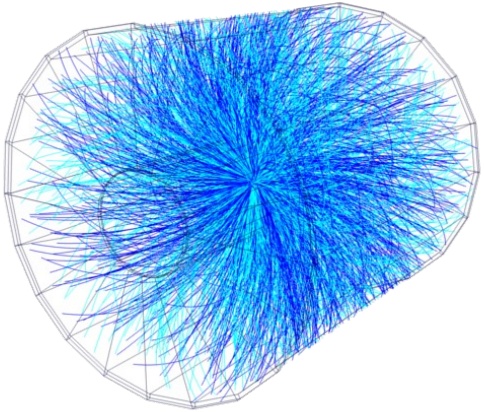

Particle production at LHC

- Particle production in pp, p-Pb, and Pb-Pb collisions shows an **equal abundance** of matter and anti-matter in the central rapidity region
- A large number of particles is produced: $dN_{ch}/d\eta \approx 2000$ (central Pb-Pb collisions)

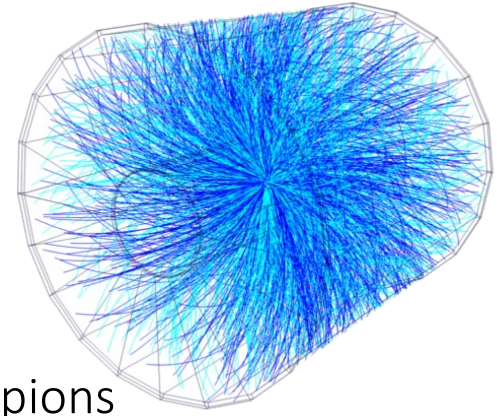

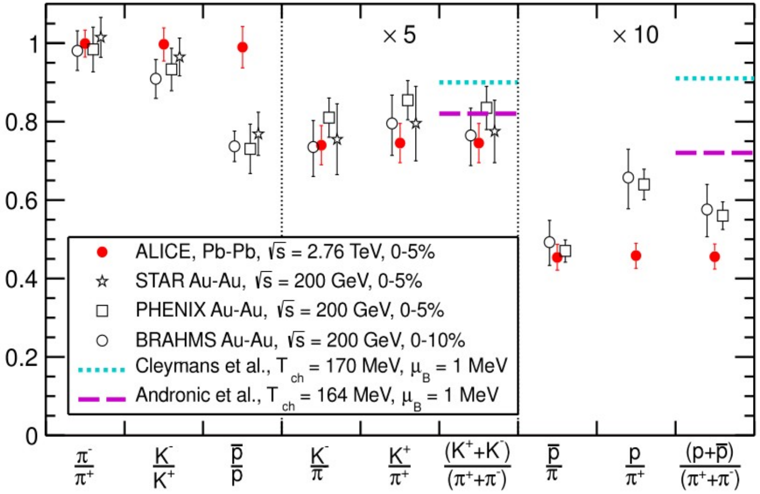

≈ 80% of all charged particles are pions
≈ 5% of all charged particles are protons

Phys. Rev. Lett.109, 252301

Particle production at LHC

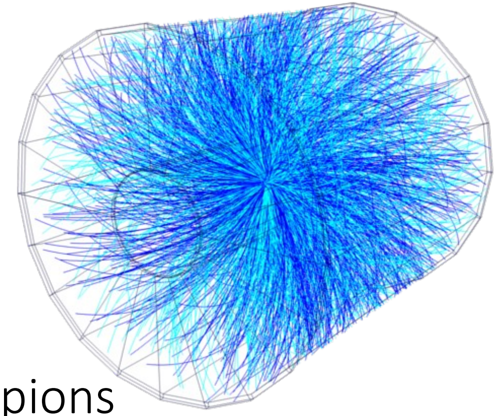

- Particle production in pp, p-Pb, and Pb-Pb collisions shows an **equal abundance** of matter and anti-matter in the central rapidity region
- A large number of particles is produced: $dN_{ch}/d\eta \approx 2000$ (central Pb-Pb collisions)

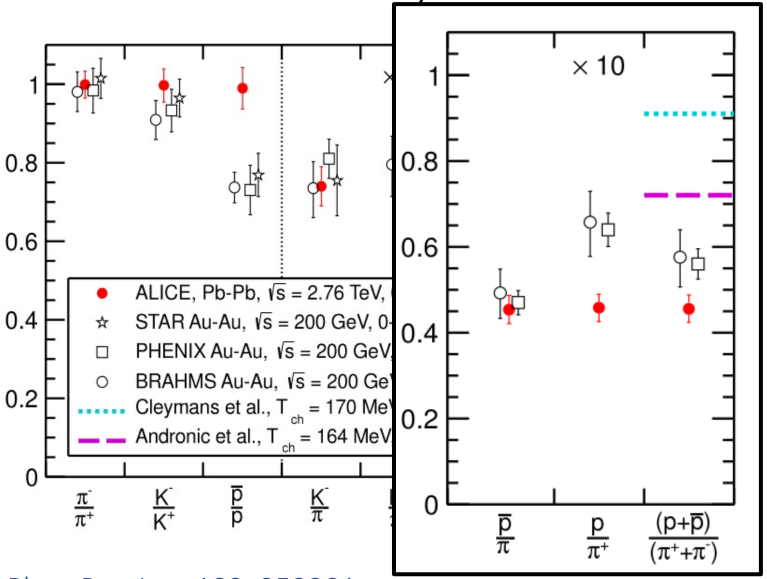

≈ 80% of all charged particles are pions
≈ 5% of all charged particles are protons

Phys. Rev. Lett.109, 252301

Particle production at LHC

- Particle production in pp, p-Pb, and Pb-Pb collisions shows an **equal abundance** of matter and anti-matter in the central rapidity region

- A large number of particles is produced: $dN_{ch}/d\eta \approx 2000$ (central Pb-Pb collisions)

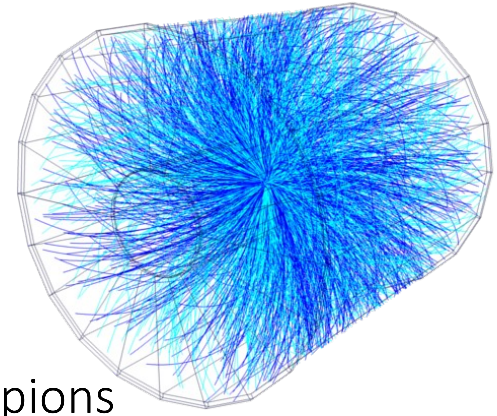

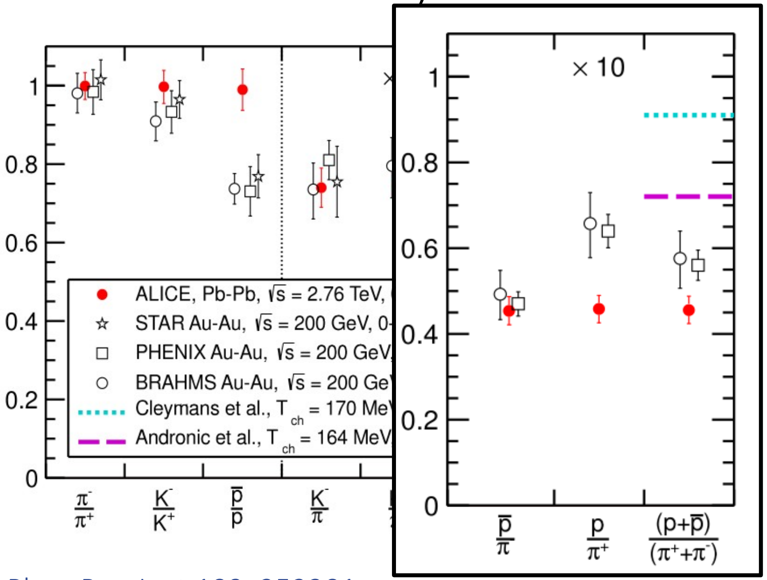

Phys. Rev. Lett.109, 252301

≈ 80% of all charged particles are pions
≈ 5% of all charged particles are protons

- Even in heavy ion collisions, light (anti-)nuclei are rarely produced:
  - (Anti-)nuclei up to A = 4 are in reach
  - For each additional nucleon the production yield at LHC decreases by a factor of about 350!

Experimental apparatus

A Large Ion Collider Experiment

ALICE particle identification capabilities are unique. Almost all known techniques are exploited: specific energy loss (dE/dx), time of flight, transition radiation, Cherenkov radiation, calorimetry and decay topology (V_0, cascade).

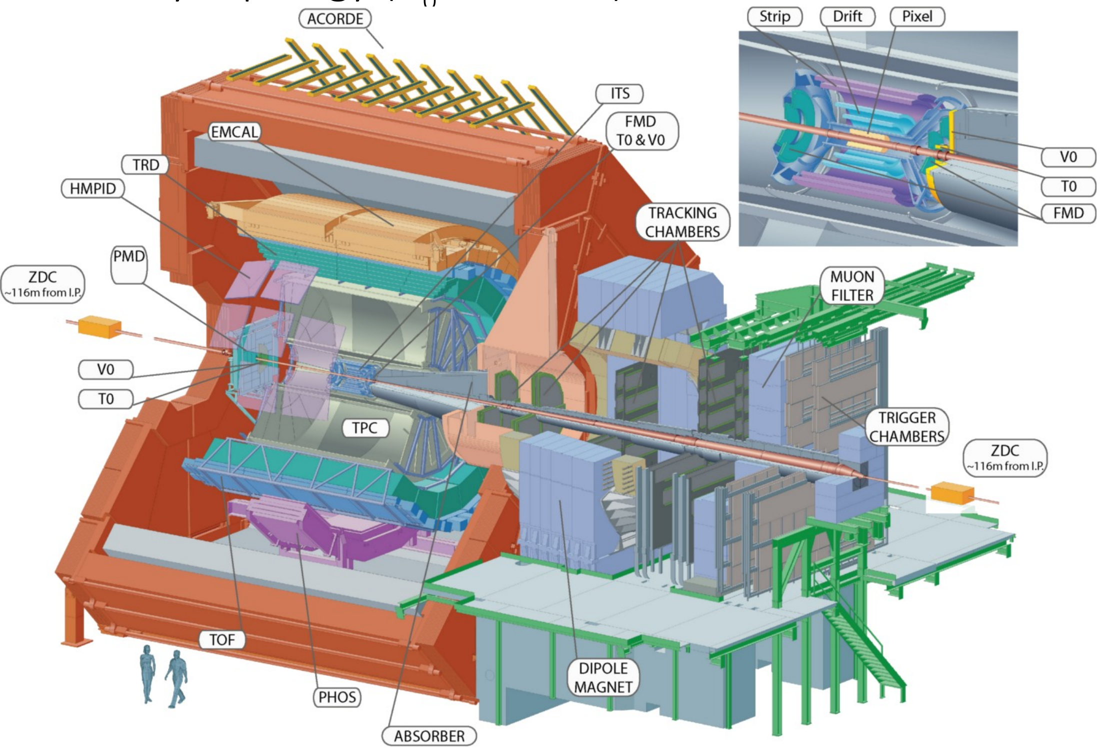

ALICE Collaboration, Int. J. Mod. Phys. A 29 (2014) 1430044

A Large Ion Collider Experiment

ALICE particle identification capabilities are unique. Almost all known techniques are exploited: specific energy loss (dE/dx), time of flight, transition radiation, Cherenkov radiation, calorimetry and decay topology (V_0, cascade).

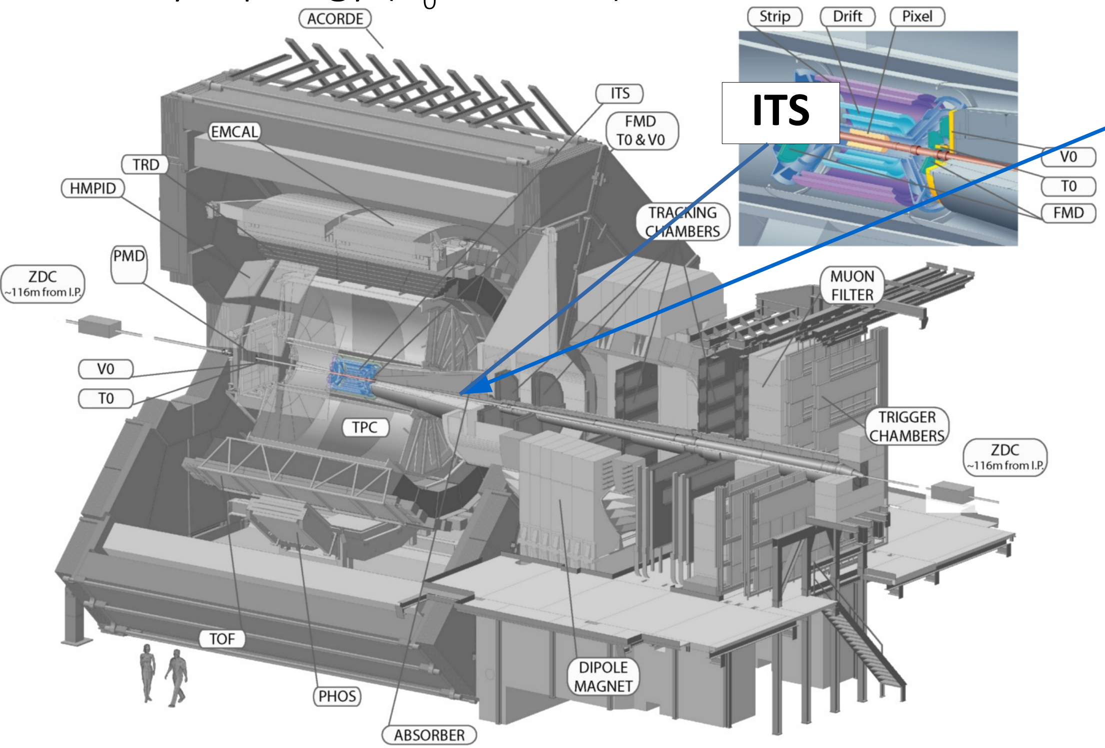

Inner Tracking System (ITS) :

- Primary vertex
- Tracking
- Particle identification via dE/dx

ALICE Collaboration, Int. J. Mod. Phys. A 29 (2014) 1430044

A Large Ion Collider Experiment

ALICE

ALICE particle identification capabilities are unique. Almost all known techniques are exploited: specific energy loss (dE/dx), time of flight, transition radiation, Cherenkov radiation, calorimetry and decay topology (V_0, cascade).

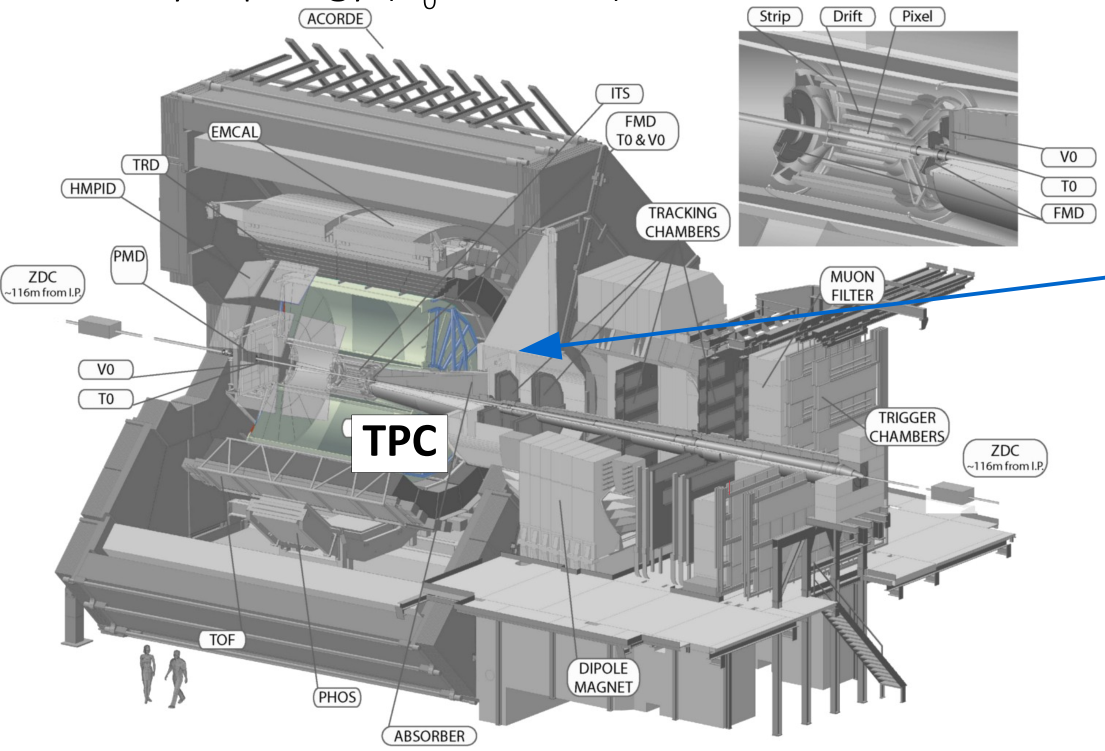

Inner Tracking System (ITS) :
- Primary vertex
- Tracking
- Particle identification via dE/dx

Time Projection Chamber (TPC):
- Global tracking
- Particle identification via dE/dx

ALICE Collaboration, Int. J. Mod. Phys. A 29 (2014) 1430044

A Large Ion Collider Experiment

ALICE particle identification capabilities are unique. Almost all known techniques are exploited: specific energy loss (dE/dx), time of flight, transition radiation, Cherenkov radiation, calorimetry and decay topology (V_0, cascade).

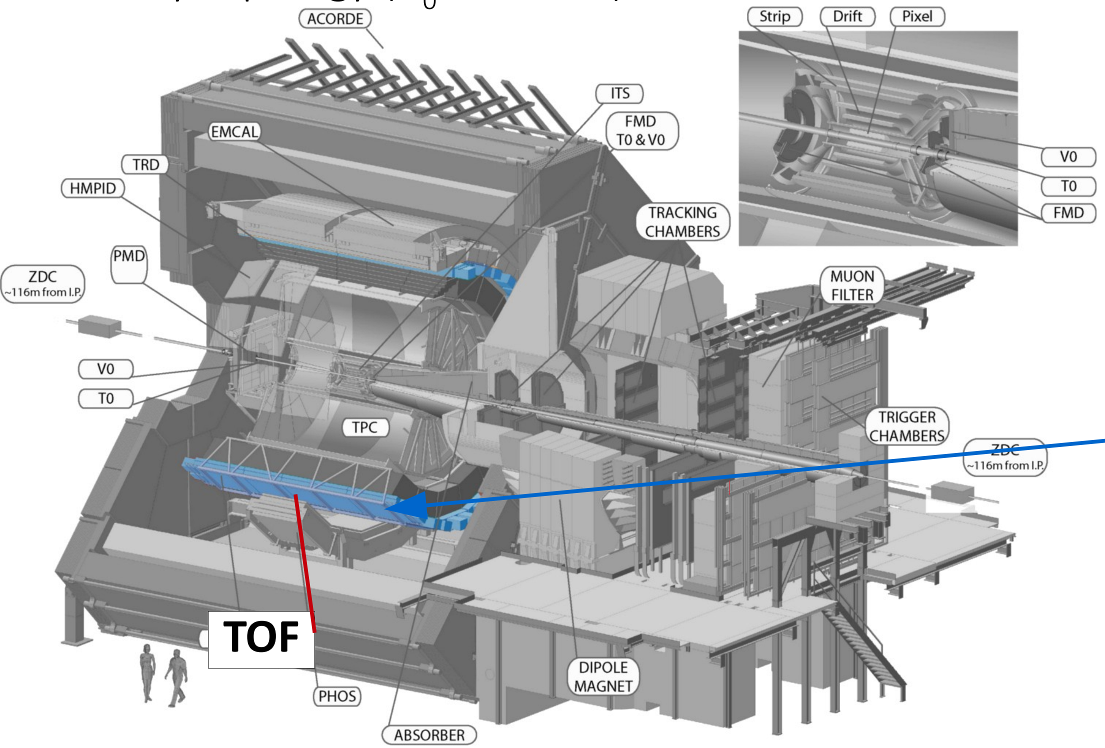

Inner Tracking System (ITS) :
- Primary vertex
- Tracking
- Particle identification via dE/dx

Time Projection Chamber (TPC):
- Global tracking
- Particle identification via dE/dx

Time Of Flight (TOF):
- Particle identification via velocity measurement

ALICE Collaboration, Int. J. Mod. Phys. A 29 (2014) 1430044

A Large Ion Collider Experiment

ALICE particle identification capabilities are unique. Almost all known techniques are exploited: specific energy loss (dE/dx), time of flight, transition radiation, Cherenkov radiation, calorimetry and decay topology (V_0, cascade).

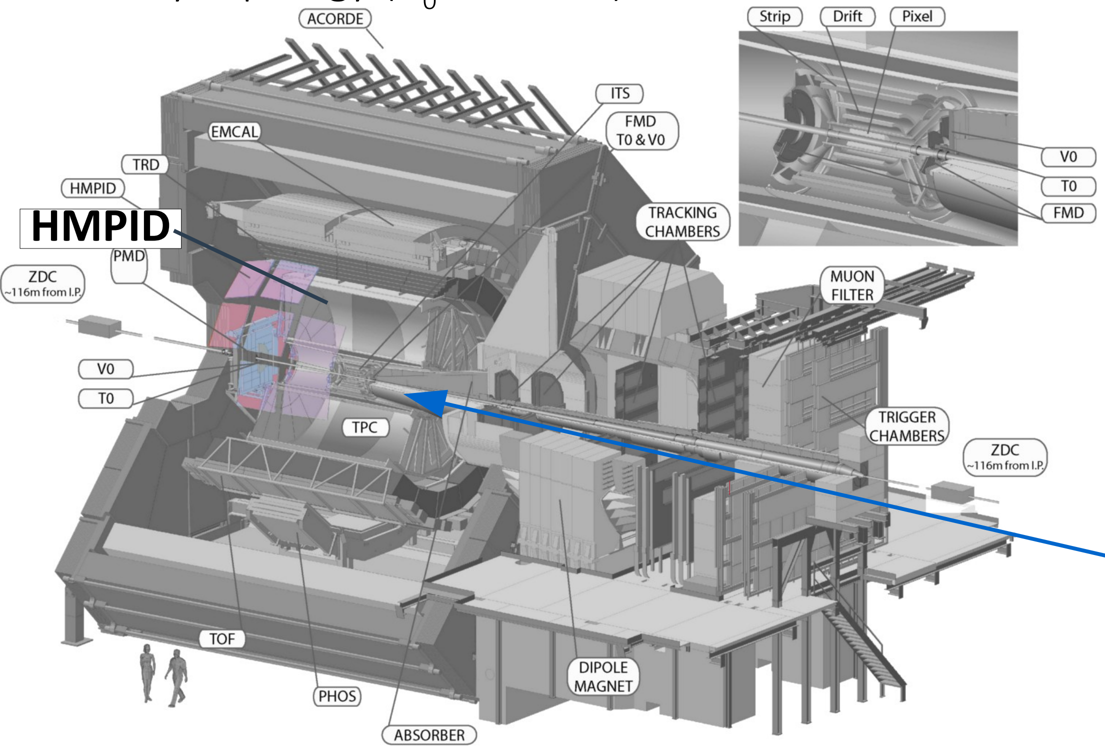

Inner Tracking System (ITS) :
- Primary vertex
- Tracking
- Particle identification via dE/dx

Time Projection Chamber (TPC):
- Global tracking
- Particle identification via dE/dx

Time Of Flight (TOF):
- Particle identification via velocity measurement

High Momentum PID (HMPID):
- particle identification via ring imaging Cherenkov

ALICE Collaboration, Int. J. Mod. Phys. A 29 (2014) 1430044

A Large Ion Collider Experiment

ALICE particle identification capabilities are unique. Almost all known techniques are exploited: specific energy loss (dE/dx), time of flight, transition radiation, Cherenkov radiation, calorimetry and decay topology (V_0, cascade).

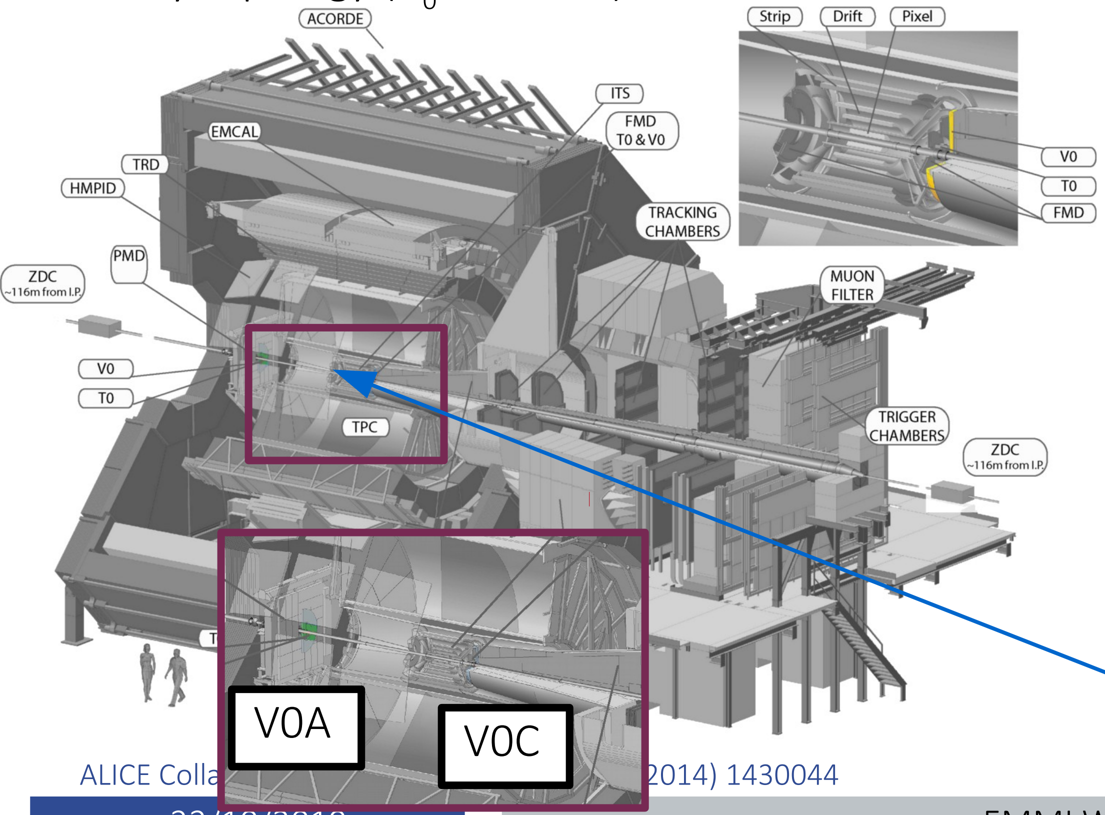

ALICE Colla... 2014) 1430044

Inner Tracking System (ITS) :
- Primary vertex
- Tracking
- Particle identification via dE/dx

Time Projection Chamber (TPC):
- Global tracking
- Particle identification via dE/dx

Time Of Flight (TOF):
- Particle identification via velocity measurement

High Momentum PID (HMPID):
- particle identification via ring imaging Cherenkov

V0 (A-C): Trigger, beam-gas event rejection, centrality, multiplicity classes

Centrality of the collisions

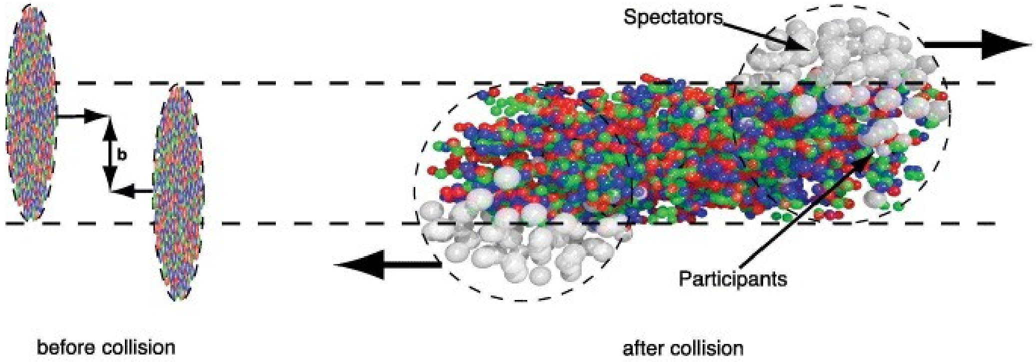

Centrality = degree of overlap of the 2 colliding nuclei

Central collisions:

- small impact parameter *b*
- high number of participant nucleons → high multiplicity

Peripheral collisions:

- large impact parameter *b*
- low number of participant nucleons → low multiplicity

Centrality connected to observables via Glauber model

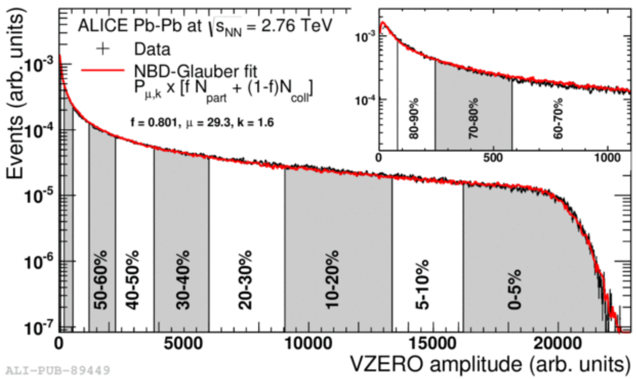

ALICE Collaboration, Phys. Rev. Lett. 106, 032301 (2011)

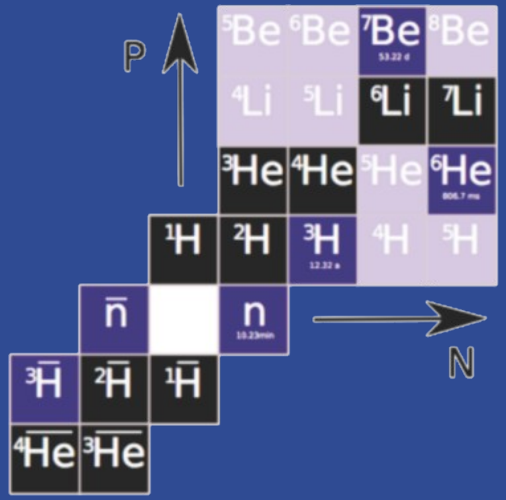

Production of light (anti-)nuclei

Identification of nuclei

Low momenta: specific energy loss in the TPC

- Nuclei identification via dE/dx measurement in the TPC:
  - ➢ dE/dx resolution in central Pb-Pb collisions: around 6.5%
  - ➢ Excellent separation of (anti-)nuclei from other particles over a wide range of momenta

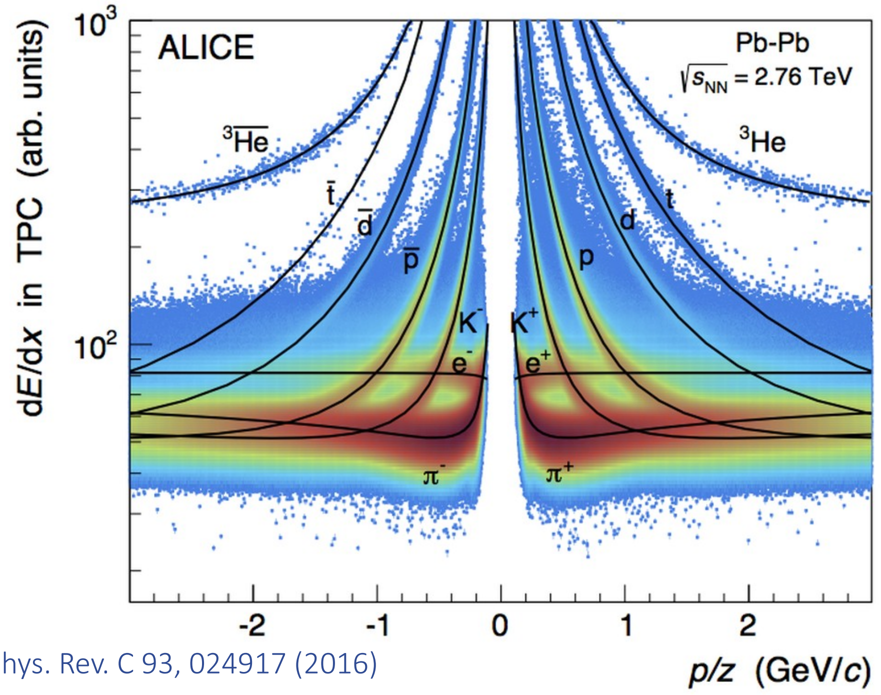

– Bethe-Bloch curves

(rigidity)

ALICE Collaboration, Phys. Rev. C 93, 024917 (2016)

Identification of nuclei

Higher momenta: time-of-flight measurement in the TOF

- Velocity measurement with the Time Of Flight detector is used to evaluate the m^2 distribution
  - ➢ Excellent TOF performance: $\sigma_{TOF} \approx 85$ ps in Pb-Pb collisions

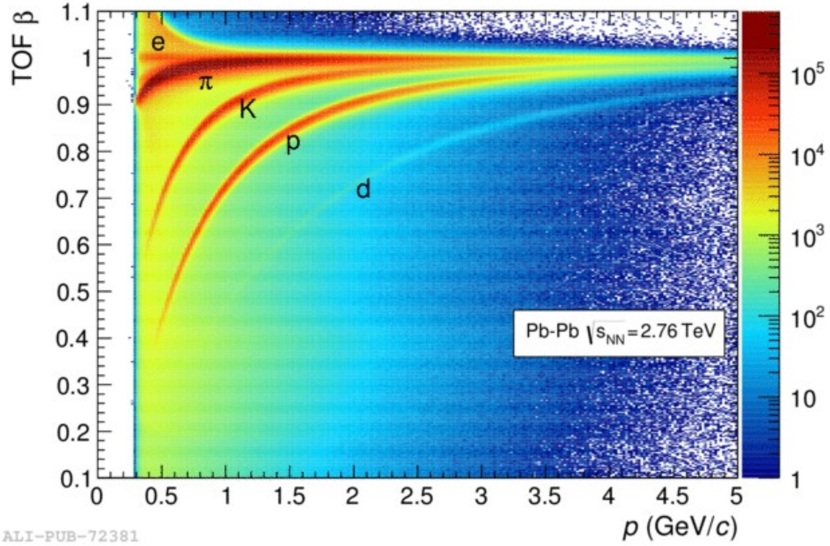

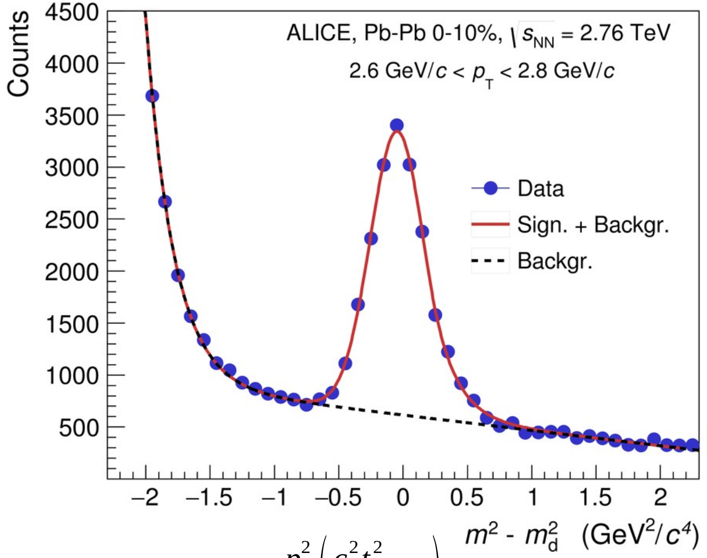

$$m^2 = \frac{p^2}{c^2}\left(\frac{c^2 t^2}{L^2} - 1\right)$$

ALICE Collaboration, Int. J. Mod. Phys. A 29 (2014) 1430044

Identification of nuclei

Higher momenta: Cherenkov angle determination in the HMPID

- The particle identification in the HMPID detector is based on the measurement of the Cherenkov radiation ($\theta_{Cherenkov}$) which allows us to determine the square mass of the particle by the following formula:

$$m^2 = p^2 (n^2 \cos^2\theta_{Cherenkov} - 1) \qquad \cos\theta_{Cherenkov} = \frac{1}{n\beta}$$

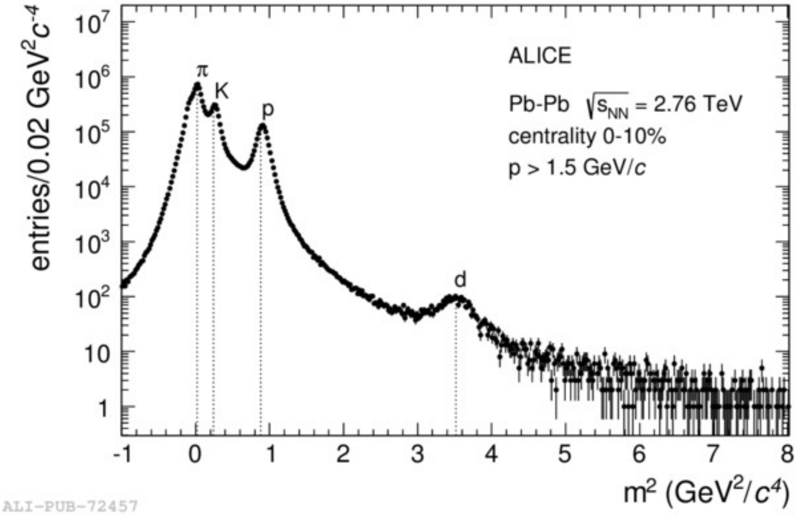

ALICE Collaboration, Int. J. Mod. Phys. A 29 (2014) 1430044

Deuteron p_T spectra in pp collisions

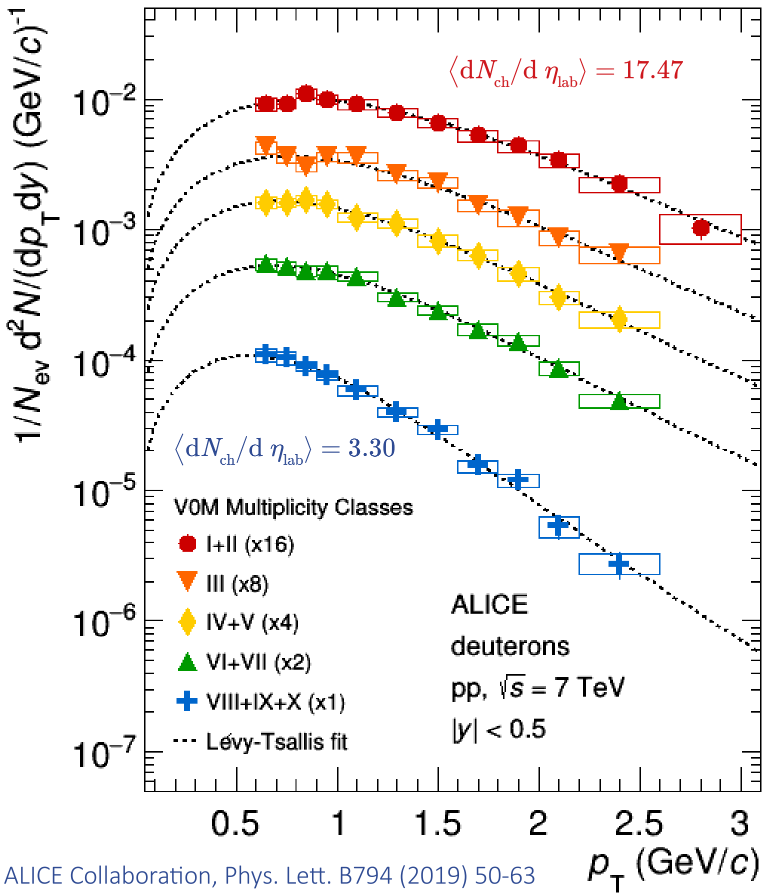

ALICE Collaboration, Phys. Lett. B794 (2019) 50-63

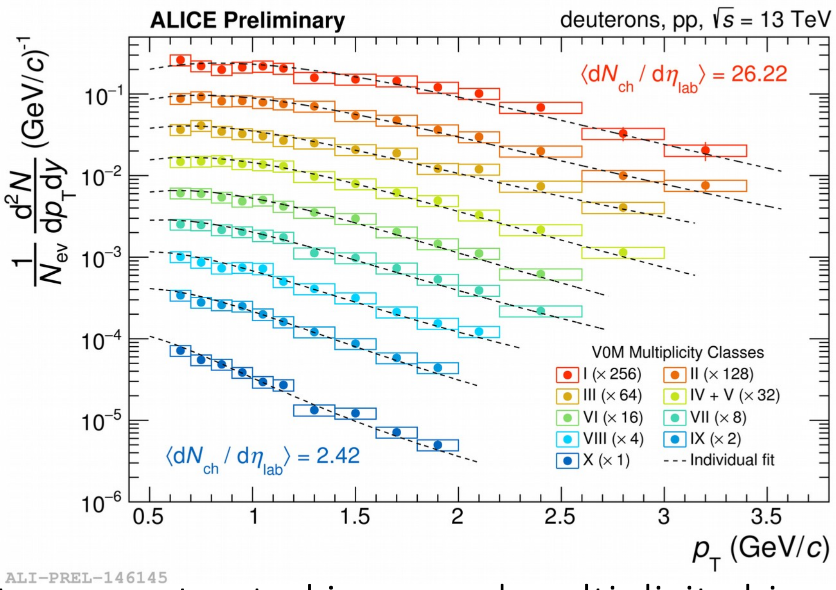

Spectra are extracted in several multiplicity bins and fitted with Lévy-Tsallis function for the extraction of yields

$$\frac{1}{2\pi p_T}\frac{d^2N}{dp_T dy} = \frac{dN}{dy}\frac{(n-1)(n-2)}{2\pi nC[nC + m_0(n-2)]}\left(1 + \frac{m_T - m_0}{nC}\right)^{-n}$$

C. Tsallis, J. Stat. Phys. 52 , 479 (1988) 980
STAR Collaboration, Phys. Rev. C75, 064901 981 (2007)

Deuteron p_T spectra in p-Pb collisions

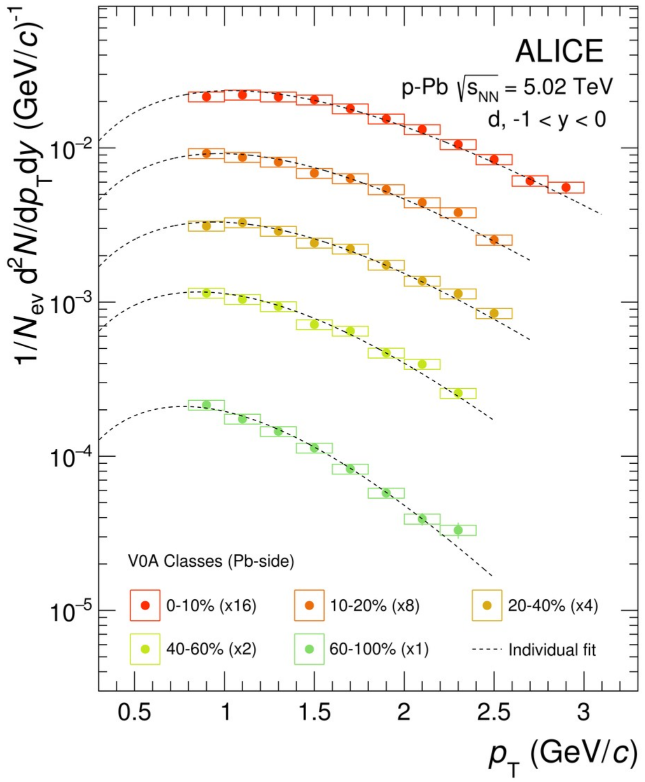

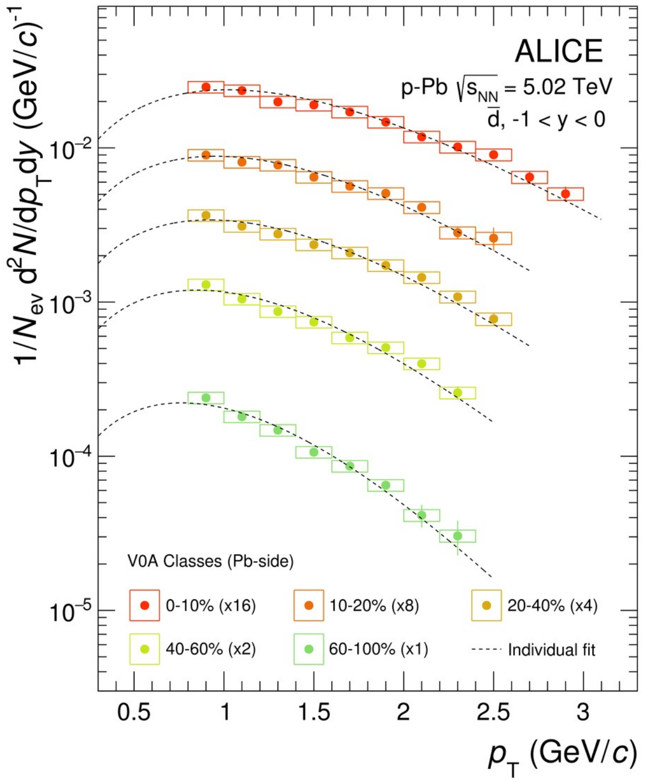

Spectra are extracted in several multiplicity bins and fitted with m_T-exponential function for the extraction of yields

ALICE Collaboration, arXiv:1906.03136

Deuteron p_T spectra in Pb-Pb collisions

ALICE-PUBLIC-2017-006

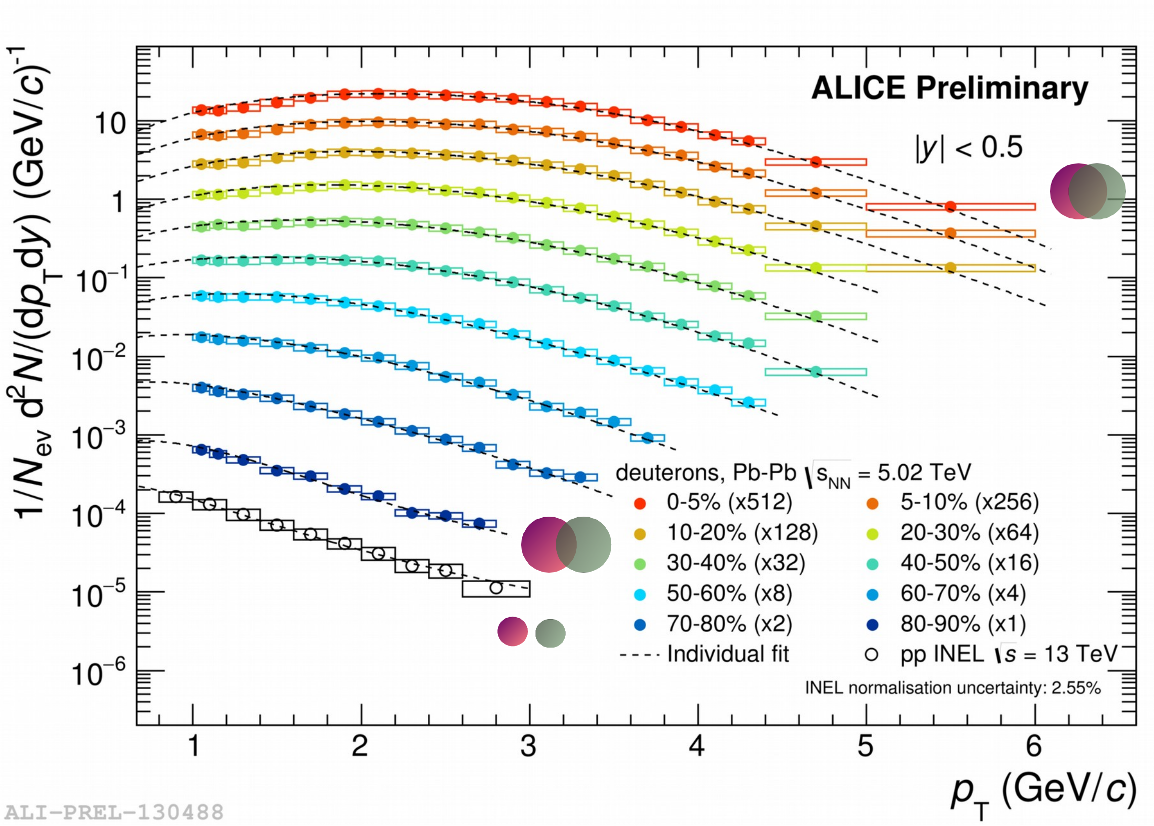

Spectra are extracted in several centrality bins and fitted with blast-wave function for the extraction of yields

$$\frac{1}{p_{\mathrm{T}}}\frac{dN}{dp_{\mathrm{T}}} \propto \int_0^R r\,dr\,m_{\mathrm{T}} I_0\left(\frac{p_{\mathrm{T}}\sinh\rho}{T_{\mathrm{kin}}}\right) K_1\left(\frac{m_{\mathrm{T}}\cosh\rho}{T_{\mathrm{kin}}}\right)$$

E. Schnedermann et al., Phys. Rev. C 48, 2462 (1993)

t and ^{3}He p_T spectra in pp collisions

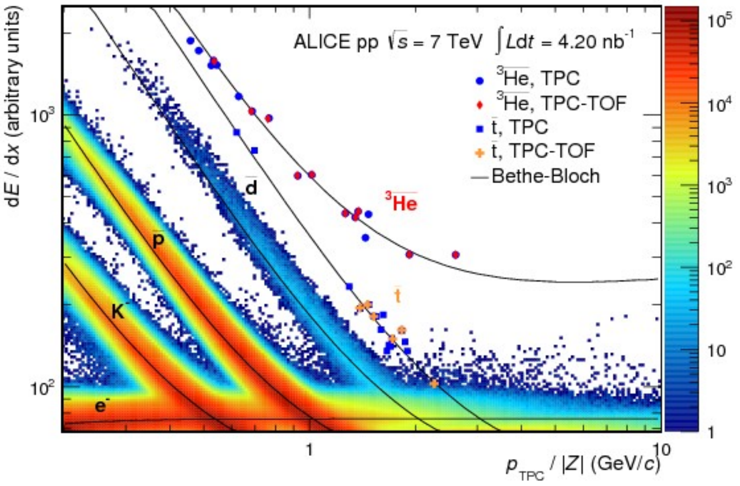

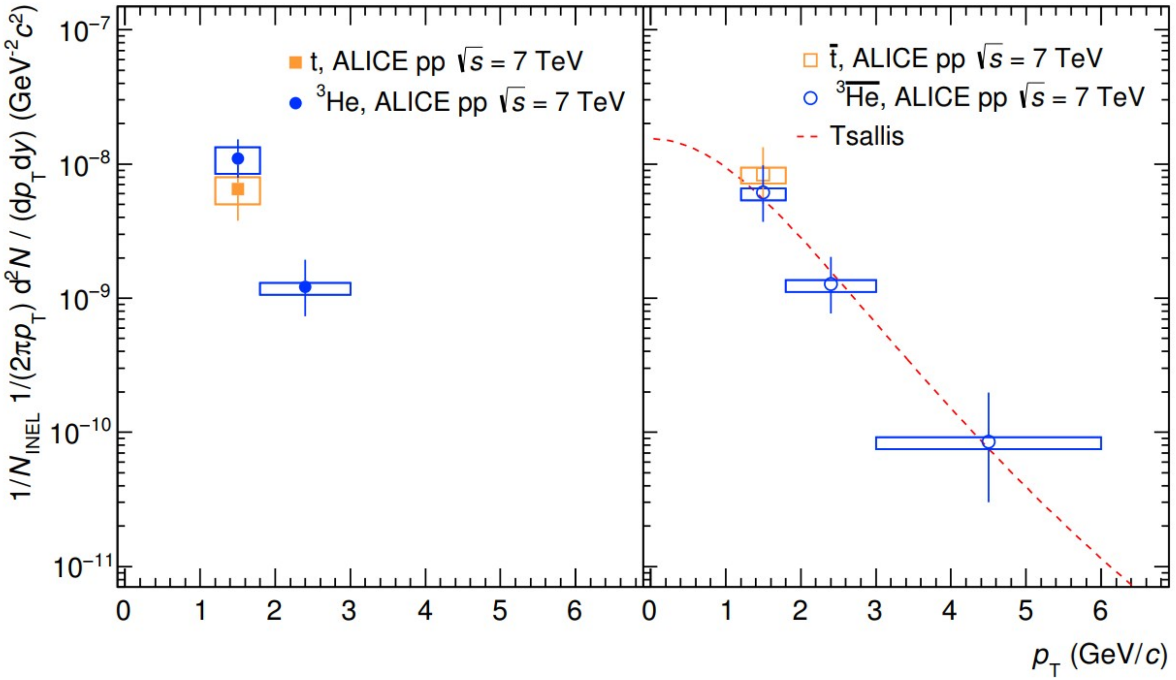

First ever measurements of t and ^{3}He nuclei in pp collisions

ALICE Collaboration, Phys. Rev. C **97**, no.2, 024615 (2018)

^{3}He p_T spectra in p-Pb collisions

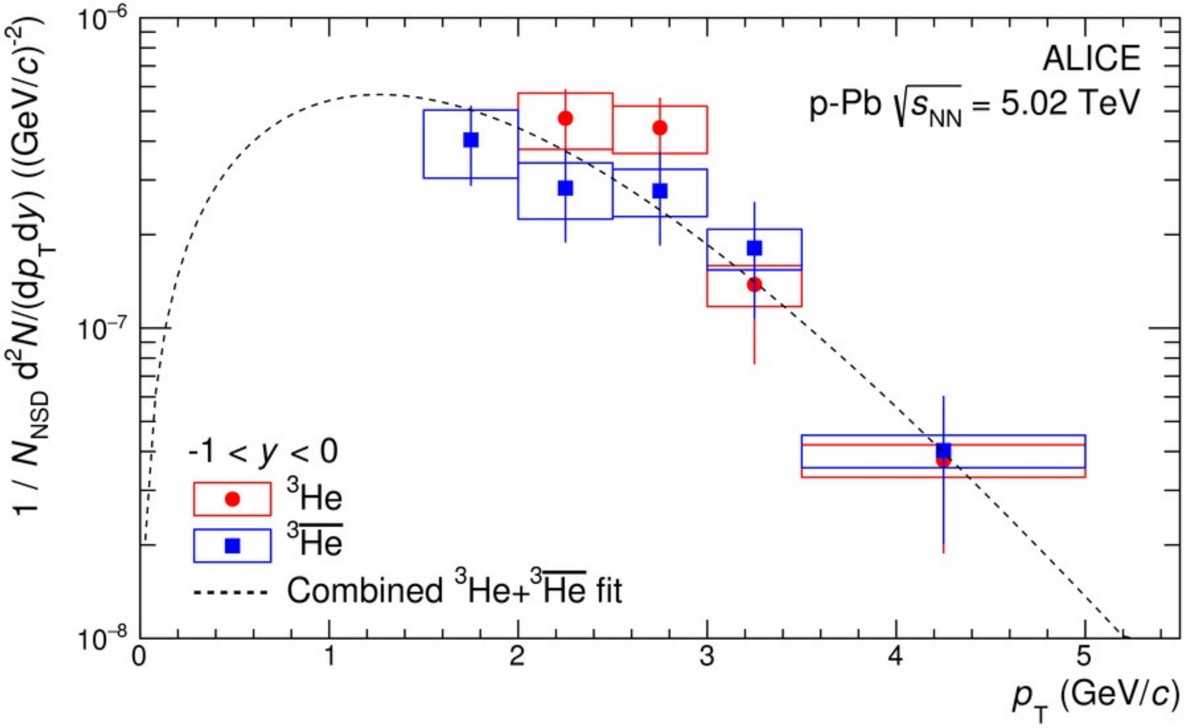

Spectra are extracted in two multiplicity bins and fitted with blast-wave function for the extraction of yields

ALICE Collaboration, arXiv:1906.03136

^{3}He p_{T} spectra in Pb-Pb collisions

ALICE-PUBLIC-2017-006

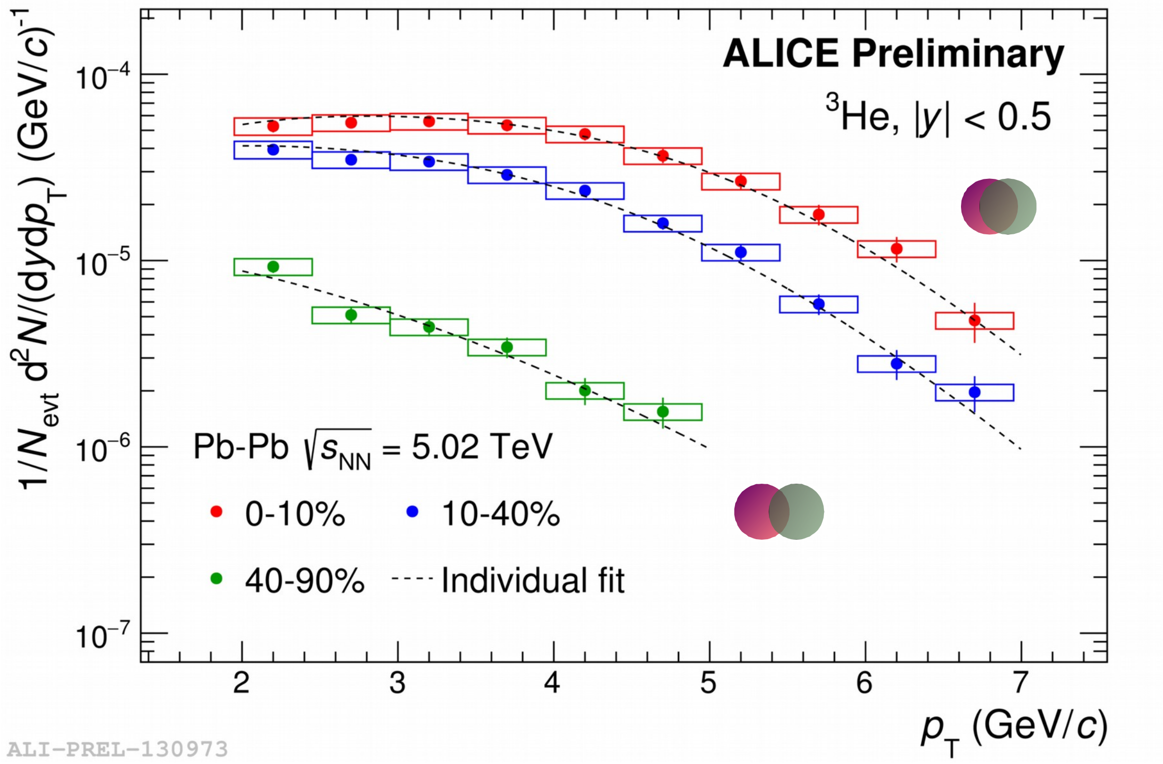

Spectra are extracted in three centrality bins and fitted with blast-wave function for the extraction of yields

Anti-Matter production

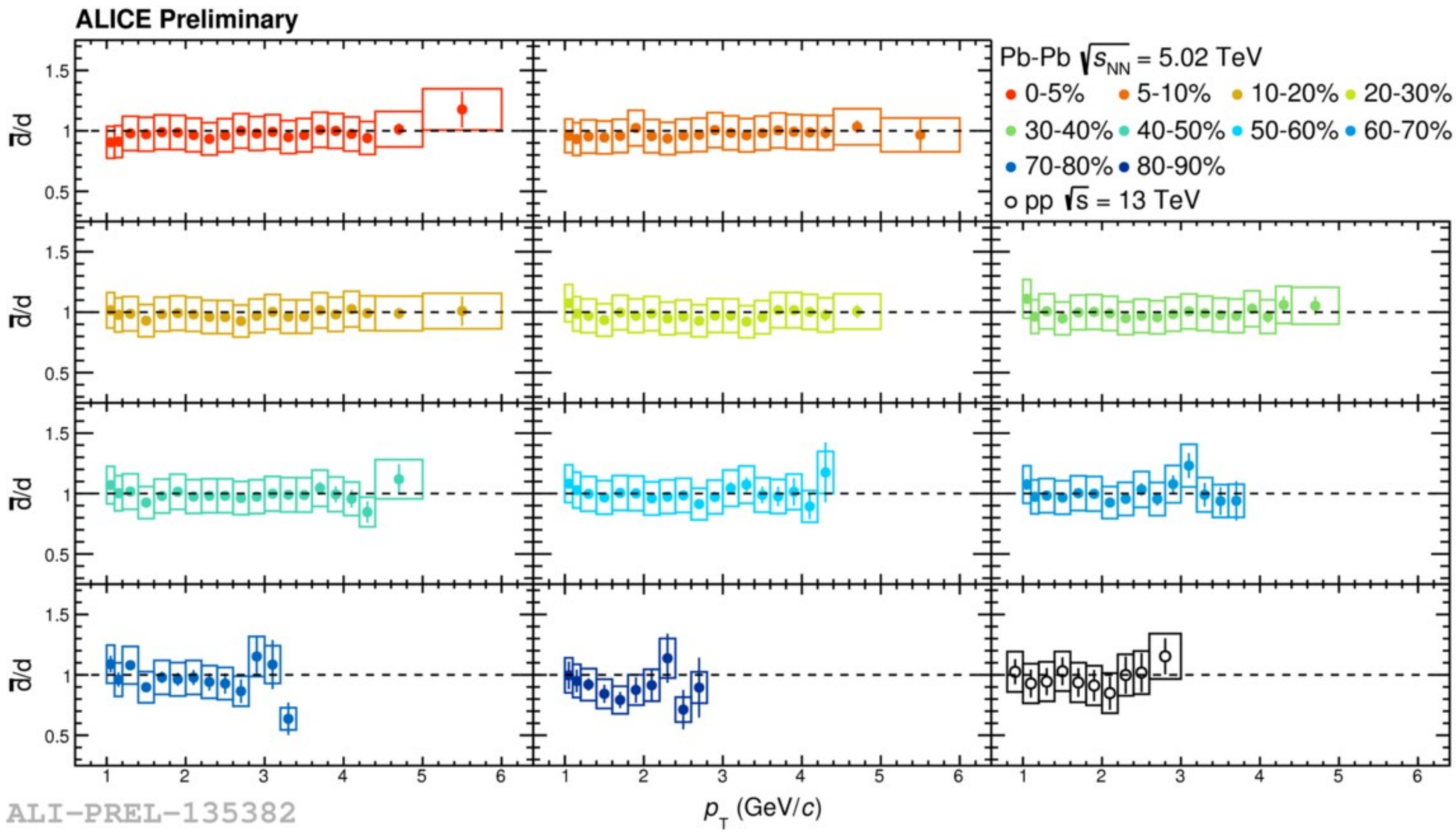

Anti-Matter production

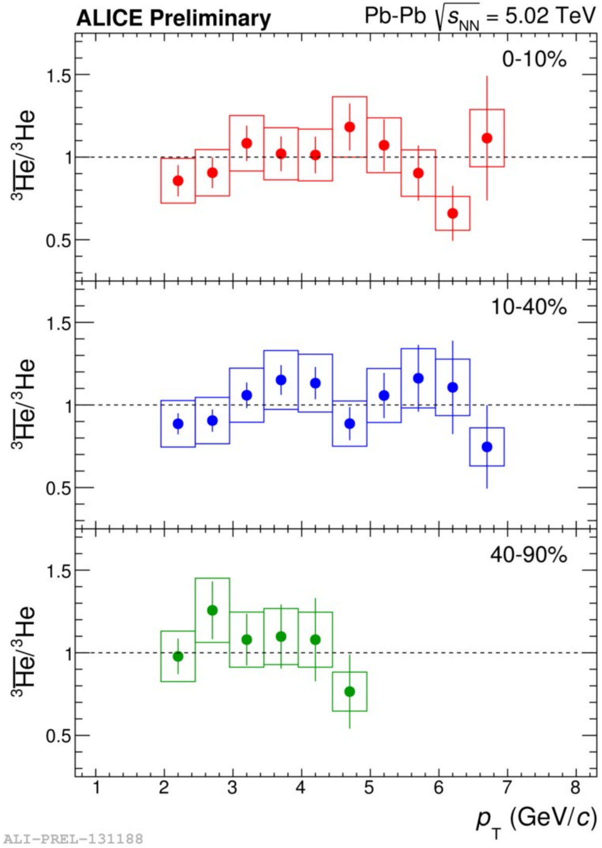

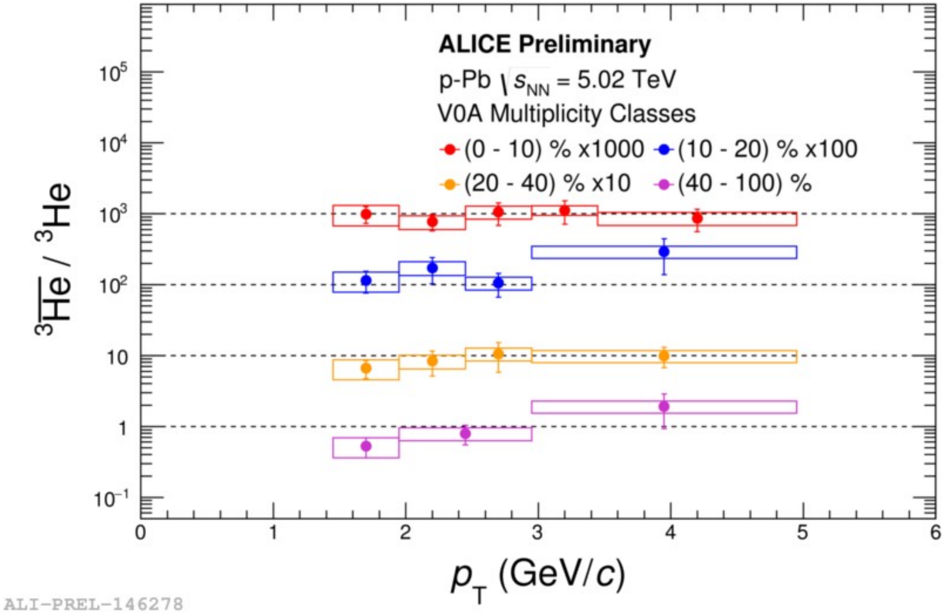

- Anti-nuclei/nuclei ratios are consistent with unity (similar to other light particle species) in the measured p_T-interval
- Ratios are constant as a function of p_T and centrality

^{4}He production in Pb-Pb collisions

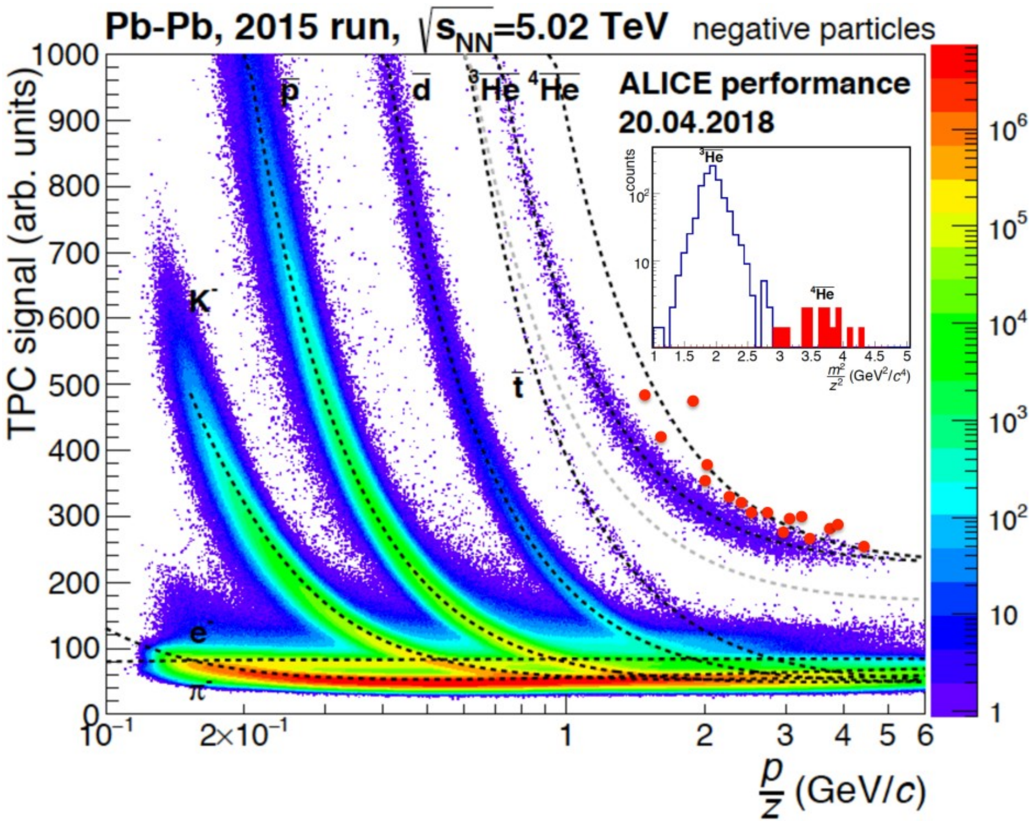

- Heaviest (anti-)nucleus observed (16 candidates in Pb-Pb at 5.02 TeV)
- Pre-selection using d*E*/d*x* measured in TPC
- ±3σ from the expected value for ^{4}He
- Signal extraction from mass squared distribution obtained using TOF

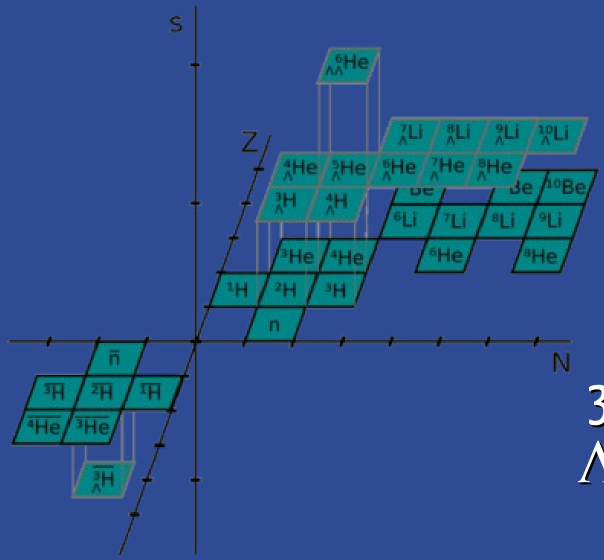

$^{3}_{\Lambda}$H identification

Hypernuclei

A hypernucleus is a nucleus which contains at least one hyperon (a baryon containing one or more strange quarks) in addition to nucleons

Hypernuclei

A hypernucleus is a nucleus which contains at least one hyperon (a baryon containing one or more strange quarks) in addition to nucleons

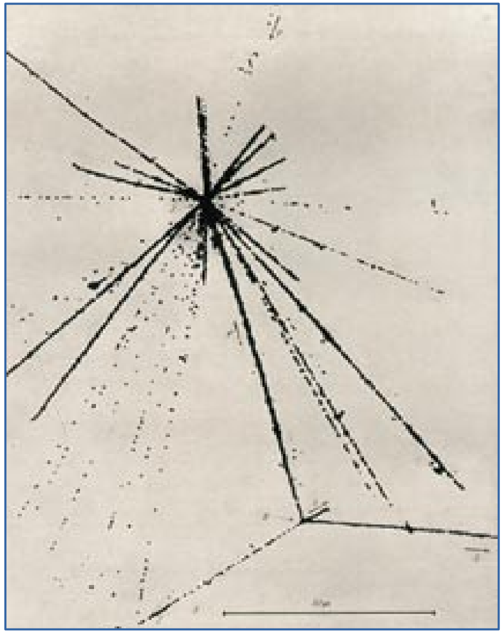

1952: first observation of hypernuclear decay from cosmic rays data

Photographic emulsion M. Danysz and J.Pniewski, Phil. Mag. 44 (1953) 348

Hypernuclei

A hypernucleus is a nucleus which contains at least one hyperon (a baryon containing one or more strange quarks) in addition to nucleons

Main goals of hypenuclear physics:

- Extension of nuclear chart
- Understand the baryon-baryon interaction in strangeness sector
- Study the structure of multi-strange systems

3D nuclear landscape

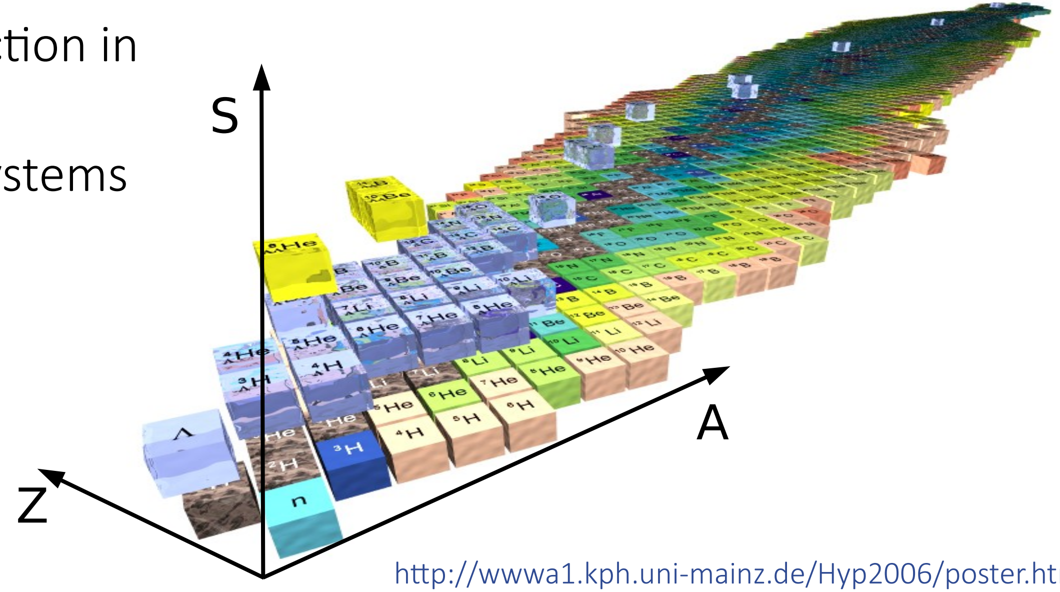

http://wwwa1.kph.uni-mainz.de/Hyp2006/poster.html

Hypertriton ($^{3}_{\Lambda}H$)

$^{3}_{\Lambda}H$ is the lightest known hypernucleus and is formed by (p,n,Λ).

- Mass = 2.991 GeV/c^2
- **B_{Λ} = 0.13 ± 0.05 MeV** (B_d = 2.2 MeV, B_t = 8.5 MeV, B_{3He} = 7.7 MeV)

($^{3}_{\Lambda}\overline{H}$) $^{3}_{\Lambda}H$ is unstable under weak decay. Possible decay modes:

$$^{3}_{\Lambda}H \rightarrow {}^{3}He + \pi^{-} \quad (\sim 25\%)$$
$$^{3}_{\Lambda}H \rightarrow {}^{3}H + \pi^{0} \quad (\sim 13\%)$$
$$^{3}_{\Lambda}H \rightarrow d + p + \pi^{-} \quad (\sim 41\%)$$
$$^{3}_{\Lambda}H \rightarrow d + n + \pi^{0} \quad (\sim 21\%)$$

$$^{3}_{\overline{\Lambda}}\overline{H} \rightarrow {}^{3}\overline{He} + \pi^{+} \quad (\sim 25\%)$$
$$^{3}_{\overline{\Lambda}}\overline{H} \rightarrow {}^{3}\overline{H} + \pi^{0} \quad (\sim 13\%)$$
$$^{3}_{\overline{\Lambda}}\overline{H} \rightarrow \overline{d} + \overline{p} + \pi^{+} \quad (\sim 41\%)$$
$$^{3}_{\overline{\Lambda}}\overline{H} \rightarrow \overline{d} + \overline{n} + \pi^{0} \quad (\sim 21\%)$$

- Branching ratios are not well known
  - Only few theoretical calculations[1] available

[1] Kamada et al., Phys. Rev. C57(1998)4

($^{3}_{\bar{\Lambda}}\overline{\mathrm{H}}$) $^{3}_{\Lambda}\mathrm{H}$ identification

Decay Channels

$^{3}_{\Lambda}\mathrm{H} \rightarrow {}^{3}\mathrm{He} + \pi^{-}$	$^{3}_{\bar{\Lambda}}\overline{\mathrm{H}} \rightarrow {}^{3}\overline{\mathrm{He}} + \pi^{+}$
$^{3}_{\Lambda}\mathrm{H} \rightarrow \mathrm{H} + \pi^{0}$	$^{3}_{\bar{\Lambda}}\overline{\mathrm{H}} \rightarrow \overline{\mathrm{H}} + \pi^{0}$
$^{3}_{\Lambda}\mathrm{H} \rightarrow d + p + \pi^{-}$	$^{3}_{\bar{\Lambda}}\overline{\mathrm{H}} \rightarrow \bar{d} + \bar{p} + \pi^{+}$
$^{3}_{\Lambda}\mathrm{H} \rightarrow d + n + \pi^{-}$	$^{3}_{\bar{\Lambda}}\overline{\mathrm{H}} \rightarrow \bar{d} + \bar{n} + \pi^{+}$

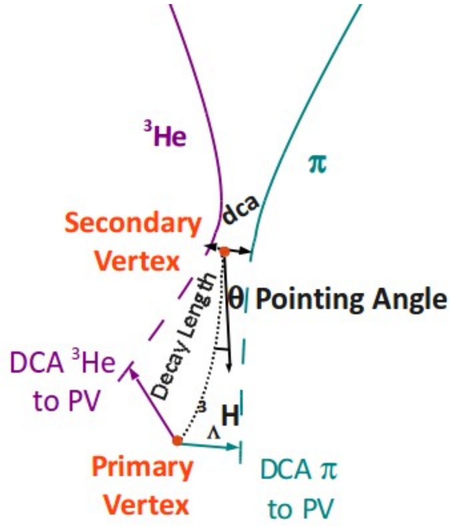

$^{3}_{\Lambda}\mathrm{H}$ and $^{3}_{\bar{\Lambda}}\overline{\mathrm{H}}$ search via two-body decays into charged particles:

- Two body decay: lower combinatorial background
- Charged particles: ALICE acceptance for charged particles higher than for neutrals

Signal Extraction:

- Identify ^{3}He and π
- Evaluate (^{3}He,π) invariant mass
- Apply topological cuts in order to:
  - identify secondary decay vertex
  - reduce combinatorial background
- Extract signal

$(^{3}_{\bar{\Lambda}}\overline{\mathrm{H}})\ ^{3}_{\Lambda}\mathrm{H}$ identification

Decay Channels

$^{3}_{\Lambda}\mathrm{H} \rightarrow {}^{3}\mathrm{He} + \pi^{-}$	$^{3}_{\bar{\Lambda}}\overline{\mathrm{H}} \rightarrow {}^{3}\overline{\mathrm{He}} + \pi^{+}$
$^{3}_{\Lambda}\mathrm{H} \rightarrow \mathrm{H} + \pi^{0}$	$^{3}_{\bar{\Lambda}}\overline{\mathrm{H}} \rightarrow \overline{\mathrm{H}} + \pi^{0}$
$^{3}_{\Lambda}\mathrm{H} \rightarrow d + p + \pi^{-}$	$^{3}_{\bar{\Lambda}}\overline{\mathrm{H}} \rightarrow \bar{d} + \bar{p} + \pi^{+}$
$^{3}_{\Lambda}\mathrm{H} \rightarrow d + n + \pi^{-}$	$^{3}_{\bar{\Lambda}}\overline{\mathrm{H}} \rightarrow \bar{d} + \bar{n} + \pi^{+}$

$^{3}_{\Lambda}\mathrm{H}$ and $^{3}_{\bar{\Lambda}}\overline{\mathrm{H}}$ search via two-body decays into charged particles:

- Two body decay: lower combinatorial background
- Charged particles: ALICE acceptance for charged particles higher than for neutrals

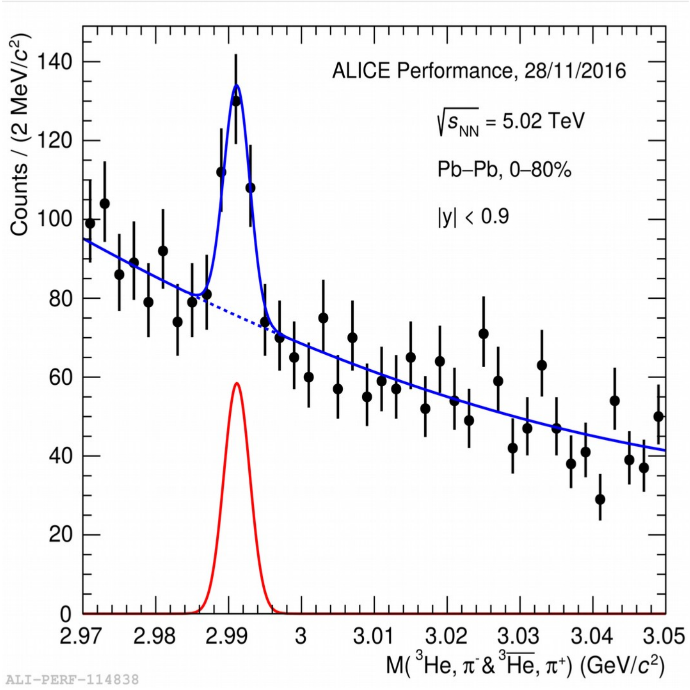

$({}^{3}_{\bar\Lambda}\overline{\mathrm{H}})\ {}^{3}_{\Lambda}\mathrm{H}$ identification

Decay Channels

${}^{3}_{\Lambda}\mathrm{H} \rightarrow {}^{3}\mathrm{He} + \pi^{-}$	${}^{3}_{\bar\Lambda}\overline{\mathrm{H}} \rightarrow {}^{3}\overline{\mathrm{He}} + \pi^{+}$
${}^{3}_{\Lambda}\mathrm{H} \rightarrow \mathrm{H} + \pi^{0}$	${}^{3}_{\bar\Lambda}\overline{\mathrm{H}} \rightarrow \overline{\mathrm{H}} + \pi^{0}$
${}^{3}_{\Lambda}\mathrm{H} \rightarrow d + p + \pi^{-}$	${}^{3}_{\bar\Lambda}\overline{\mathrm{H}} \rightarrow \bar{d} + \bar{p} + \pi^{+}$
${}^{3}_{\Lambda}\mathrm{H} \rightarrow d + n + \pi^{-}$	${}^{3}_{\bar\Lambda}\overline{\mathrm{H}} \rightarrow \bar{d} + \bar{n} + \pi^{+}$

${}^{3}_{\Lambda}\mathrm{H}$ and ${}^{3}_{\bar\Lambda}\overline{\mathrm{H}}$ search via three-body decays into charged particles:

- Higher combinatorial background
- Higher B.R. (~41%)

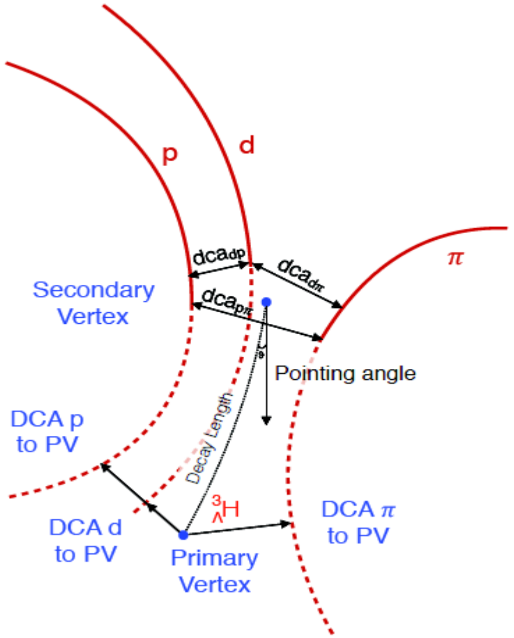

$(^{3}_{\bar{\Lambda}}\overline{H})\ ^{3}_{\Lambda}H$ identification

Decay Channels

$^{3}_{\Lambda}H \rightarrow {}^{3}He + \pi^{-}$	$^{3}_{\bar{\Lambda}}\overline{H} \rightarrow {}^{3}\overline{He} + \pi^{+}$
$^{3}_{\Lambda}H \rightarrow H + \pi^{0}$	$^{3}_{\bar{\Lambda}}\overline{H} \rightarrow \overline{H} + \pi^{0}$
$^{3}_{\Lambda}H \rightarrow d + p + \pi^{-}$	$^{3}_{\bar{\Lambda}}\overline{H} \rightarrow \bar{d} + \bar{p} + \pi^{+}$
$^{3}_{\Lambda}H \rightarrow d + n + \pi^{-}$	$^{3}_{\bar{\Lambda}}\overline{H} \rightarrow \bar{d} + \bar{n} + \pi^{+}$

$^{3}_{\Lambda}H$ and $^{3}_{\bar{\Lambda}}\overline{H}$ search via three-body decays into charged particles:

- Higher combinatorial background
- Higher B.R. (~41%)

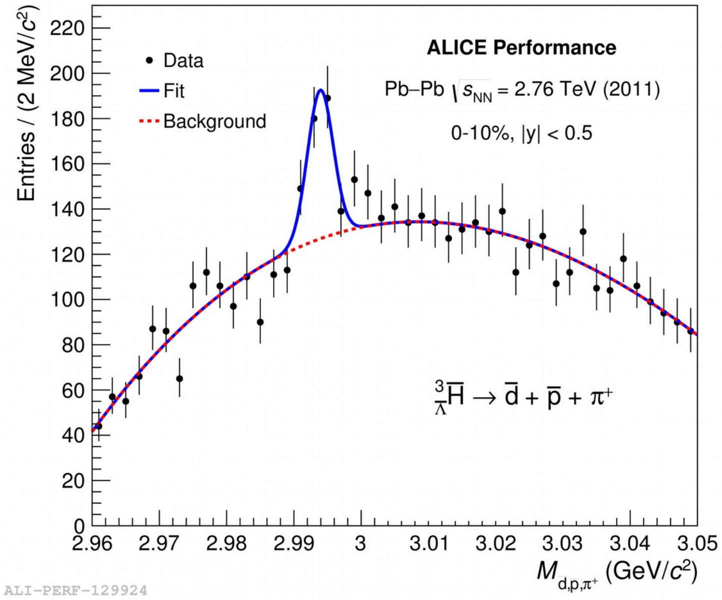

${}^{3}_{\Lambda}H$ lifetime determination

Direct decay time measurement is difficult (~ps), but the excellent determination of primary and decay vertex allows measurement of lifetime via:

$$N(t) = N(0)\exp\left(-\frac{L}{\beta\gamma c\tau}\right)$$

Where $c\tau = mL/p$
With m the hypertriton mass, L the decay length and p the total momentum

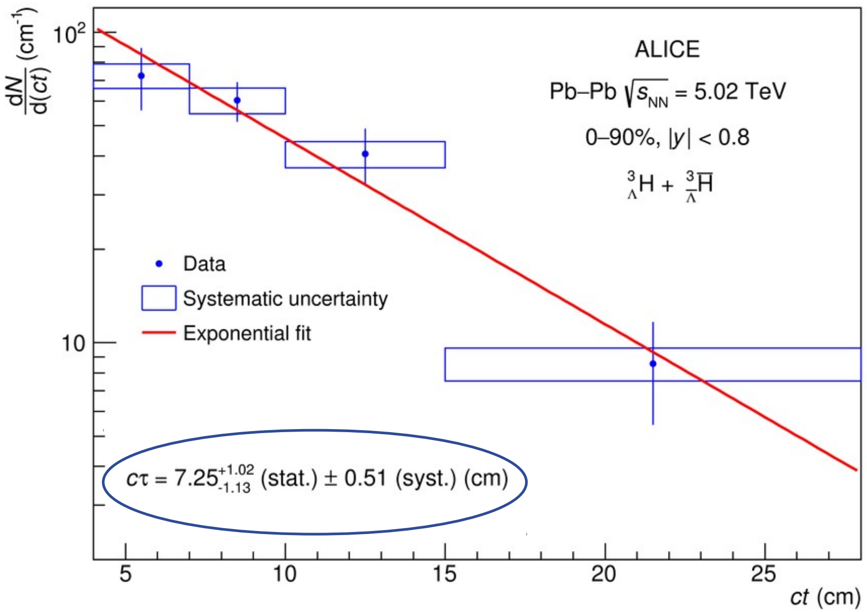

$^{3}_{\Lambda}H$ lifetime determination

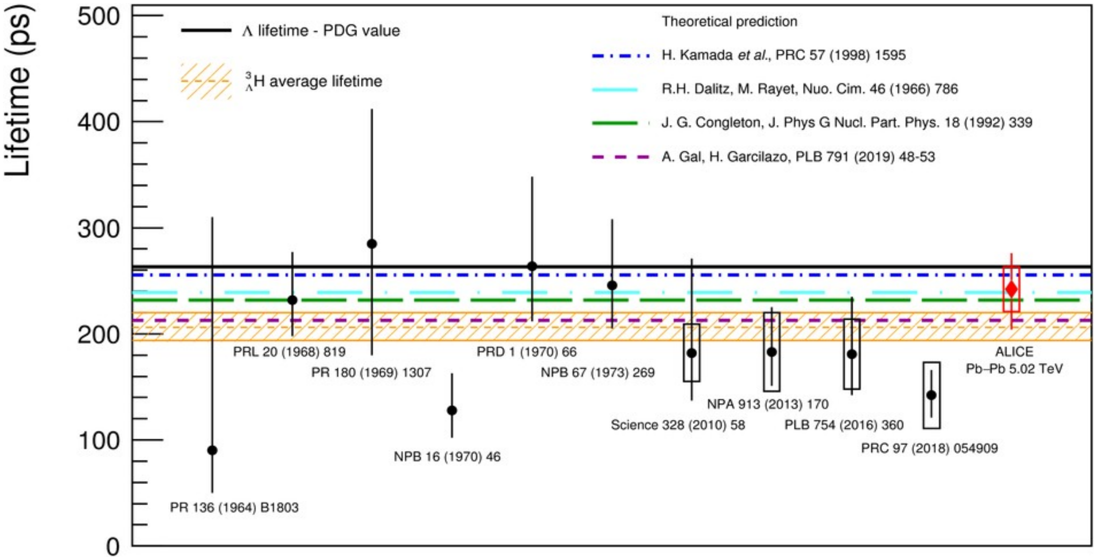

- ALICE can be used also for hypernuclear physics measurements:
  - ➢ the present data are one of the most precise measurement of $^{3}_{\Lambda}H$ life:
  - More precision can be reached:
    - ✓ increasing the statistics → another Pb-Pb data sample was collected in 2018 at the LHC → preliminary results show a lifetime closer to the free Λ one
    - ✓ lifetime measured in the 3-body decay channel
  - In the next future constraints also on the B.R. determination can be set

Production of nuclei: coalescence model

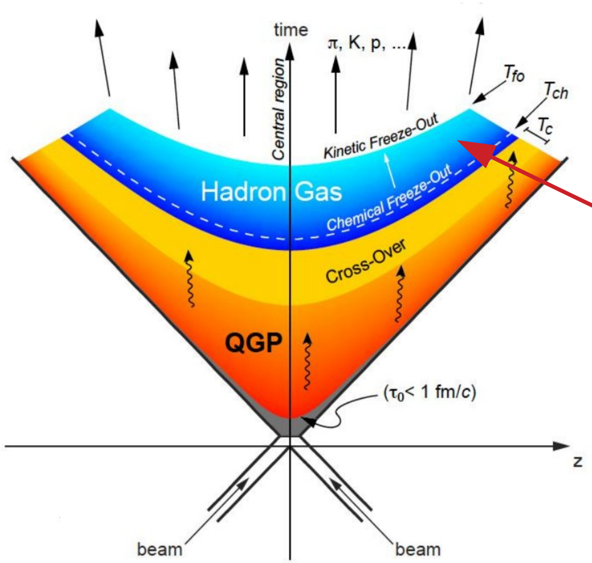

Are nuclei produced inside the hadron gas?

Coalescence model

- If baryons at freeze-out are close enough in phase space (i.e. geometrically and in momentum) and match spin state a (anti-)nucleus can be formed

Coalescence model

- If baryons at freeze-out are close enough in phase space (i.e. geometrically and in momentum) and match spin state a (anti-)nucleus can be formed
- Usually, since the nucleus is larger w.r.t. the source, the phase space is reduced to the momentum space

J. I. Kapusta, Phys.Rev. C21, 1301 (1980)

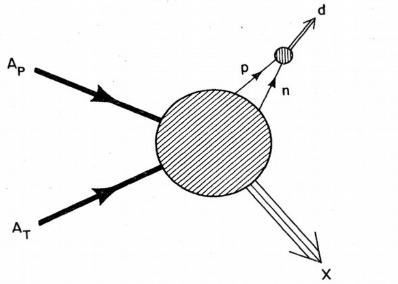

FIG. 1. Schematic for the production of a deuteron in the final state of a relativistic collision between two heavy nuclei.

Coalescence model

- If baryons at freeze-out are close enough in phase space (i.e. geometrically and in momentum) and match spin state a (anti-)nucleus can be formed
- Usually, since the nucleus is larger w.r.t. the source, the phase space is reduced to the momentum space
- Assuming that p an n have the same mass and have the same p_{T} spectra, the yield of any nucleus can be determined as

$$E_A \frac{\mathrm{d}^3 N_A}{\mathrm{d}p_A^3} = B_A \left(E_{\mathrm{p}} \frac{\mathrm{d}^3 N_{\mathrm{p}}}{\mathrm{d}p_{\mathrm{p}}^3} \right)^A$$

Coalescence model

ALICE

- If baryons at freeze-out are close enough in phase space (i.e. geometrically and in momentum) and match spin state a (anti-)nucleus can be formed
- Usually, since the nucleus is larger w.r.t. the source, the phase space is reduced to the momentum space
- Assuming that p an n have the same mass and have the same p_T spectra, the yield of any nucleus can be determined as

$$E_A \frac{d^3 N_A}{dp_A^3} = B_A \left(E_p \frac{d^3 N_p}{dp_p^3} \right)^A$$

$$\boxed{B_A = \left(\frac{4\pi}{3} p_0^3 \right)^{(A-1)} \frac{1}{A!} \frac{M}{m^A}}$$

Coalescence model

- If baryons at freeze-out are close enough in phase space (i.e. geometrically and in momentum) and match spin state a (anti-)nucleus can be formed
- Usually, since the nucleus is larger w.r.t. the source, the phase space is reduced to the momentum space
- Assuming that p an n have the same mass and have the same p_T spectra, the yield of any nucleus can be determined as

$$E_A \frac{d^3 N_A}{dp_A^3} = B_A \left(E_p \frac{d^3 N_p}{dp_p^3} \right)^A$$

$$\boxed{B_A = \left(\frac{4\pi}{3} p_0^3 \right)^{(A-1)} \frac{1}{A!} \frac{M}{m^A}}$$

$$\boxed{\begin{array}{r} d \propto p^2 \\ {}^3He \propto p^3 \end{array}}$$

Coalescence parameter B_2

$$E_A \frac{d^3 N_A}{dp_A^3} = B_A \left(E_p \frac{d^3 N_p}{dp_p^3} \right)^A$$

Measured deuteron p_T-spectra

Measured proton p_T-spectra

Coalescence parameter B_2

$$E_A \frac{\mathrm{d}^3 N_A}{\mathrm{d}p_A^3} = B_A \left(E_\mathrm{p} \frac{\mathrm{d}^3 N_\mathrm{p}}{\mathrm{d}p_\mathrm{p}^3} \right)^A$$

Measured deuteron p_T-spectra

Measured proton p_T-spectra

pp

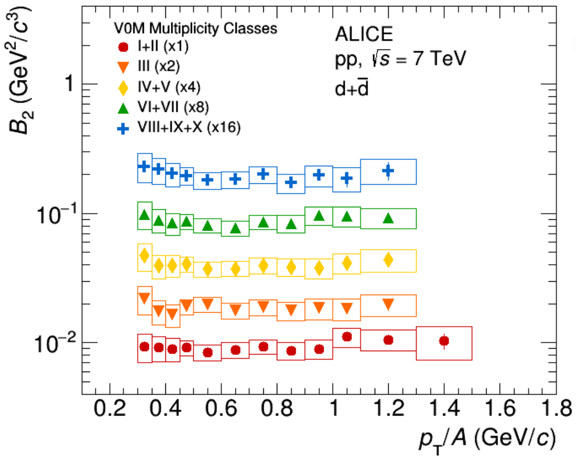

p-Pb

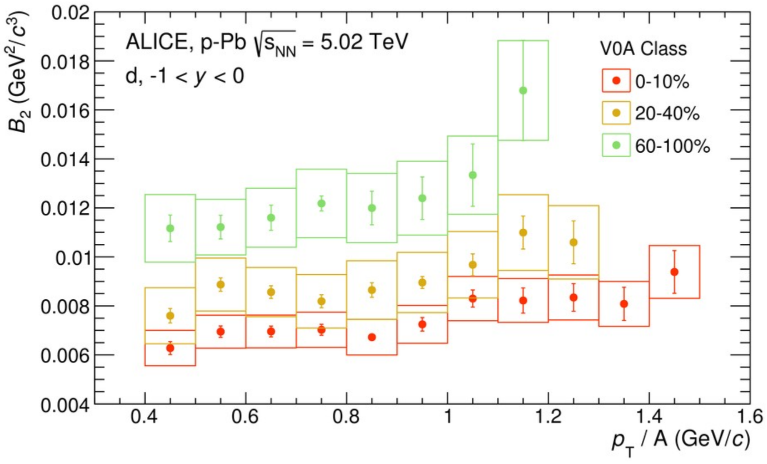

Pb-Pb

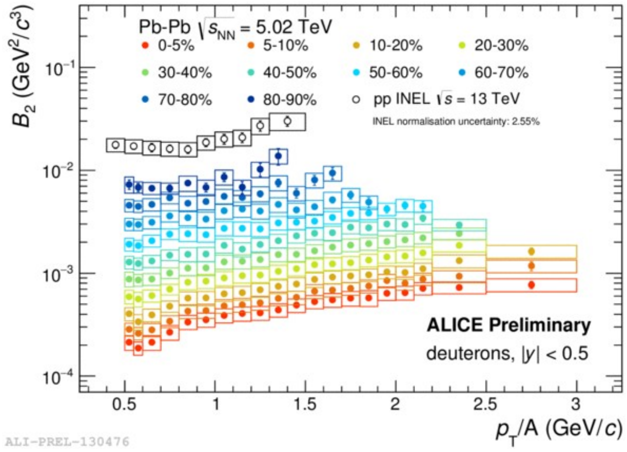

Coalescence parameter B_2

$$E_A \frac{d^3N_A}{dp_A^3} = B_A \left(E_p \frac{d^3N_p}{dp_p^3} \right)^A$$

Measured deuteron p_T-spectra

Measured proton p_T-spectra

pp

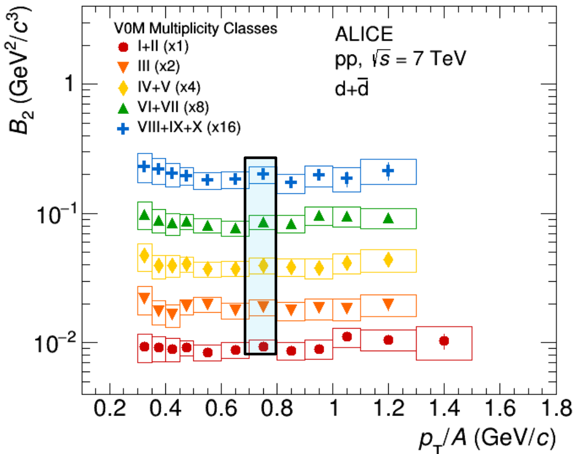

p-Pb

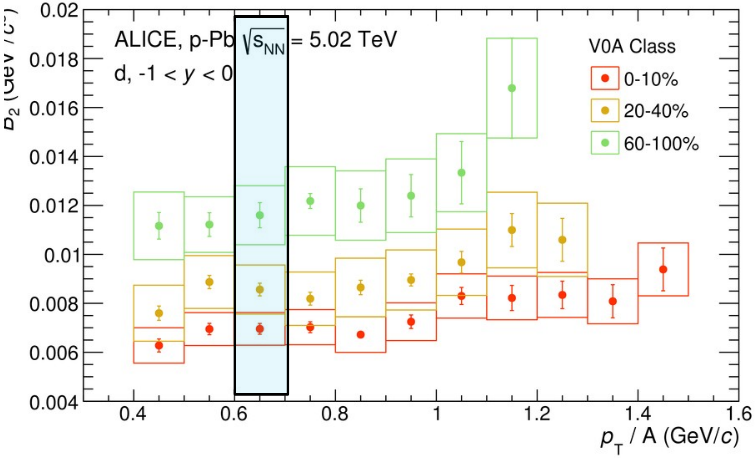

Pb-Pb

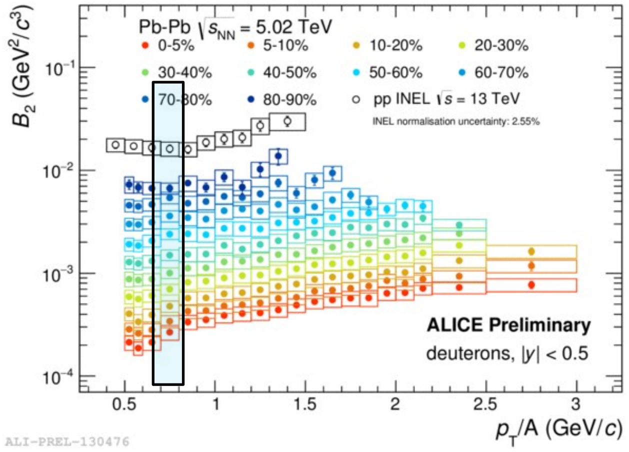

p_T/A = 0.75 GeV/c

Coalescence parameter B_2

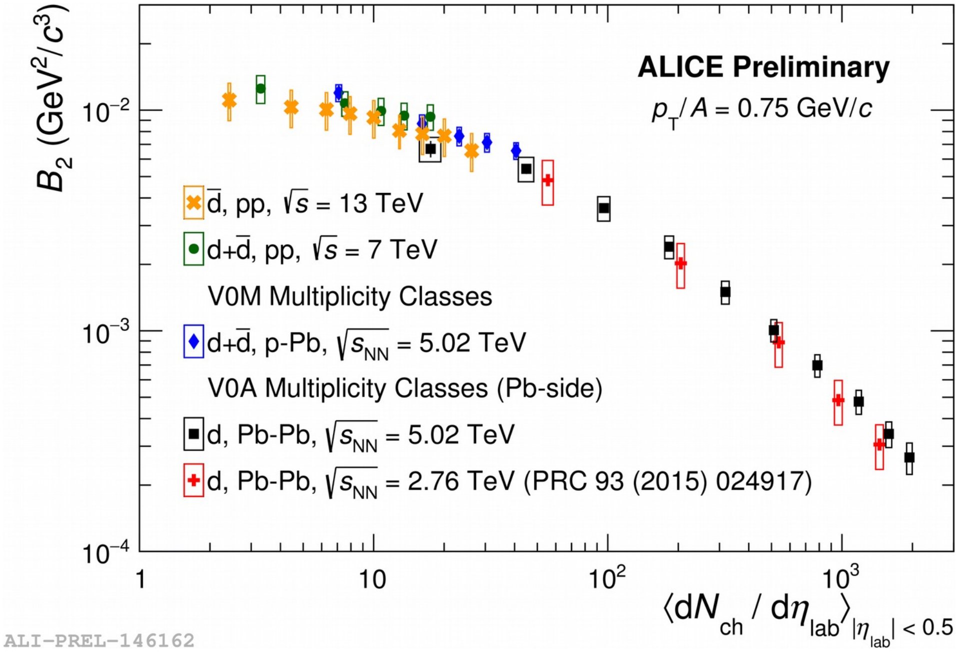

Simple coalescence model

- Flat B_2 vs p_T and no dependence on multiplicity/centrality
  - ✔ Observed "small systems": pp, p-Pb and peripheral Pb-Pb

Coalescence parameter B_2

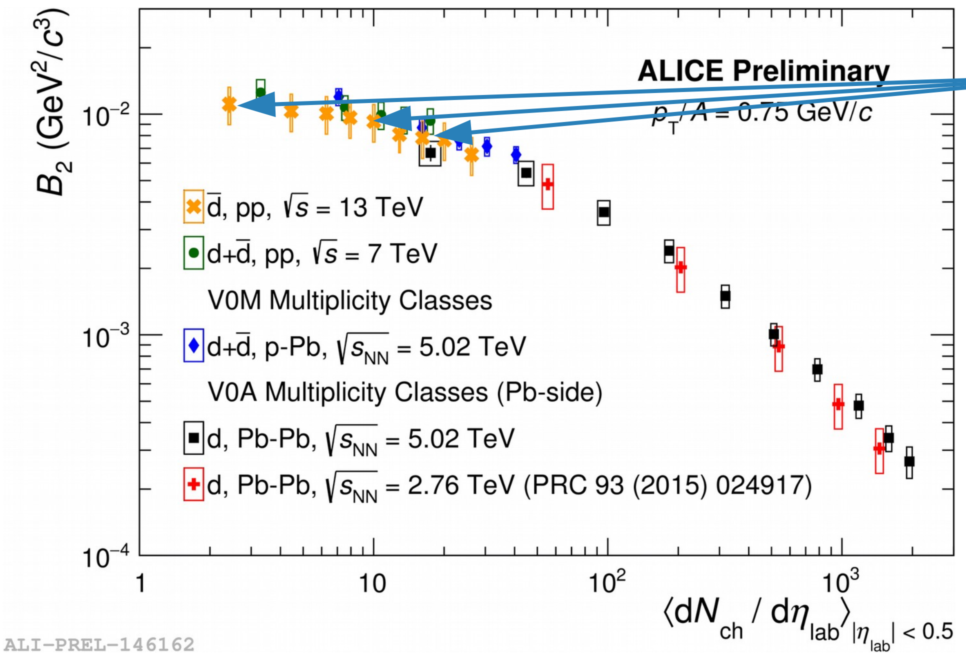

Simple coalescence model

- Flat B_2 vs p_T and no dependence on multiplicity/centrality
  - ✔ Observed "small systems": pp, p-Pb and peripheral Pb-Pb

Coalescence parameter B_2

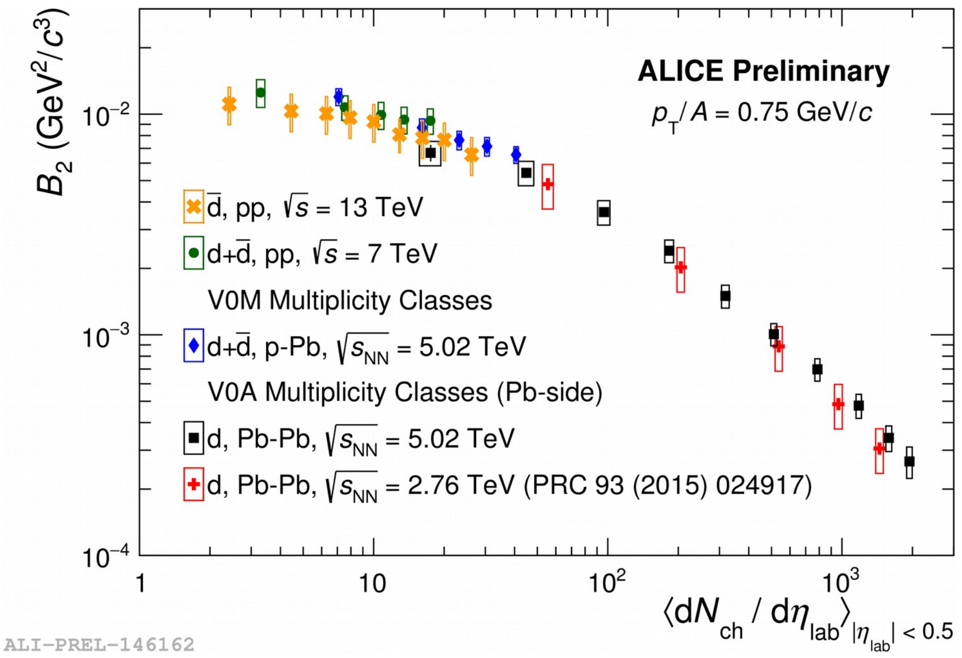

Simple coalescence model

- Flat B_2 vs p_T and no dependence on multiplicity/centrality
  - ✔ Observed "small systems": pp, p-Pb and peripheral Pb-Pb

More elaborated coalescence model takes into account the volume of the source:

$$\boxed{B_2 = \frac{3\pi^{3/2}\langle C_d \rangle}{2m_T R_\perp^2(m_T) R_\parallel(m_T)}}$$

- B_2 scales like HBT radii
  - ➢ decrease with centrality in Pb-Pb is explained as an increase in the source volume
  - ➢ increasing with p_T in central Pb-Pb reflects the K_T-dependence of the homogeneity volume (i.e. volume with similar flow properties) in HBT
    - ✔ Qualitative agreement in central Pb-Pb collisions

Coalescence parameter B_2

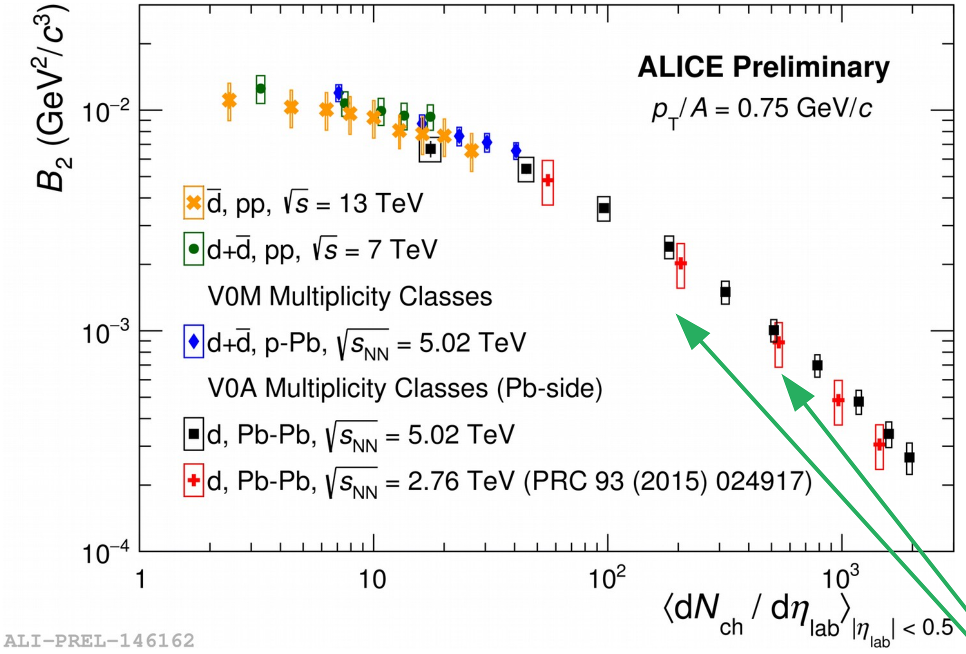

Simple coalescence model

- Flat B_2 vs p_T and no dependence on multiplicity/centrality
  - ✔ Observed "small systems": pp, p-Pb and peripheral Pb-Pb

More elaborated coalescence model takes into account the volume of the source:

$$B_2 = \frac{3\pi^{3/2}\langle C_d \rangle}{2m_T R_\perp^2(m_T) R_\parallel(m_T)}$$

- B_2 scales like HBT radii
  - ➢ decrease with centrality in Pb-Pb is explained as an increase in the source volume
  - ➢ increasing with p_T in central Pb-Pb reflects the K_T-dependence of the homogeneity volume (i.e. volume with similar flow properties) in HBT
  - ✔ Qualitative agreement in central Pb-Pb collisions

"More elaborated" coalescence model

- For "large" systems, the size of the emitting volume (V_{eff}) has to be taken into account:
  - the larger the distance between the protons and neutrons which are created in the collision, the less likely it is that they coalesce
- The source can be parameterized as rapidly expanding under radial flow (hydro)
- The coalescence process is governed by the same correlation volume ("length of homogeneity") which can be extracted from HBT interferometry
- The source radius enters in the B_A and in the quantum-mechanical correction $\langle C_A \rangle$ factor that accounts for the size of the object being produced (d, ^{3}He, …)

$$B_A = \frac{2J_A+1}{2^A} A \langle \mathcal{C}_A \rangle \frac{V_{\rm eff}(A, M_t)}{V_{\rm eff}(1, m_t)} \left(\frac{(2\pi)^3}{m_t V_{\rm eff}(1, m_t)} \right)^{A-1}$$

R. Scheibl, U. Heinz, PRC 59 (1999) 1585-1602
K. Blum et al., PRD 96 (2017) 103021

F.Bellini and A. P.Kalweit, arXiv:1807.05894 [hep-ph].

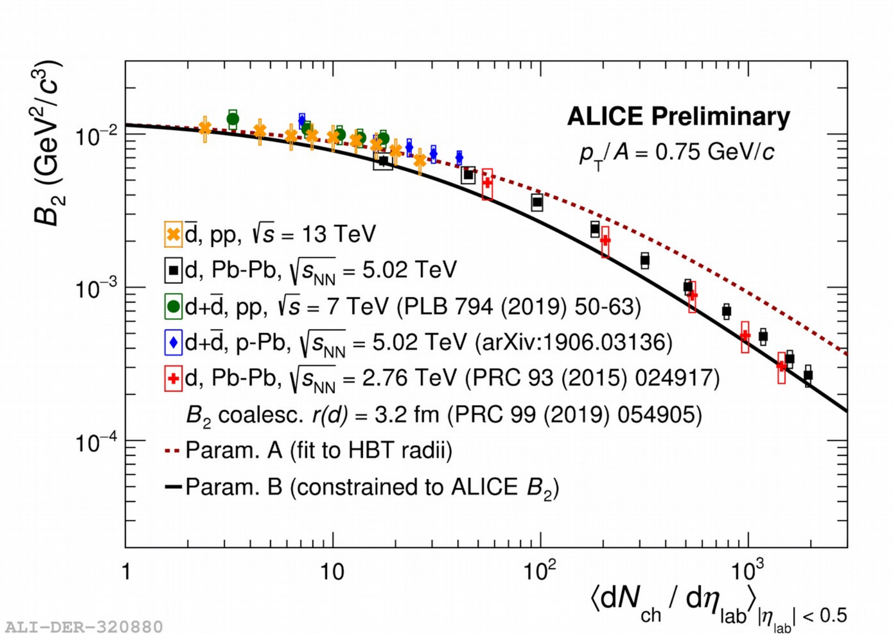

Anti-nuclei in pp collisions

Searches for dark matter WIMP candidate decaying in $\overline{d}$ and $^{3}\overline{He}$ require estimate of expected secondary astrophysical background (secondary anti-nuclei produced in cosmic ray interactions)

Precise measurement of coalescence parameters at the LHC can provide constraints for models

Predicted flux of $\overline{p}$, $\overline{d}$, $^{3}\overline{He}$ in AMS (5-yr, 95%CL)

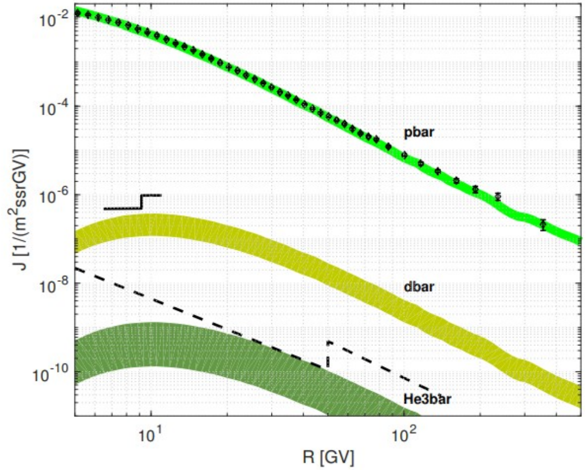

Poisson probability for detecting N≥1, 2, 3, 4 $^{3}\overline{He}$ events in a 5-yr analysis of AMS02

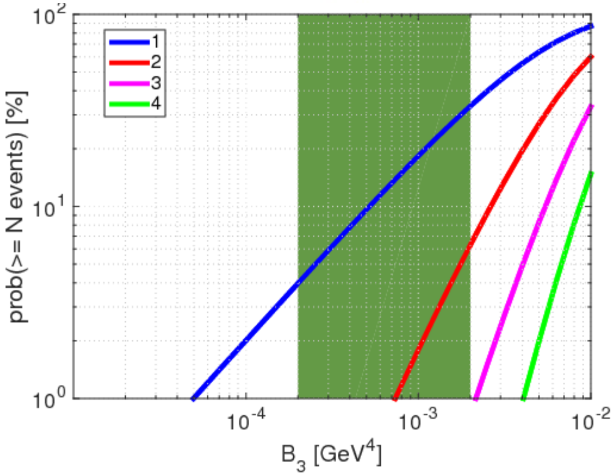

K. Blum et al., arXiv:1704.05431

Anti-nuclei in pp collisions

Searches for dark matter WIMP candidate decaying in $\overline{d}$ and $^{3}\overline{He}$ require estimate of expected secondary astrophysical background (secondary anti-nuclei produced in cosmic ray interactions)

Precise measurement of coalescence parameters at the LHC can provide constraints for models

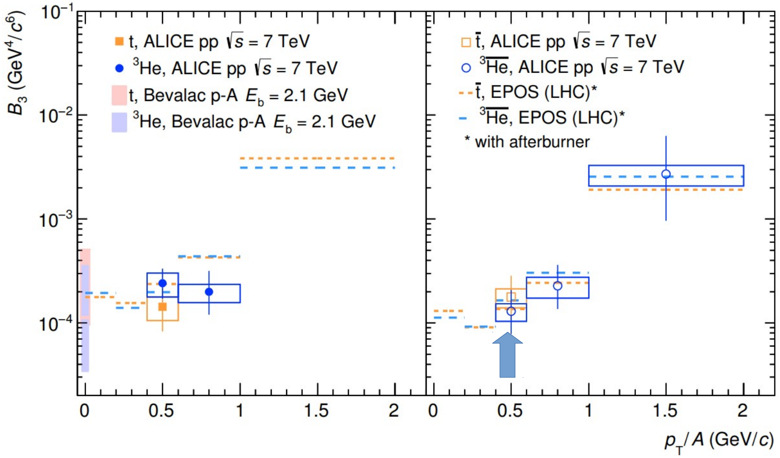

ALICE Collaboration, arXiv:1709.08522

Predicted flux of $\overline{p}$, $\overline{d}$, $^{3}\overline{He}$ in AMS (5-yr, 95%CL)

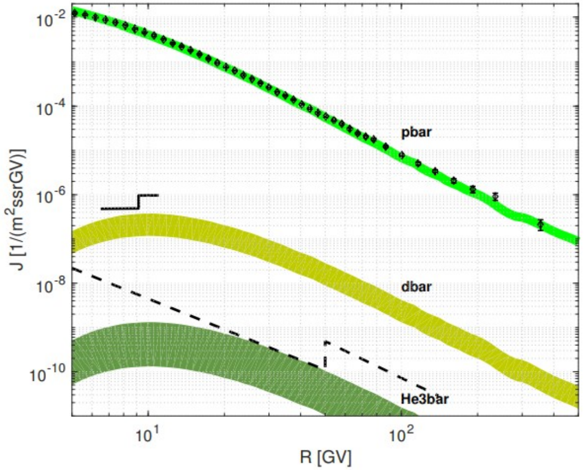

Poisson probability for detecting N≥1, 2, 3, 4 $^{3}\overline{He}$ events in a 5-yr analysis of AMS02

After ALICE

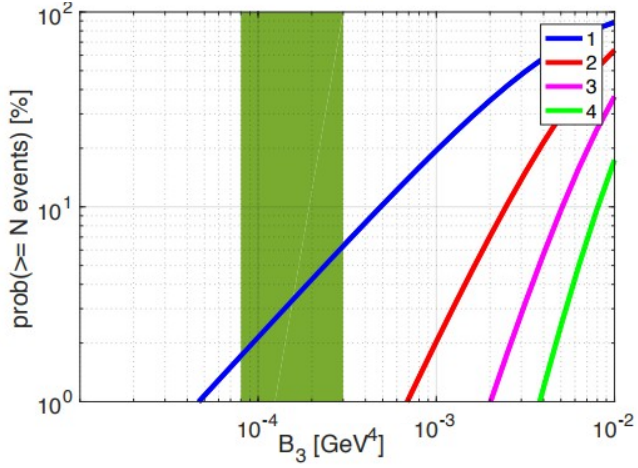

K. Blum, EMMI Workshop 2017

Light nuclei flow measurement

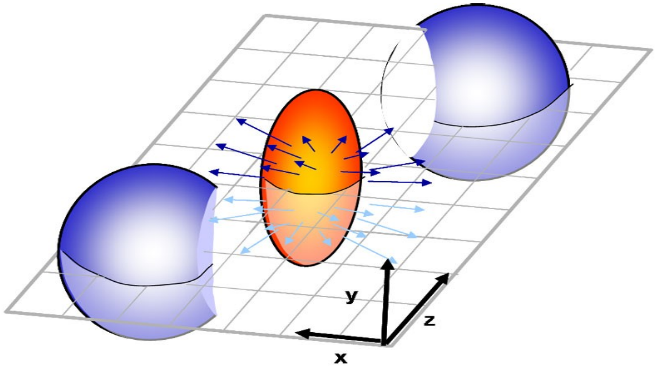

Light nuclei flow

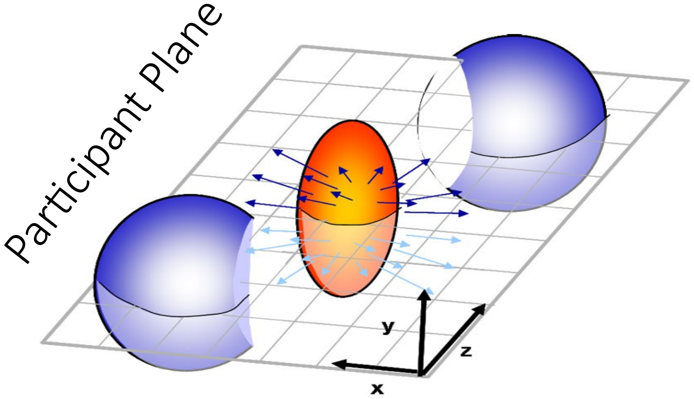

Angular distribution of reconstructed charged particles can be expanded into a Fourier series w.r.t. symmetry plane Ψ_n :

$$E\frac{d^3N}{dp^3}=\frac{1}{2\pi}\frac{d^2N}{p_T dp_T dy}\left(1+\sum_{n=1}^{\infty}2v_n\cos\left(n\left(\phi-\Psi_n\right)\right)\right)$$

$$v_n=\left\langle\cos\left(n\left(\phi-\Psi_n\right)\right)\right\rangle$$

Light nuclei flow

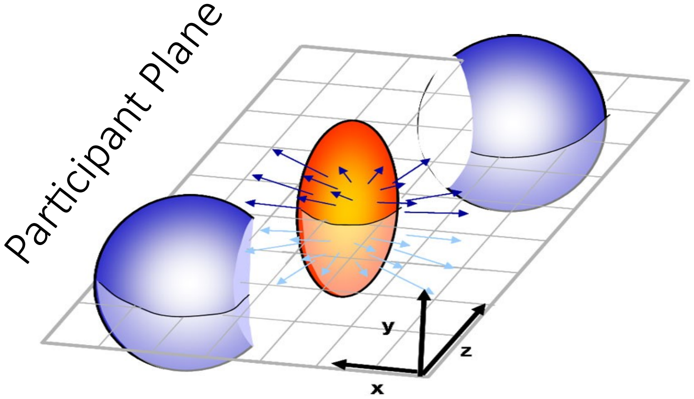

Angular distribution of reconstructed charged particles can be expanded into a Fourier series w.r.t. symmetry plane Ψ_n :

$$E\frac{d^3N}{dp^3}=\frac{1}{2\pi}\frac{d^2N}{p_T dp_T dy}\left(1+\sum_{n=1}^{\infty}2v_n\cos\left(n\left(\phi-\Psi_n\right)\right)\right)$$

$$v_n=\left\langle\cos\left(n\left(\phi-\Psi_n\right)\right)\right\rangle$$

- Elliptic flow (v_2) is sensitive to the system evolution:
  - It probes initial conditions and constrains particle production mechanisms

Light nuclei flow

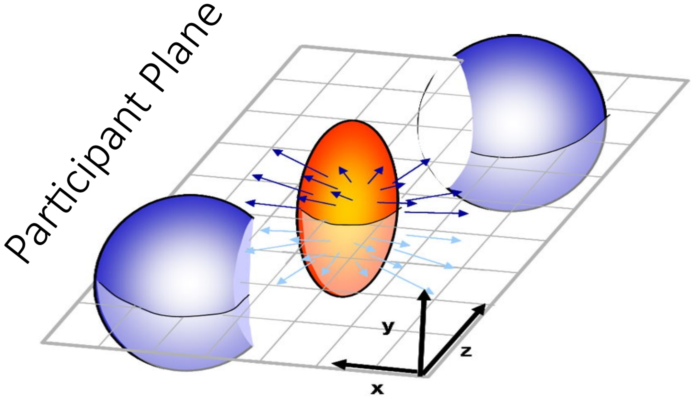

Angular distribution of reconstructed charged particles can be expanded into a Fourier series w.r.t. symmetry plane Ψ_n :

$$E\frac{d^3N}{dp^3} = \frac{1}{2\pi}\frac{d^2N}{p_T\,dp_T\,dy}\left(1+\sum_{n=1}^{\infty} 2v_n\cos\left(n\left(\phi-\Psi_n\right)\right)\right)$$

$$v_n = \left\langle \cos\left(n\left(\phi-\Psi_n\right)\right)\right\rangle$$

- Elliptic flow (v_2) is sensitive to the system evolution:
  - ➢ It probes initial conditions and constrains particle production mechanisms
- The measurement of light nuclei v_n will help in the understanding of particle production mechanisms
  - ➢ Do light nuclei follow the mass ordering observed for lighter particles?
  - ➢ Do light nuclei follow a quark/baryon number scaling (coalescence) or follow mass scaling (hydro)?

Light nuclei flow measurement

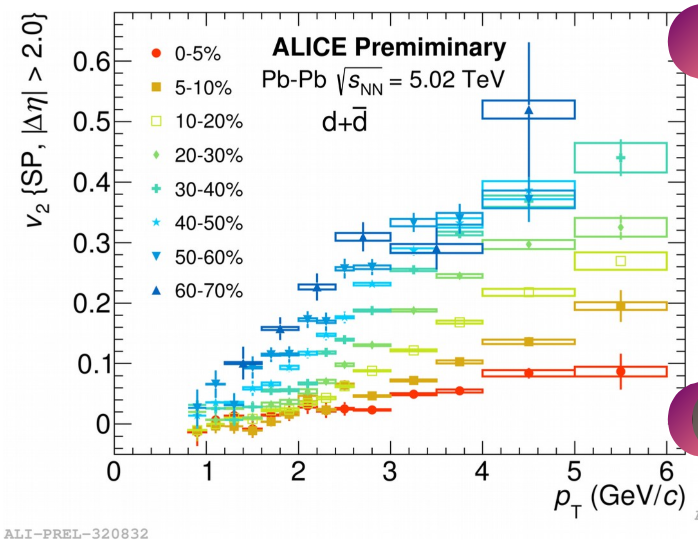

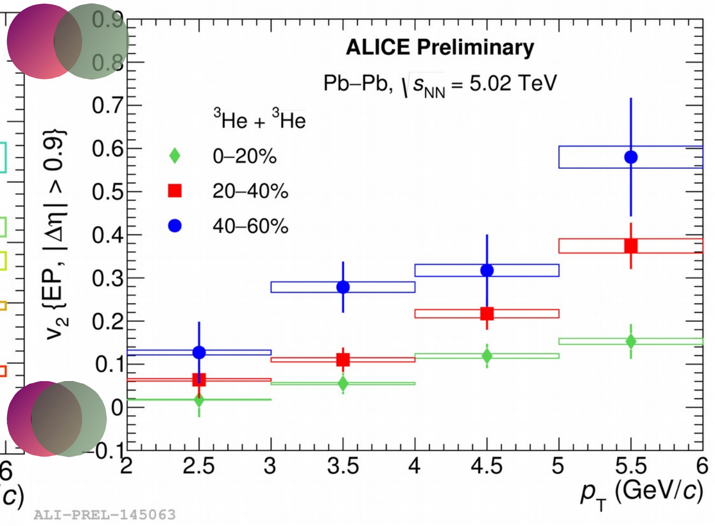

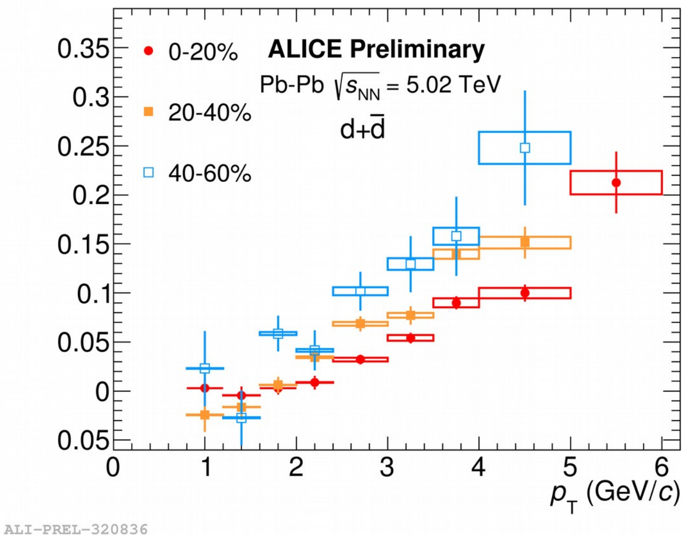

- A significant v_2 is observed for deuterons and ^{3}He. The value of v_2 (p_T) increases progressively from central to semi-central collisions
- v_3 of (anti-)deuterons measured for the **first measurement**: effects of initial state fluctuations of energy density in the colliding nuclei visible also for (anti-)deuterons

A-scaling of v_n of (anti-)deuterons

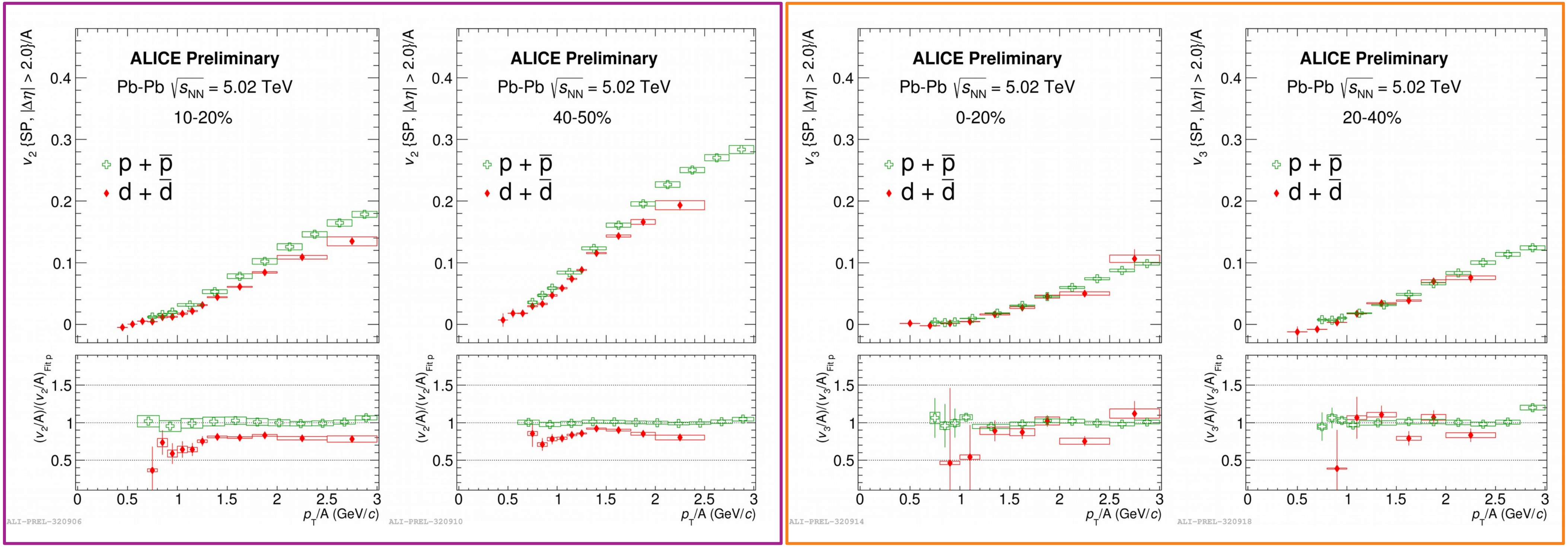

- Simple coalescence approach:
  - Scaling of v_n with the mass number A
  - Overestimates the data in all centrality ranges, even if smaller deviations in more peripheral collisions
  - Mass number scaling seems to be approximately valid for v_3

Blast-Wave model

- Blast-Wave model: simplified hydro model which can be used to describe spectra and flow at the same time
- The transverse mass spectrum can be expressed as

$$\frac{\mathrm{dN}}{\mathrm{d}y\mathrm{d}m_{\mathrm{T}}^2\mathrm{d}\phi_p} \sim \int_0^{2\pi} \mathrm{d}\phi_s\, K_1(\beta_t(\phi_s))\, e^{\alpha_t(\phi_s)\cos(\phi_s-\phi_p)}$$

- Taking the azimuthal average over $\cos(2\phi_{\mathrm{p}})$ [1]
- Blast-Wave fit matched data better after the STAR Collaboration[2] added a fourth parameter, s_2 which takes into account the density modulation in the source

$$v_2(p_{\mathrm{T}}) = \frac{\int_0^{2\pi} \mathrm{d}\phi_s \cos(2\phi_s) I_2[\alpha_t(\phi_s)] K_1[\beta_t(\phi_s)][1+2s_2\cos(2\phi_s)]}{\int_0^{2\pi} \mathrm{d}\phi_s I_0[\alpha_t(\phi_s)] K_1[\beta_t(\phi_s)][1+2s_2\cos(2\phi_s)]}$$

Blast-Wave model:
[1] P. Huovinen et al. Phys. Lett. B 503, 58-64 (2001), [2] STAR Collaboration, Phys. Rev. Lett. 87, 182301 (2001)

Blast-Wave model

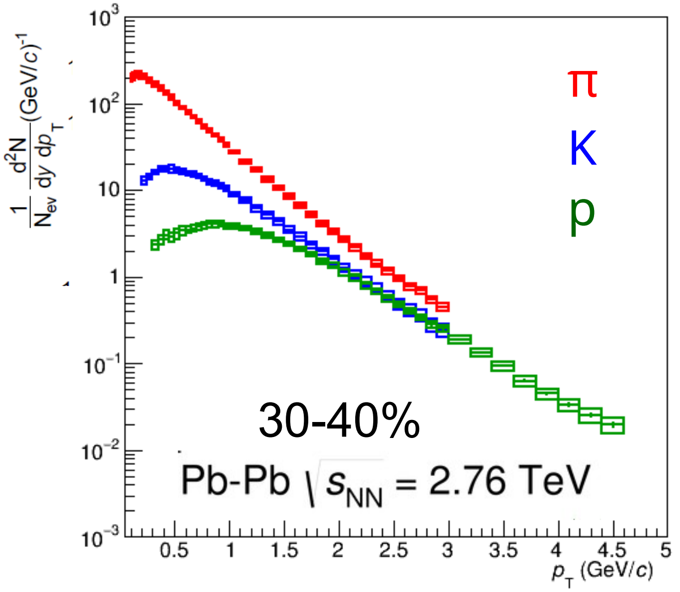

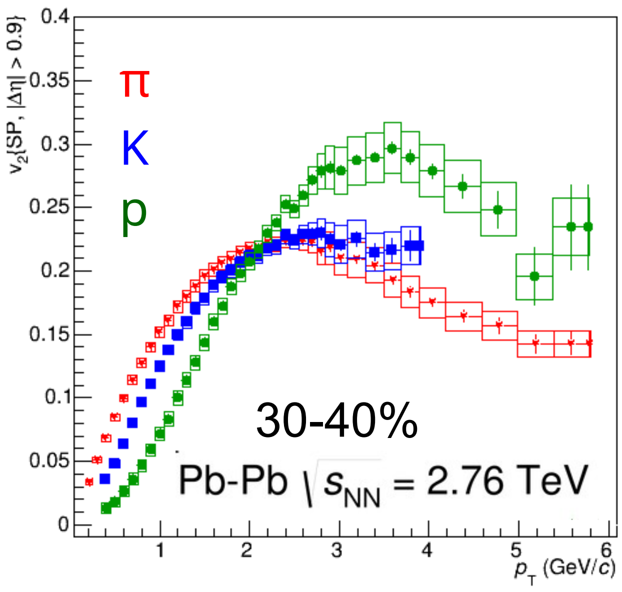

Data from [1,2]

- The measured π, K and p p_T spectra and v_2 (p_T)fitted simultaneously (mass used as fixed par)
  - ✔ **Parameters from fit used to predict deuteron p_T spectra and $v_2(p_T)$**

Fit range for the combined fit:

- [0.5-1,0] GeV/c for π
- [0.2-1.2] GeV/c for K
- [0.3-1.7] GeV/c for p

v_2 of (anti-)deuterons vs Blast-Wave

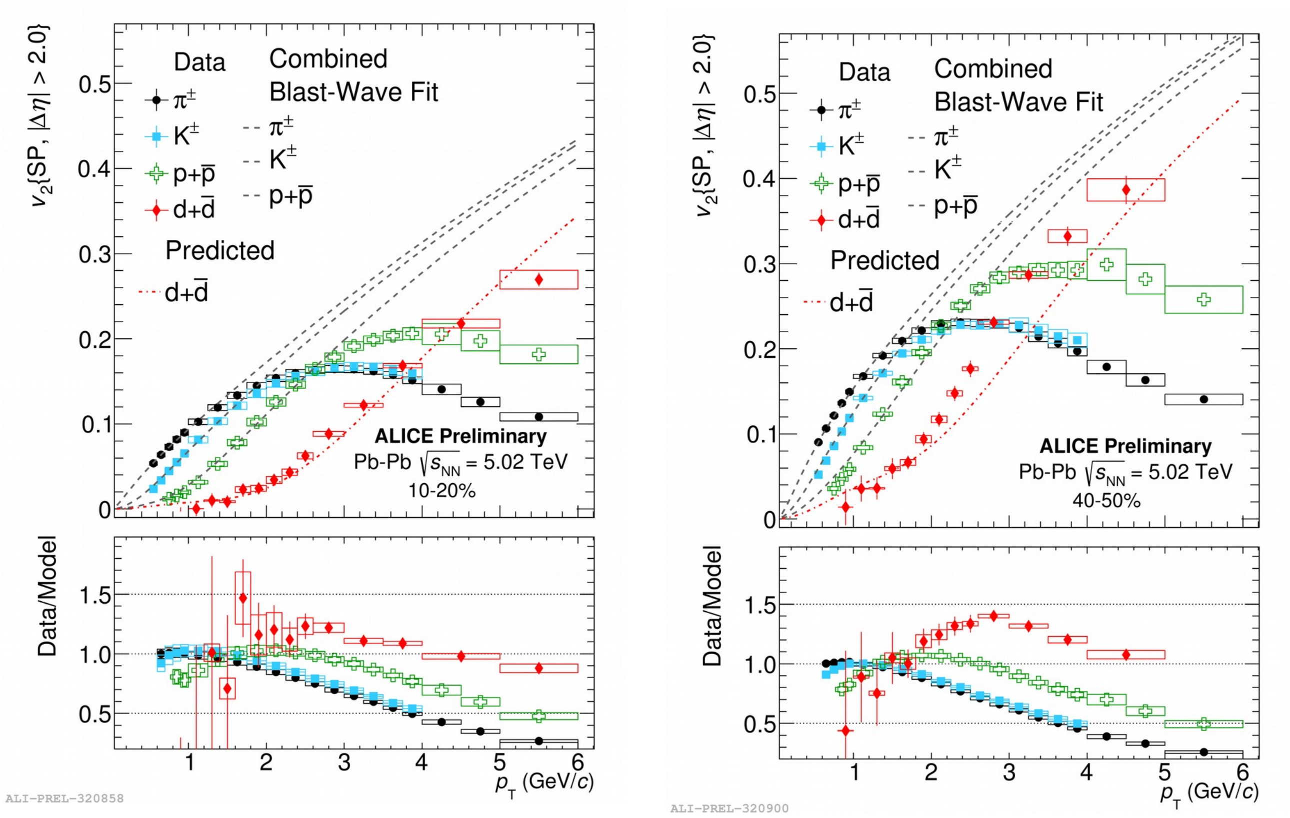

- Blast-Wave (BW) predictions for the (anti-)deuteron v_2 fromcombined fits of v_2 and p_T spectra of π,K,p in the p_T ranges:

  - Consistent with the data in more central collisions
  - Deviations in more peripheral collisions

Elliptic flow of ^3He

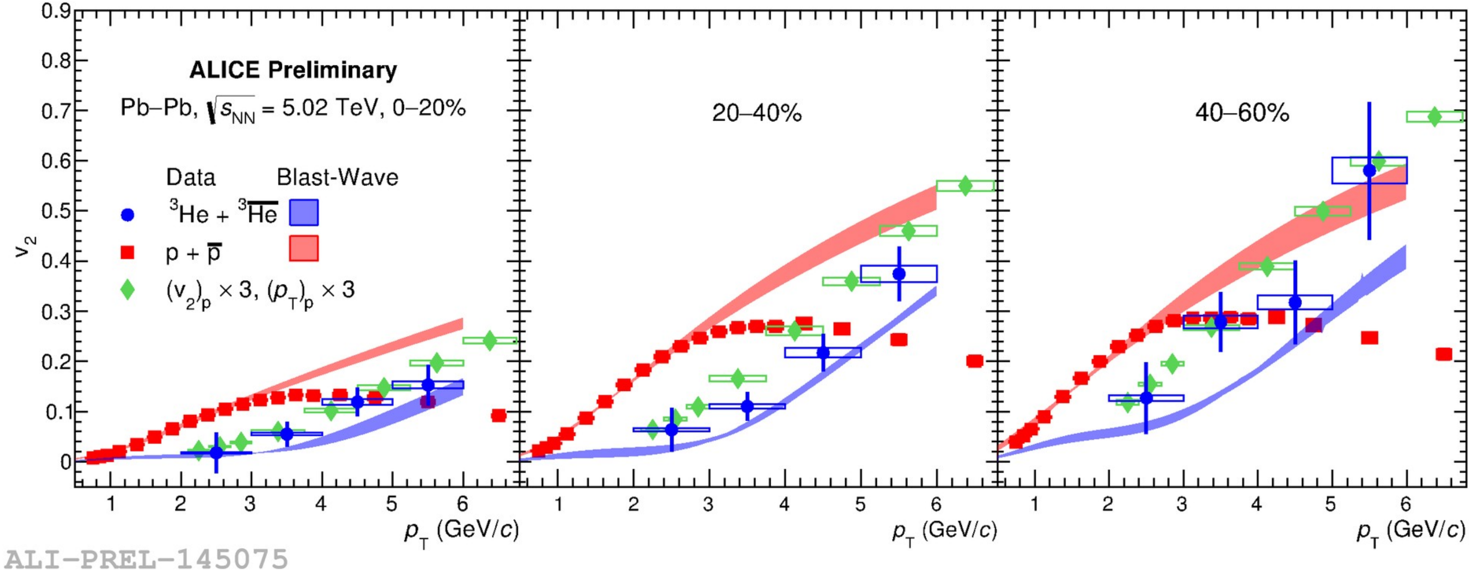

- Blast-Wave prediction with parameters fixed to lighter species is better in the most central collisions
  - Simple coalescence expectation (green points) gets closer to the measured ^3He for 40-60% centrality
- More statistics in the next Pb-Pb run and in the Run3 and Run4 of LHC will help to better undestrand light nuclei production mechanism

v_2 & v_3 : iEBE-VISHNU + Coalescence

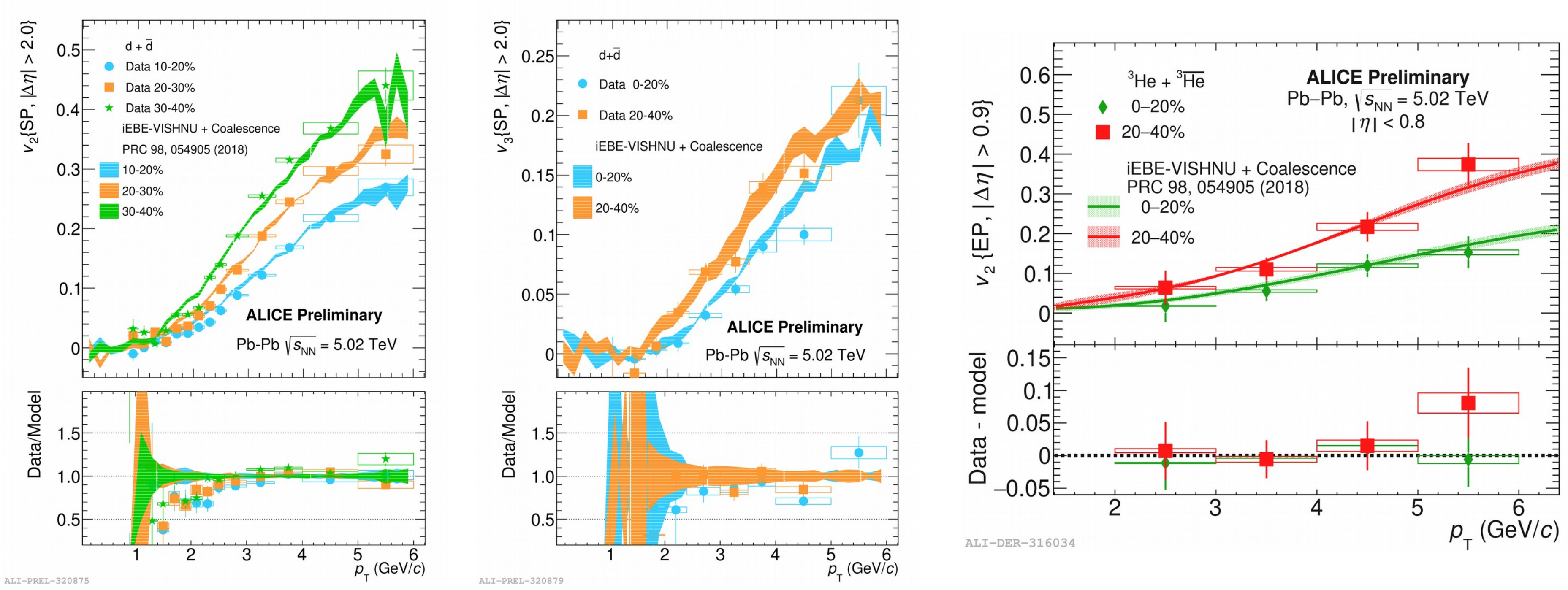

- Coalescence model with phase space distributions of nucleons generated by iEBE-VISHNU (PRC 98, 054905 (2018)):
- AMPT initial conditions ((1+2)d hydro (VISHNU) + UrQMD)
- Good description of the data in 0-40%
  - no predictions for more peripheral collisions

Production of nuclei: thermal model

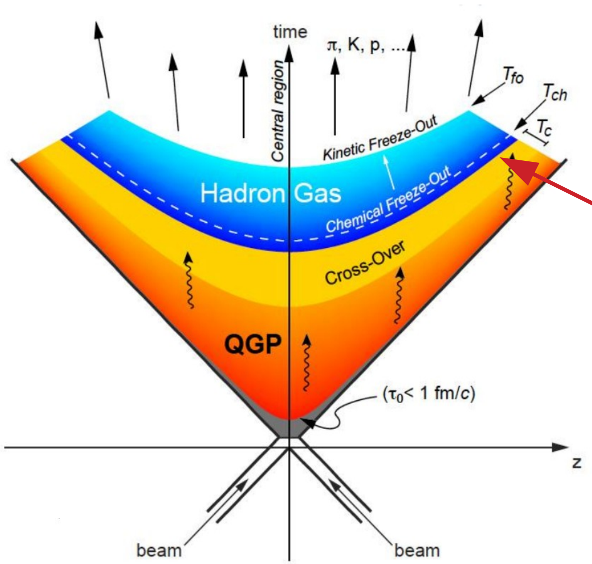

Are nuclei produced with all the other particles at the chemical freeze-out?

Thermal model

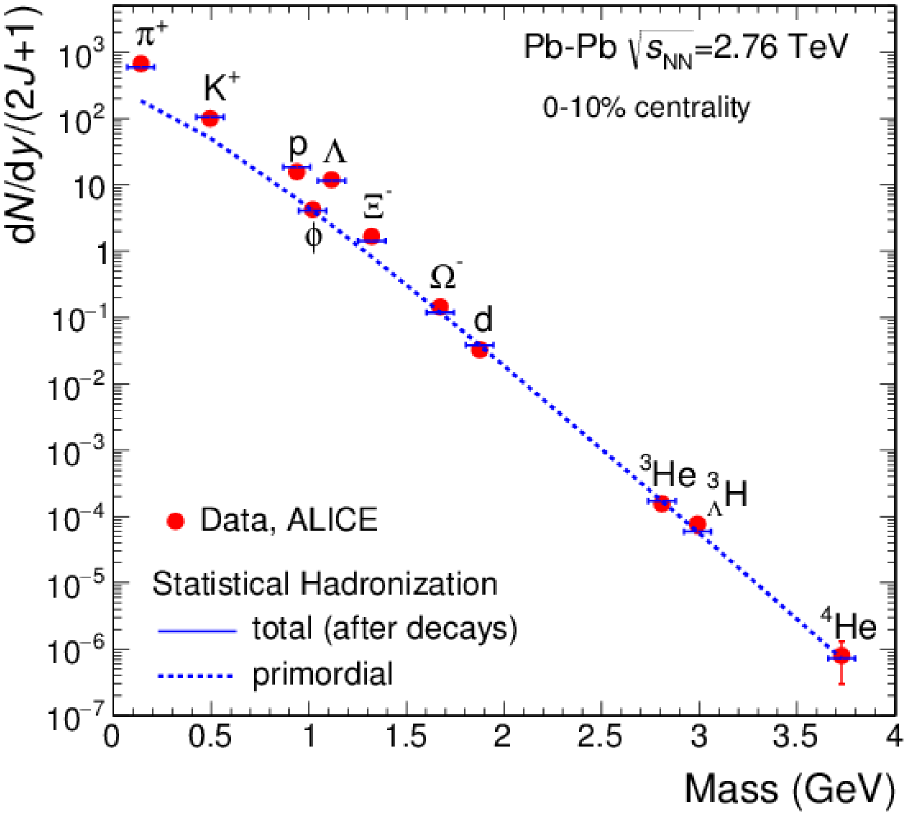

Nature 561 (2018) no.7723, 321-330 arXiv:1710.09425 [nucl-th]

Statistical hadronization model: thermal emission from equilibrated source

Particle abundances fixed at chemical freeze-out

$$N_i = \frac{g_i V}{2\pi^2} \int_0^{+\infty} \frac{p^2 dp}{\exp\left[-\left(\frac{E-\mu_B}{T_{\rm chem}}\right)\right] \pm 1}$$

- Primordial yields modified by hadron decays:
  - Contribution obtained from calculations based on known hadron spectrum
  - Excellent agreement with data with only 2 free parameters: T_{chem} , V

Nuclei production in Pb – Pb collisions

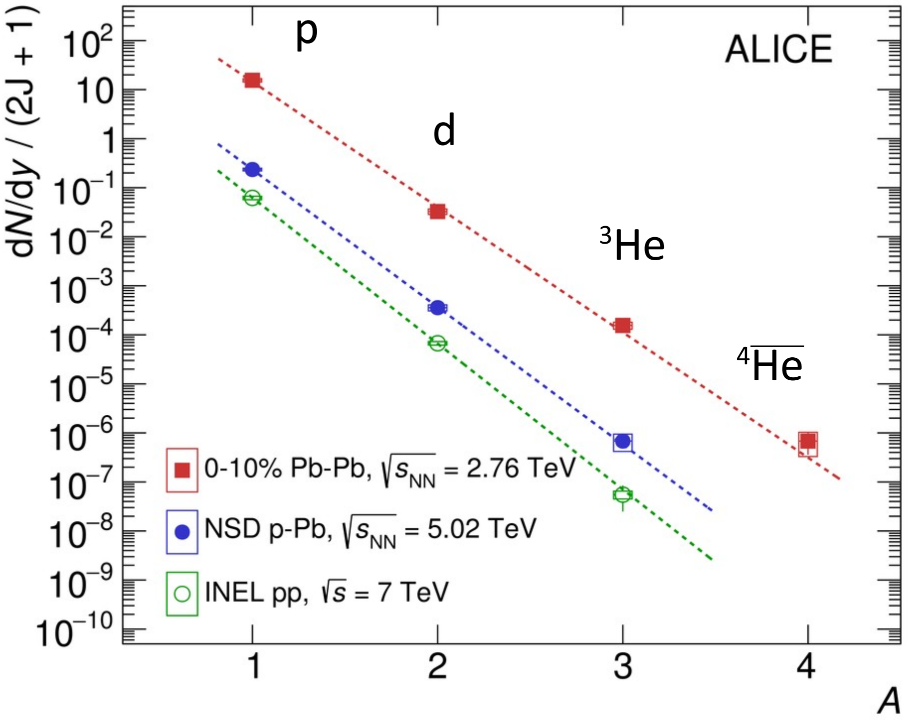

Thermal model prediction:

$$\frac{dN}{dy} \propto \exp\left(-\frac{m}{T_{chem}}\right)$$

- Nuclei follow nicely the exponential fall predicted by the thermal model
- Each added baryon gives a factor of ~350 less production yield in Pb-Pb collisions, ~600 in p-Pb collisions, and ~1000 in pp collisions

Thermal model fit to ALICE data

THERMUS: S. Wheaton, et al., CPC 180, 84 (2009)
GSI-Heidelberg: A. Andronic, et al., PLB 697, 203 (2011); PLB 673, 142 (2009) 142
SHARE3: G. Torrieri, et al., CPC 167, 229 (2005); CPC 175, 635 (2006); CPC 185, 2056 (2014)

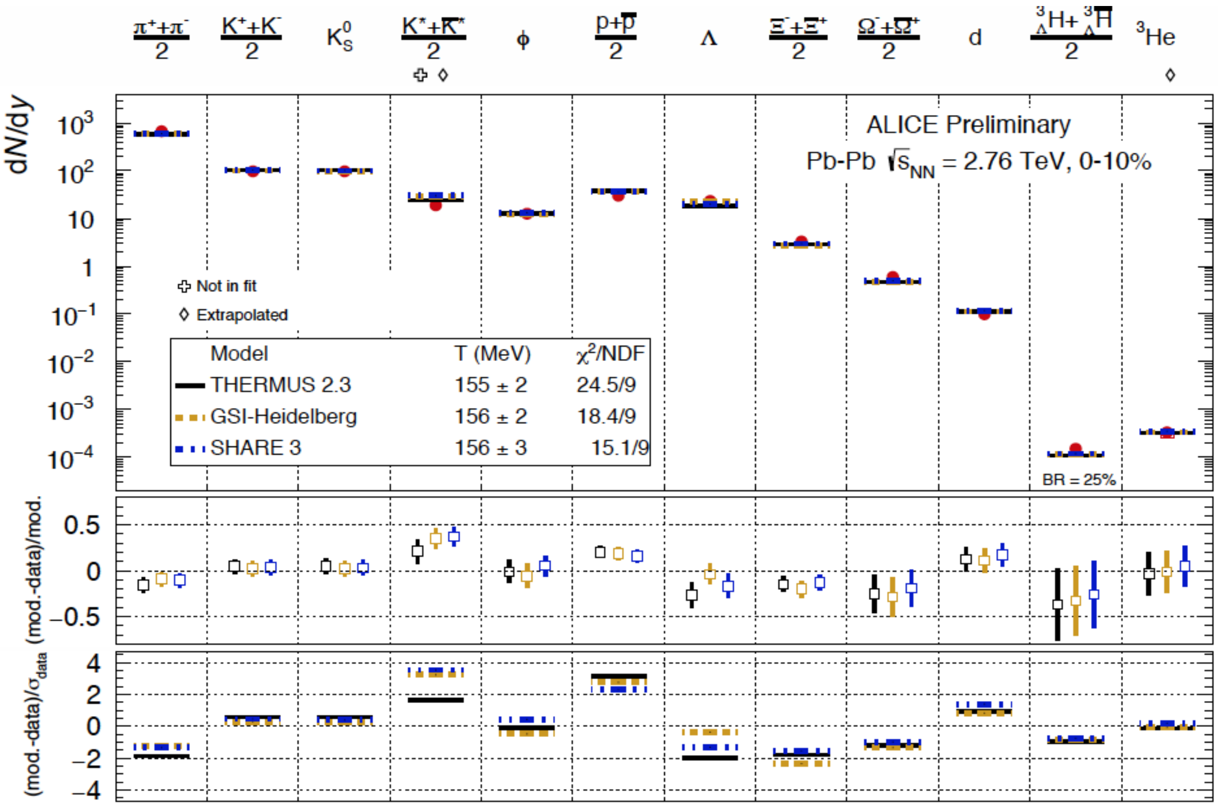

K* not included in the fit

- The p_T-integrated yields and ratios can be interpreted in terms of statistical (thermal) models
- Particle yields of light flavor hadrons (including nuclei) are described with a common chemical freeze-out temperature (T_{chem} = 156 ± 2 MeV)

Light nuclei production: Nucleon to proton ratio

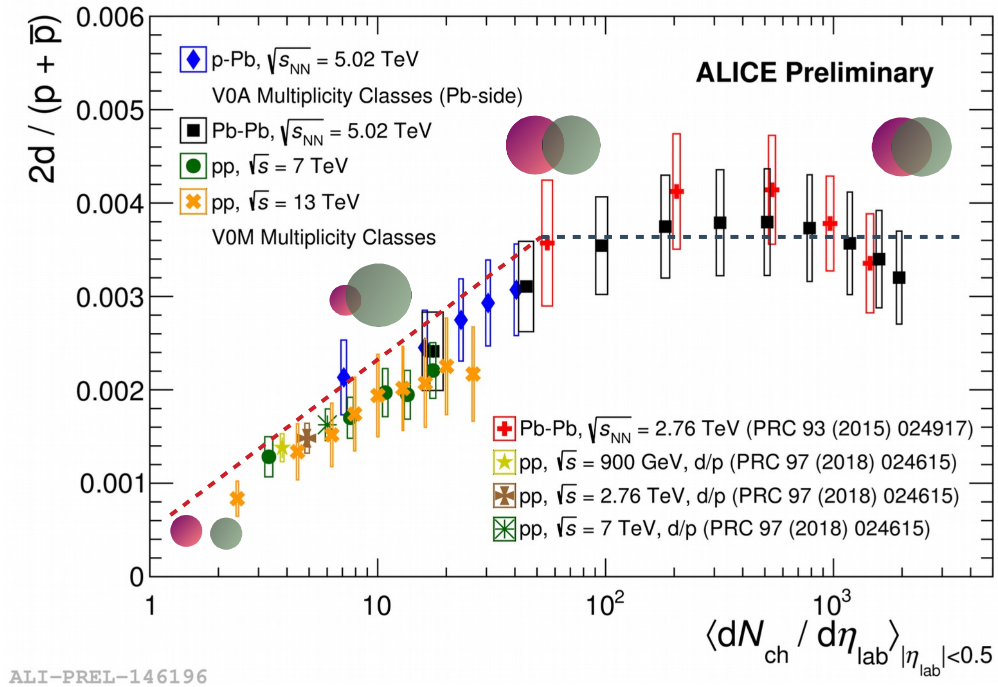

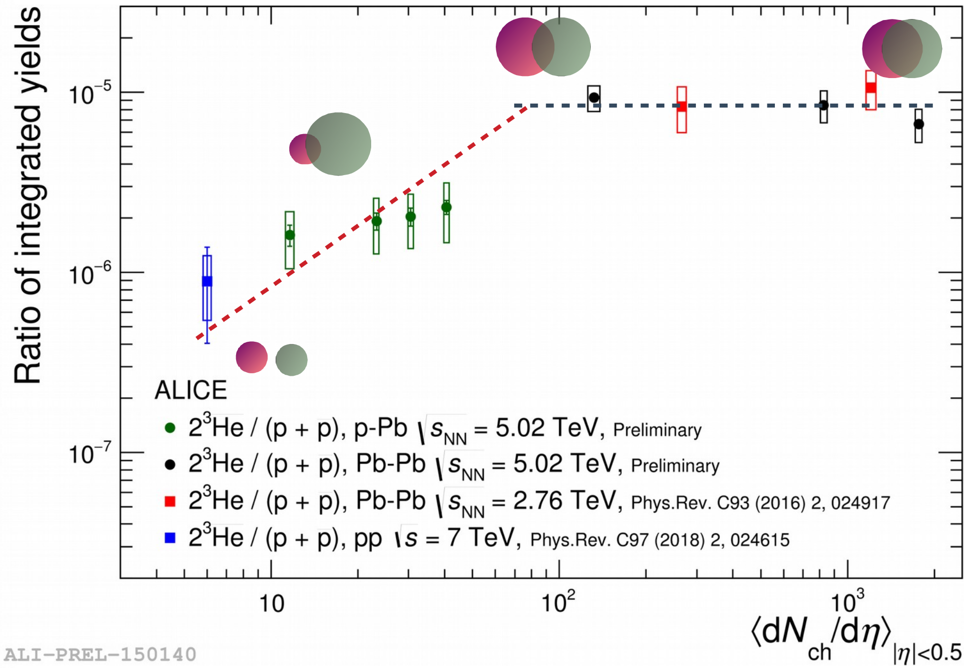

- Ratio increases with multiplicity going from pp to peripheral Pb-Pb : consistent with simple coalescence (d ∝ p^2, ^{3}He ∝ p^3)
- No significant centrality dependence in Pb-Pb : consistent with thermal model (yield fixed by T_{chem})
  - Smooth transition: is there a single particle production mechanism?

Light nuclei production: Nucleon to proton ratio

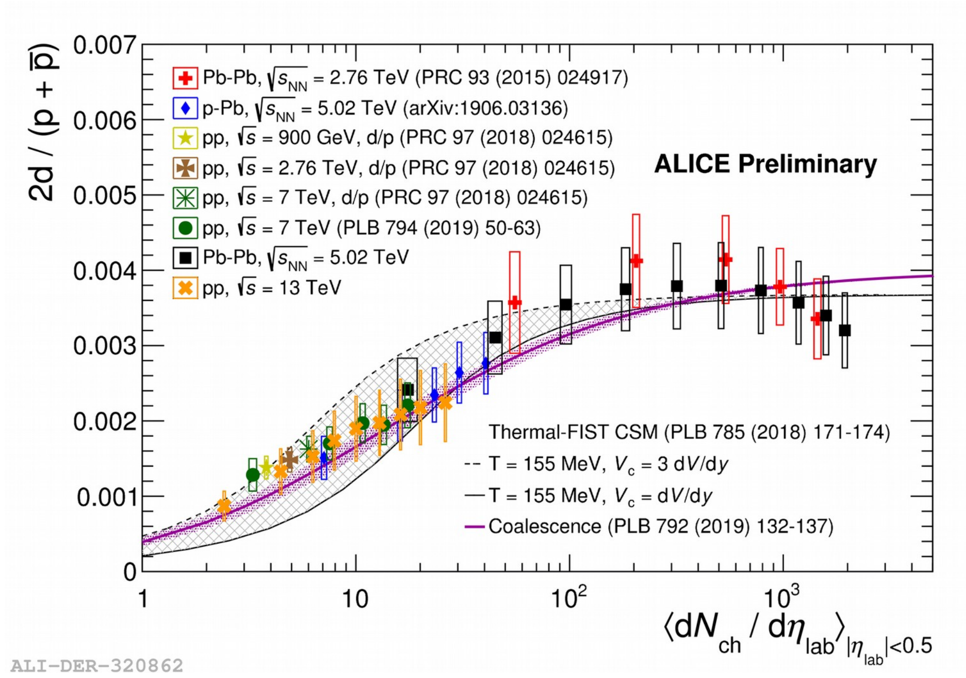

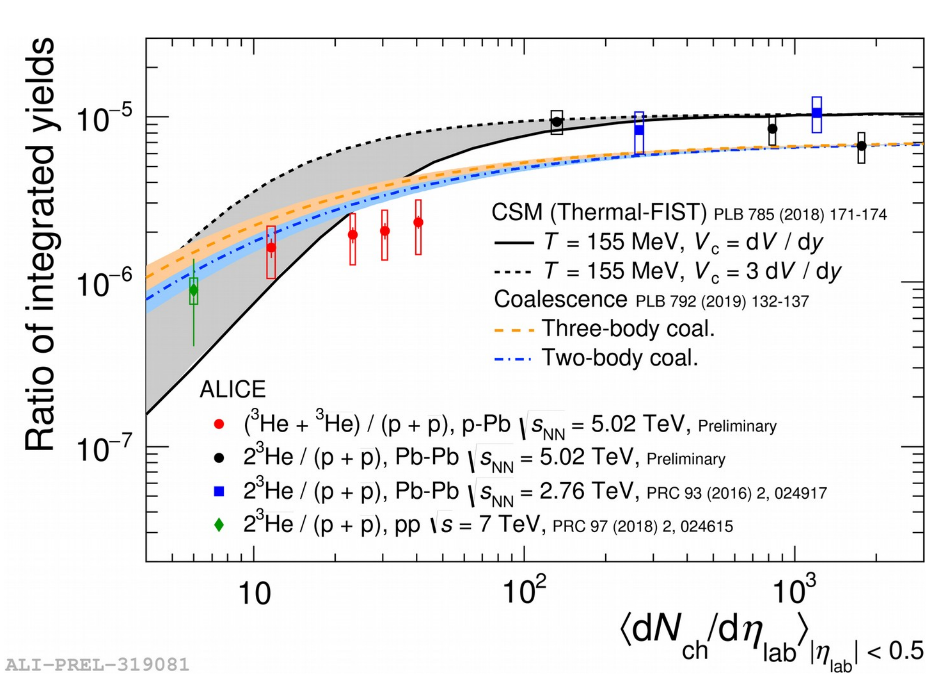

- Increasing trend at low and intermediate multiplicities
  - SHM: Canonical suppression, but tension for ALICE p/π
  - Coalescence: increasing phase space
- No dependence of the ratio on multiplicity for high multiplicities
  - In agreement with both SHM and coalescence
- Coalescence prediction below data for ^{3}He

Outlook – ALICE upgrade

After the LS2 ALICE will be able to collect data with better performance at higher luminosity

- Expected integrated luminosity: ~10 nb^{-1} (~ $8x10^9$ collisions in the 0-10% centrality class)
- New ITS: less material budget and more precise tracking for the identification of hyper-nuclei
- All the physics which is now done for A = 2 and A = 3 (hyper-)nuclei will be done for A = 4

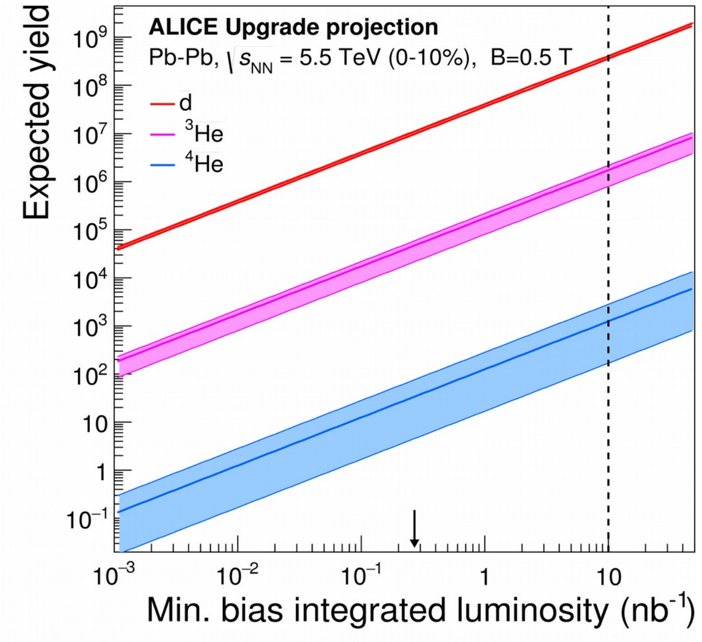

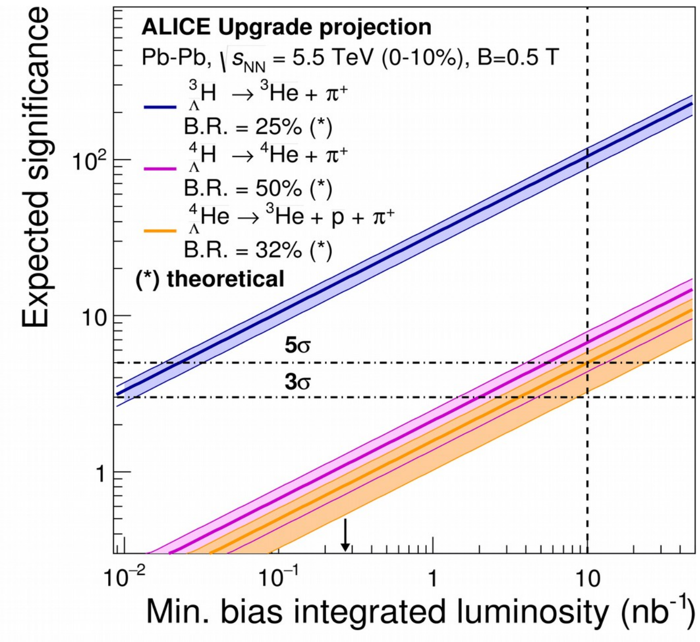

Conclusions

- Excellent ALICE performance allows for the detection of light (anti-)nuclei and (anti-)hypernuclei

Conclusions

ALICE

- Excellent ALICE performance allows for the detection of light (anti-)nuclei and (anti-)hypernuclei

	Spectra and B_2		d/p vs. multiplicity		Yield		$v_2(p_T)$
	pp, p-Pb	Pb-Pb	pp, p-Pb	Pb-Pb	pp, p-Pb	Pb-Pb	Pb-Pb
Simple Coalescence							
Thermal model							
Blast-Wave model							

Conclusions

ALICE

- Excellent ALICE performance allows for the detection of light (anti-)nuclei and (anti-)hypernuclei

	Spectra and B_2		d/p vs. multiplicity		Yield		$v_2(p_T)$
	pp, p-Pb	Pb-Pb	pp, p-Pb	Pb-Pb	pp, p-Pb	Pb-Pb	Pb-Pb
Simple Coalescence	🙂	☹️ ✶	🙂	☹️ ✶			☹️ ✶
Thermal model			☹️ ✶	🙂 ✶	☹️	🙂	
Blast-Wave model	☹️	🙂					😐

✶ Coalescence models which take into account the volume of the source can describe data

✶ Coalescence models with rescattering seem to be able to describe data

✶ Coalescence model with phase space distributions generated by iEBE-VISHNU and AMPT initial conditions is able to describe data

✶ Canonical Standard Models are able to reproduce the increasing trend observed in data

Conclusions

- Excellent ALICE performance allows for the detection of light (anti-)nuclei and (anti-)hypernuclei

	Spectra and B_2		d/p vs. multiplicity		Yield		$v_2(p_T)$
	pp, p-Pb	Pb-Pb	pp, p-Pb	Pb-Pb	pp, p-Pb	Pb-Pb	Pb-Pb
Simple Coalescence	🙂	☹ ✶	🙂	☹ ✶			☹ ✶
Thermal model			☹ ✶	🙂 ✶	☹	🙂	
Blast-Wave model	☹	🙂					😐

✶ Coalescence models which take into account the volume of the source can describe data

✶ Coalescence models with rescattering seem to be able to describe data

✶ Coalescence model with phase space distributions generated by iEBE-VISHNU and AMPT initial conditions is able to describe data

✶ Canonical Standard Models are able to reproduce the increasing trend observed in data

- Light nuclei "puzzle": deuteron yield and $v_2(p_T)$ in Pb-Pb collisions suggest an early "freeze out", while large effects of re-interactions (favoring late stage coalescence) should be expected

Conclusions

- Excellent ALICE performance allows for the detection of light (anti-)nuclei and (anti-)hypernuclei

	Spectra and B_2		d/p vs. multiplicity		Yield		$v_2(p_T)$
	pp, p-Pb	Pb-Pb	pp, p-Pb	Pb-Pb	pp, p-Pb	Pb-Pb	Pb-Pb
Simple Coalescence	🙂	🙁 ✶	🙂	🙁 ✶			🙁 ✶
Thermal model			🙁 ✶	🙂 ✶	🙁	🙂	
Blast-Wave model	🙁	🙂					😐

✶ Coalescence models which take into account the volume of the source can describe data

✶ Coalescence models with rescattering seem to be able to describe data

✶ Coalescence model with phase space distributions generated by iEBE-VISHNU and AMPT initial conditions is able to describe data

✶ Canonical Standard Models are able to reproduce the increasing trend observed in data

- Light nuclei "puzzle": deuteron yield and $v_2(p_T)$ in Pb-Pb collisions suggest an early "freeze out", while large effects of re-interactions (favoring late stage coalescence) should be expected
- New and more precise data are expected from the LHC on the presented topics in the next years. These will provide stricter constraints to the theoretical models

Backup

Searches for weakly decaying exotic bound states

H-Dibaryon (ΛΛ) and ΛN bound state

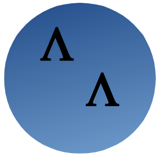

H-Dibaryon : Hypothetical bound state of *uuddss* (ΛΛ) first predicted by Jaffe in a bag model calculation. Recent lattice calculations suggest a bound state (20-50 MeV/c^2 or 13 MeV/c^2)

If : $m_H <$ ΛΛ threshold

- weakly bound: measurable channel

  $H \rightarrow \Lambda p \pi$

R.L. Jaffe, Phys. Rev. Lett. 38, 195 (1977), erratum ibid 38, 617 (1977)
Inoue et al., PRL 106, 162001 (2011)
Beane et al., PRL 106, 162002 (2011)

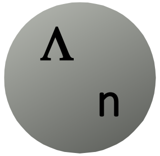

Bound state of Λn? HypHI experiment at GSI sees evidence of a new state: $\Lambda n \rightarrow d + \pi^-$

C. Rappold et al. (HypHI collaboration), Phys. Rev. C88, 041001(R) (2013)

H-Dibaryon (ΛΛ) and ΛN bound state

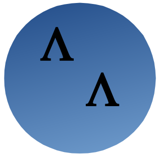

H-Dibaryon : Hypothetical bound state of *uuddss* (ΛΛ) first predicted by Jaffe in a bag model calculation. Recent lattice calculations suggest a bound state (20-50 MeV/c^2 or 13 MeV/c^2)

If : m_H < ΛΛ threshold

- weakly bound: measurable channel

  H → Λpπ

R.L. Jaffe, Phys. Rev. Lett. 38, 195 (1977), erratum ibid 38, 617 (1977)
Inoue et al., PRL 106, 162001 (2011)
Beane et al., PRL 106, 162002 (2011)

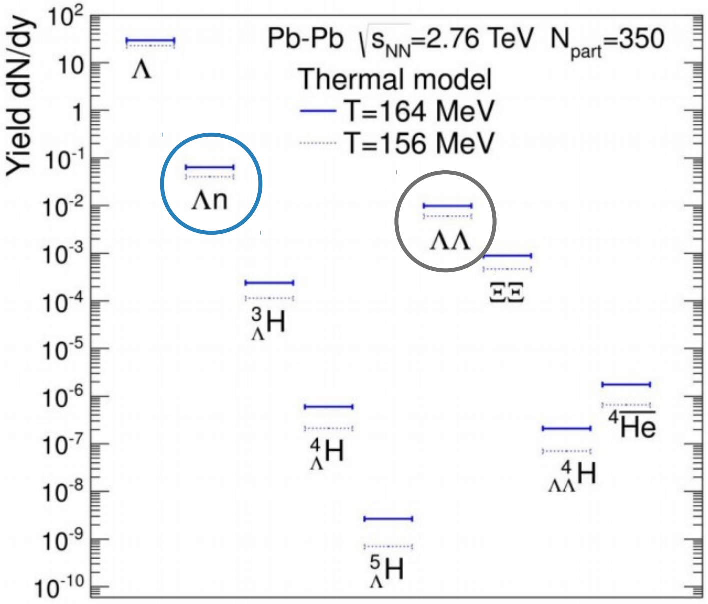

A. Andronic et al., Phys. Lett. B 697, 203 (2011)

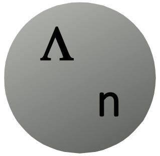

Bound state of Λn? HypHI experiment at GSI sees evidence of a new state: Λn → d+ π^-

C. Rappold et al. (HypHI collaboration), Phys. Rev. C88, 041001(R) (2013)

H-Dibaryon (ΛΛ) and ΛN bound state

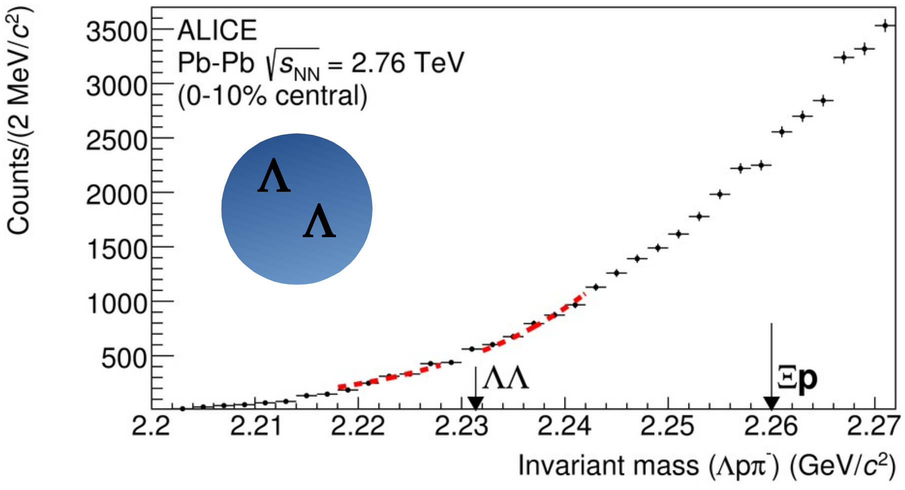

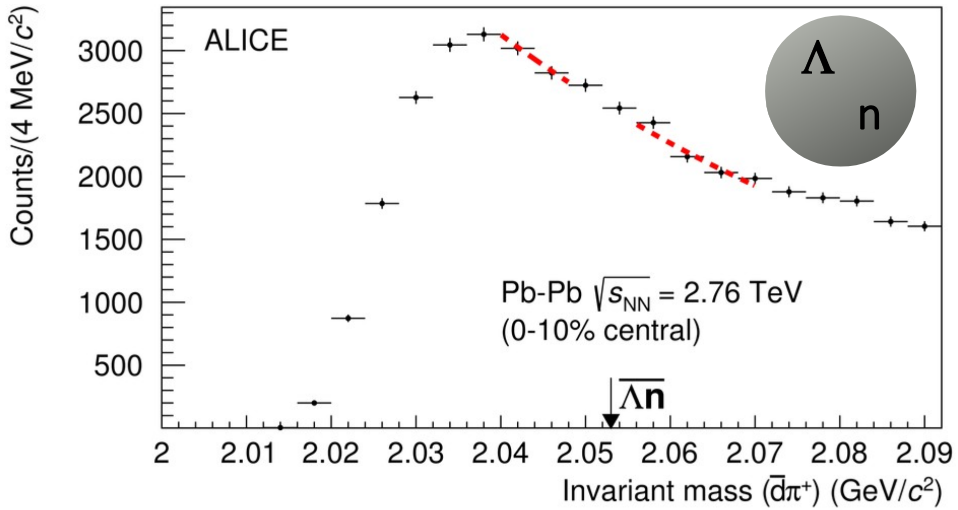

ALICE Collaboration: PLB 752, 267 (2016)

Invariant mass analyses of the two hypothetical particles lead to no visible signal
→ Upper limits set

Comparison to different models

ALICE Collaboration,
Phys. Lett. B 752, 267 (2016)

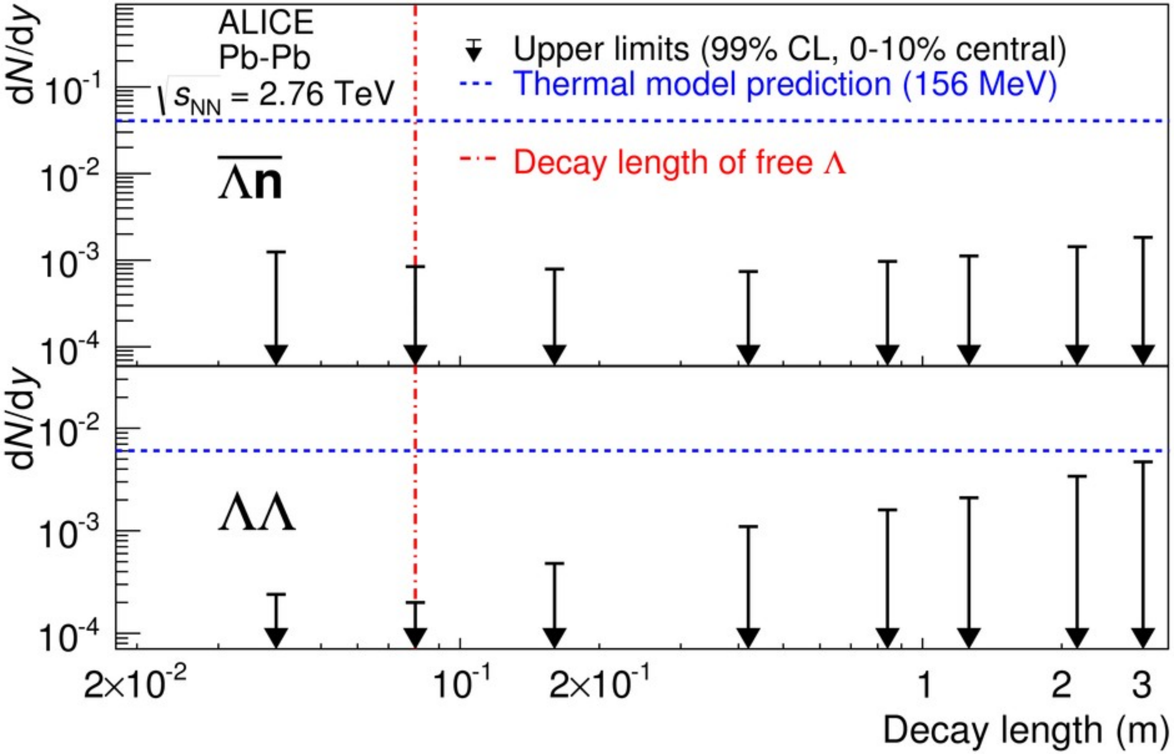

- Search for a bound state of Λn and ΛΛ shows upper limits of signal
  - ➢ set upper of limits for different lifetime assumptions of the hypothetic bound states

Coalescence vs Blast-wave : <p_T>

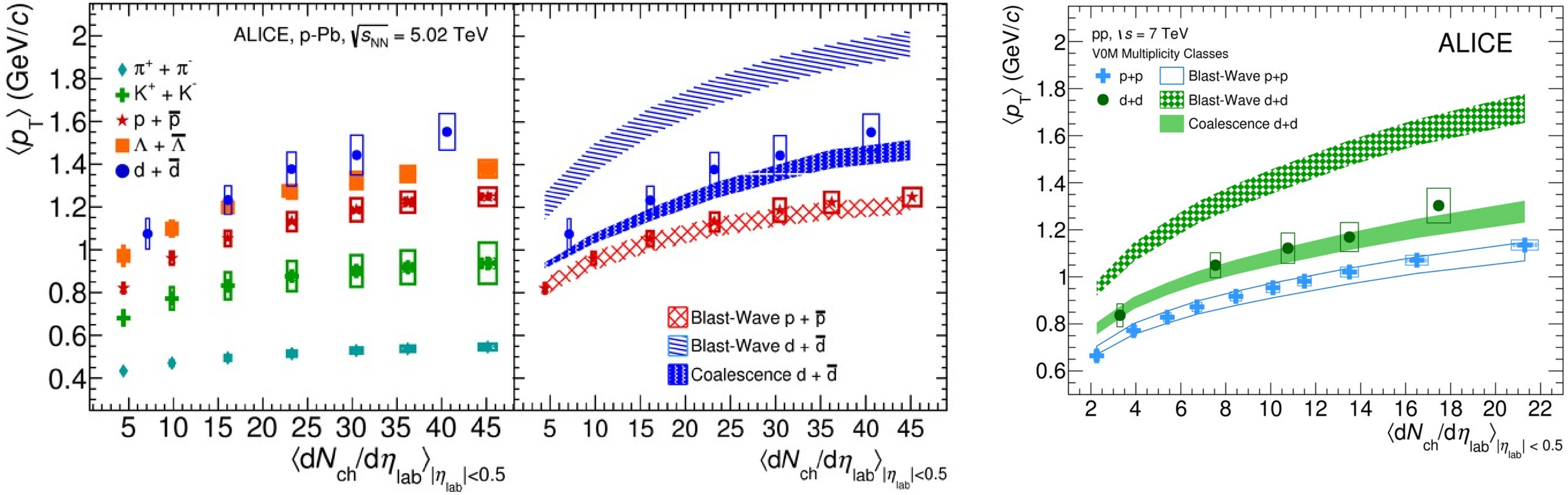

- <p_T> is consistent with the coalescence model expectations in both p-Pb and pp collisions for all multiplicity classes.
- Blast-wave model fails to describe <p_T> for deuterons using common kinetic freeze-out parameters used for pi, K, and p in both pp and p-Pb collisions
- In contrast with the observation in Pb-Pb collisions.

v2 of light (anti-)nuclei vs. v2 of π, K and p

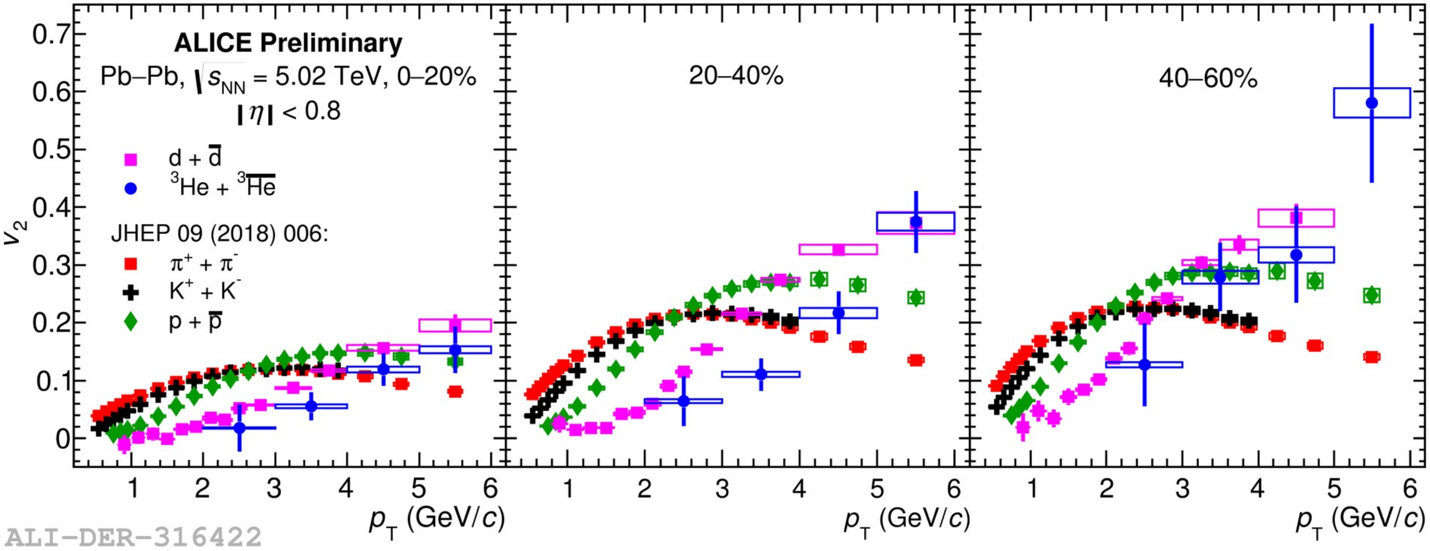

Mass ordering at low p_T & slower rise for heavier particles as expected from relativistic hydrodynamics

Coalescence + AMPT

- Phase-space distributions of p and n at kinetic freeze-out generated from iEBE-VISHNU hybrid model with AMPT initial conditions

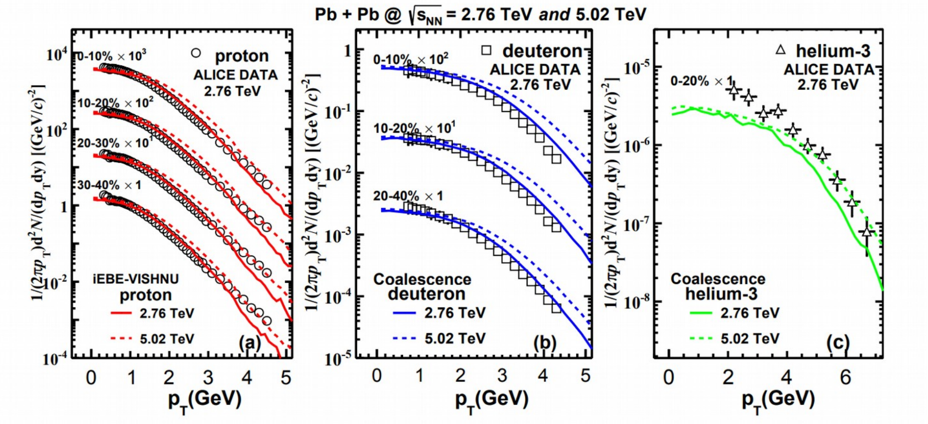

- The coalescence model describes the v_2 of d and ^{3}He at RHIC and the LHC
- There exists a discrepancy between the calculated and measured p_T spectrum of ^{3}He in Pb + Pb collisions at $\sqrt{s_{NN}}$ = 2.76 TeV
- The reason for this discrepancy may be due ^{3}He earlier formation than the deuteron in collisions at higher energies

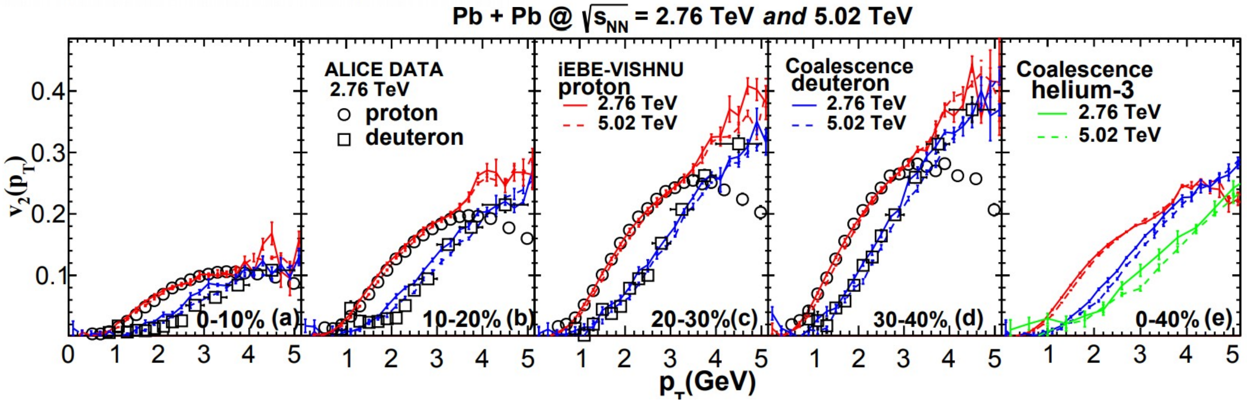

arXiv:1807.02813 [nucl-th]

Identification of nuclei: secondaries

The measurement of nuclei is strongly affected by background from knock-out from material

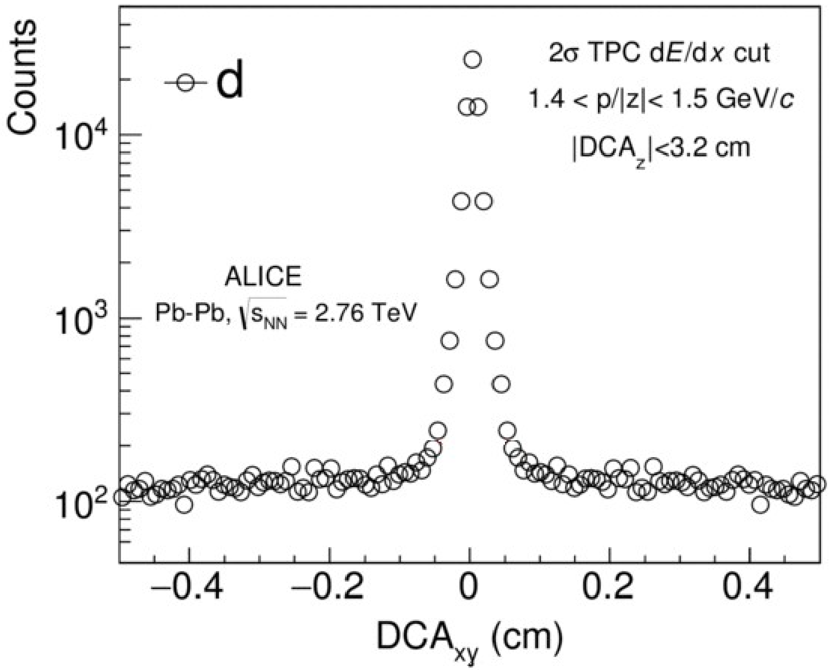

Identification of nuclei: secondaries

The measurement of nuclei is strongly affected by background from knock-out from material

➔ Rejection is possible via fitting the DCA_{XY} distributions with templates

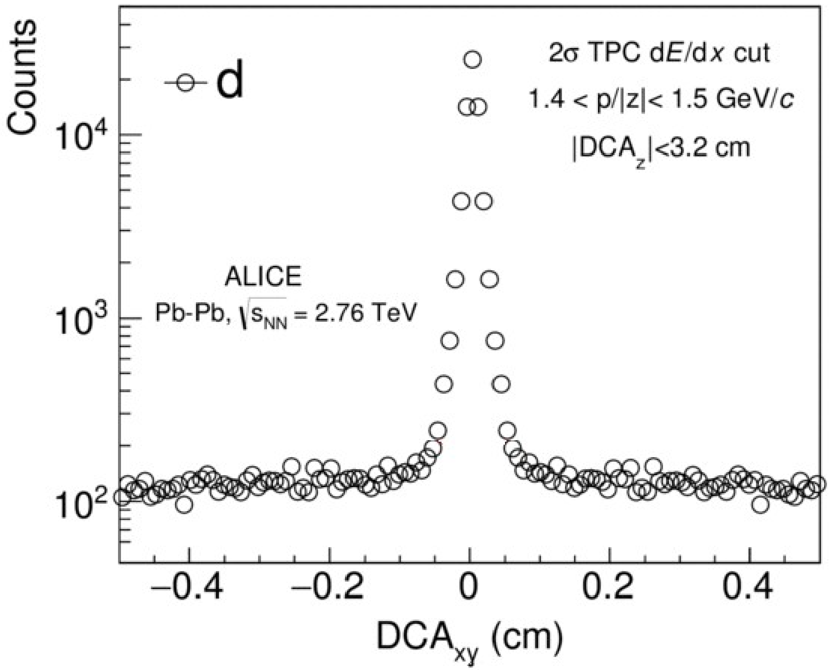

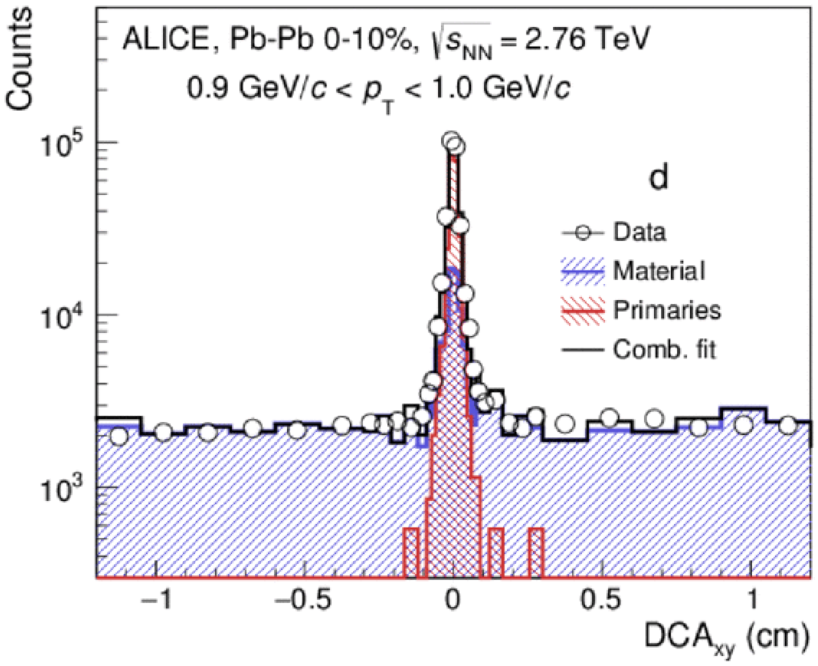

Identification of nuclei: secondaries

The measurement of nuclei is strongly affected by background from knock-out from material

➔ Rejection is possible via fitting the DCA_{XY} distributions with templates

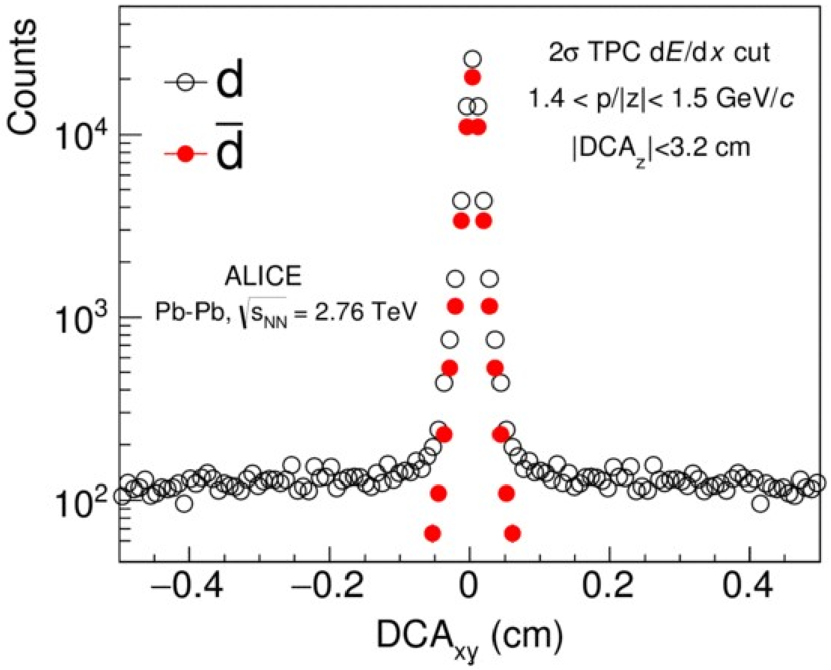

Not relevant for anti-nuclei.
However, larger systematic uncertainty from hadronic interaction cross section

Precise mass measurement

- The precise measurement of the mass difference between nuclei and their anti-counterparts allows to probe any difference in the interaction between nucleons and anti-nucleons.
- Looking at the mass difference between nuclei and their anti-nuclei it is possible to test the **CPT invariance** of the residual **QCD "nuclear force"**

ALICE Collaboration: Nature Phys. 11, 811 (2015)

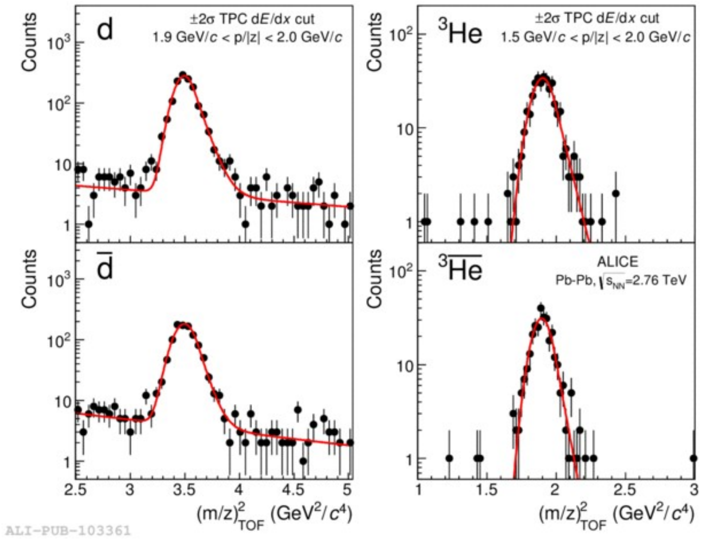

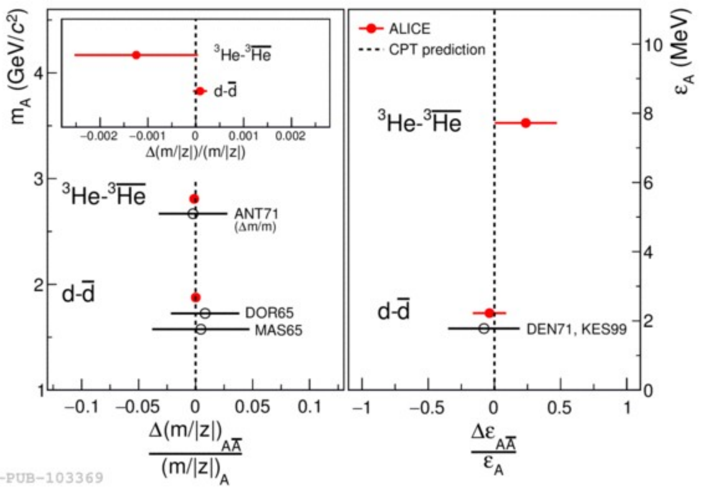

- Masses and binding energies of nuclei and anti-nuclei are compatible within uncertainties
- **Measurement confirms the CPT invariance for light nuclei**

Precise mass measurement

- The precise measurement of the mass difference between nuclei and their anti-counterparts allows to probe any difference in the interaction between nucleons and anti-nucleons.
- Looking at the mass difference between nuclei and their anti-nuclei it is possible to test the **CPT invariance** of the residual **QCD "nuclear force"**

ALICE Collaboration: Nature Phys. 11, 811 (2015)

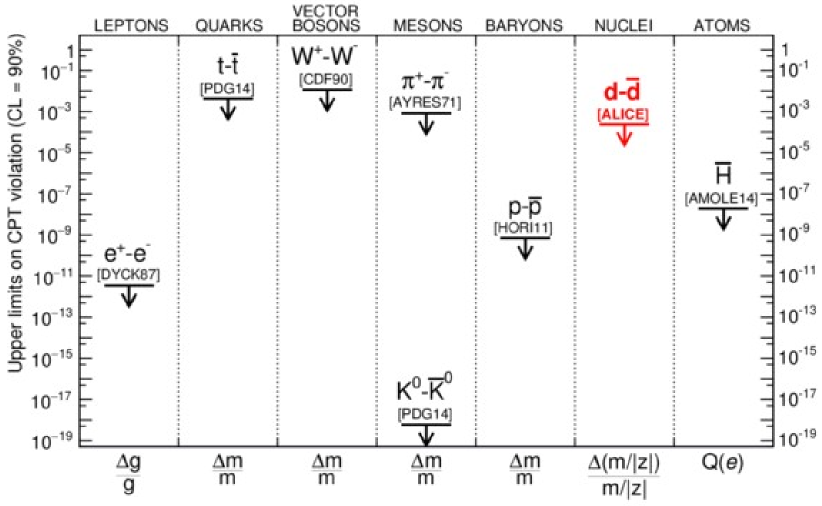

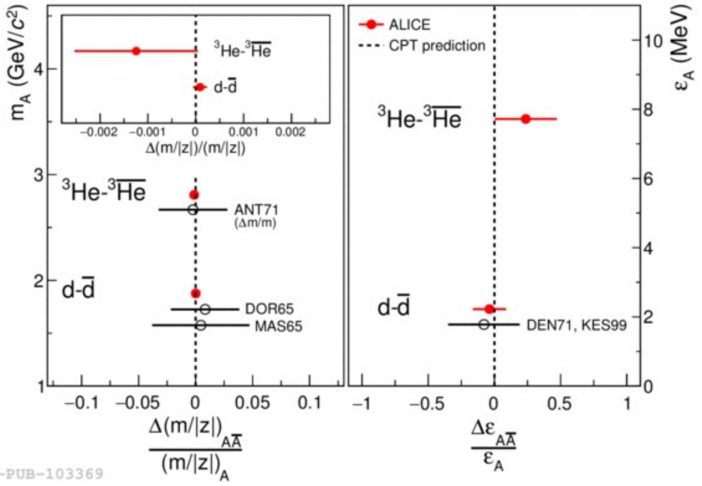

- Masses and binding energies of nuclei and anti-nuclei are compatible within uncertainties
- **Measurement confirms the CPT invariance for light nuclei**

Flow analysis method

- v_2 is measured using the scalar product method
  - Hits measured by V0A ($2.8 < \eta < 5.1$) and V0C ($-3.7 < \eta < -1.7$) are used as reference particles
  - Deuteron candidates are the particles of interest ($|\eta|<0.8$)

$$v_n\{SP\} = \frac{\left\langle u_{n,i}(p_T,\eta)\cdot \frac{Q_n^*}{M}\right\rangle}{\sqrt{\left\langle \frac{Q_{n,A}^*}{M_A}\cdot\frac{Q_{n,B}^*}{M_B}\right\rangle}}$$

- The contribution to the measured elliptic flow (v_2^{Tot}) due to misidentified deuterons (v_2^{Bkg}) was removed by studying the azimuthal correlations versus ΔM ($\Delta M = m_{TOF} - m_d$)

$$v_2^{Tot}(\Delta M) = v_2^{Sig}(\Delta M)\frac{N^{Sig}}{N^{Tot}}(\Delta M) + v_2^{Bkg}(\Delta M)\frac{N^{Bkg}}{N^{Tot}}(\Delta M),$$

- The yields N^{Sig} and N^{Bkg} are extracted from fits of the invariant mass distribution obtained with the TOF detector

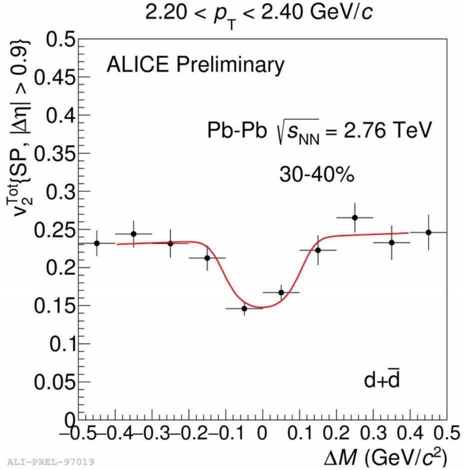

Coalescence Model and HBT

The size of the emitting volume (V_{eff}) has to be taken into account: the larger the distance between the protons and neutrons which are created in the collision, the less likely is that they coalesce

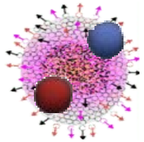
(small fireball)

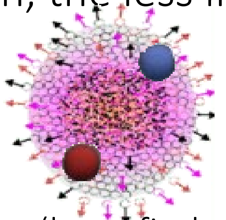
(large fireball)

In detail, it turns out [1] that the coalescence process is governed by the same "length of homogeneity in the source" which can be extracted from two particle Bose-Einstein correlation (HanburyBrown – Twiss (HBT) interferometry [2]): → $B_2 \sim 1/V_{eff}$

$$B_2 = \frac{3\pi^{3/2}\langle C_d \rangle}{2 m_t \Re_T^2(m_t) \Re_p^2(m_t)} e^{2(m_t - m)\left(\frac{1}{T^* p} - \frac{1}{T^* d}\right)}$$

The strong decrease of B_2 with centrality in Pb-Pb collisions can be naturally explained as an increase in the emitting volume: particle densities are relevant and not absolute multiplicities

[1]R. Scheibl and U. Heinz, Phys.Rev. C59, 1585 (1999)
[2]A review can be found in : U. Heinz, Nucl. Phys. A 610 , 264c (1996)

Coalescence parameter B_3

pp

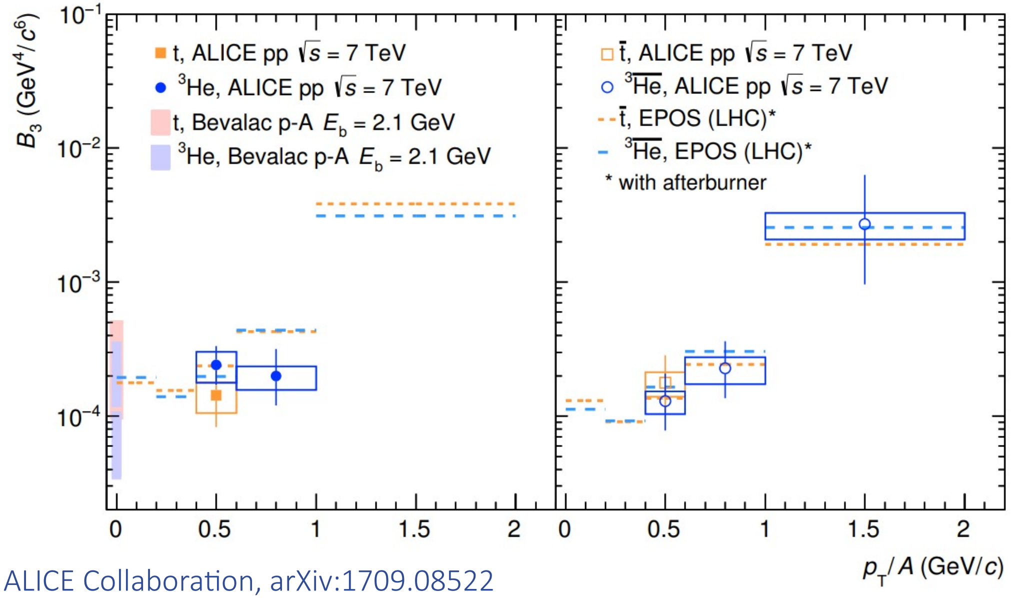

ALICE Collaboration, arXiv:1709.08522

Pb-Pb

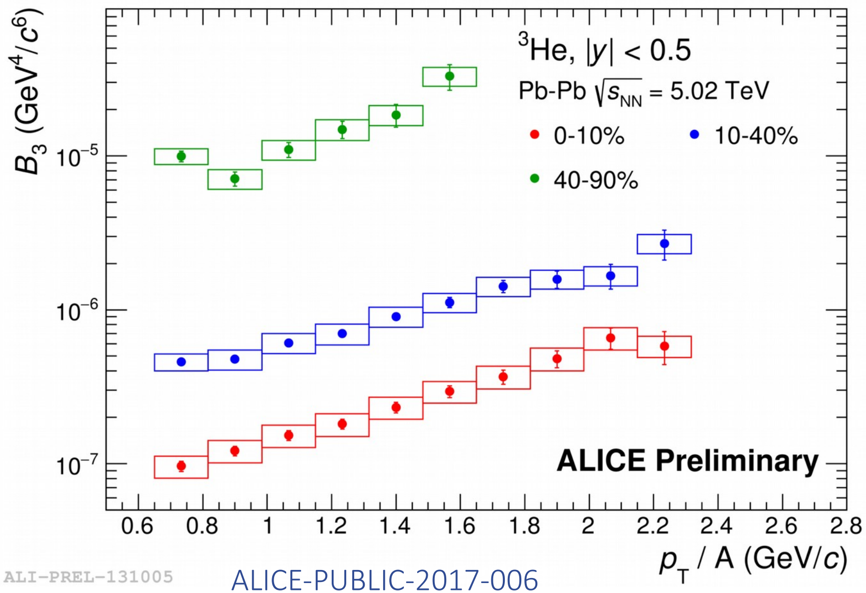

ALICE-PUBLIC-2017-006

B_3 of ($\bar{t}$)t and ($^3\overline{He}$)^{3}He measured in pp and Pb-Pb collisions

First ever measurements of the B_3 of $\bar{t}$ and $^3\overline{He}$ in pp collisions

Increasing trend with p_T and centrality observed in Pb-Pb collision

Anti-nuclei production

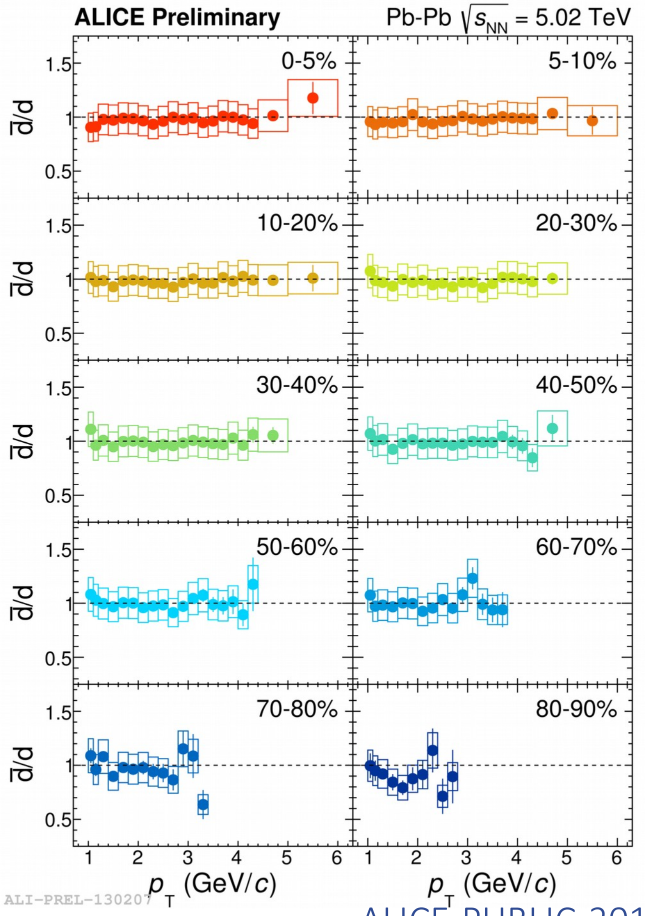

ALICE-PUBLIC-2017-006

- Anti-nuclei/nuclei ratios are consistent with unity (similar to other light particle species) in the measured p_T-interval
- Ratios are constant as a function of p_T and centrality

Anti-nuclei production

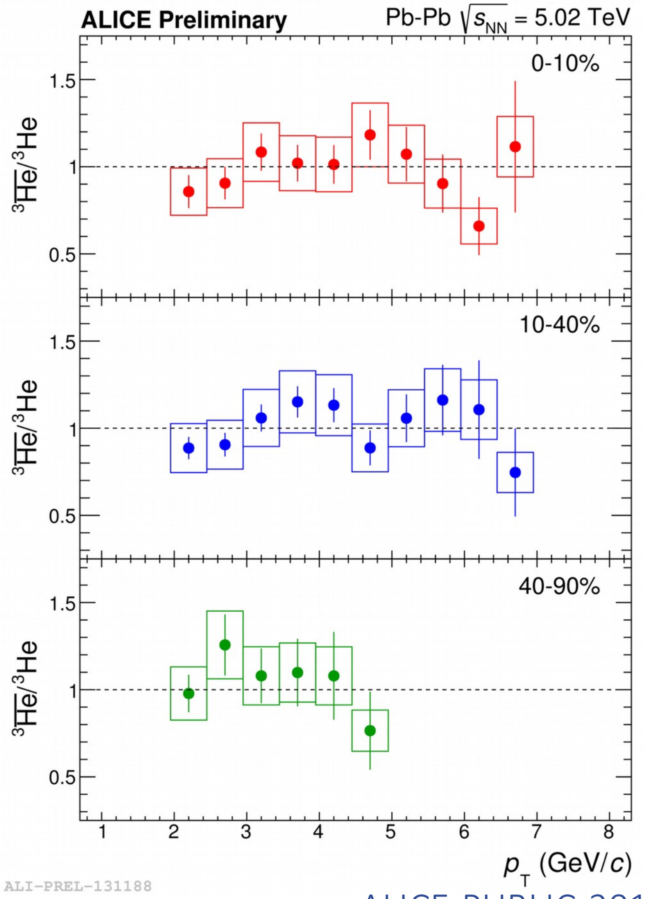

ALICE-PUBLIC-2017-006

- Anti-nuclei/nuclei ratios are consistent with unity (similar to other light particle species) in the measured p_T-interval
- Ratios are constant as a function of p_T and centrality

Centrality of the collisions: p-Pb and pp

Multiplicity estimator: slices in VZERO-A (V0A) amplitude

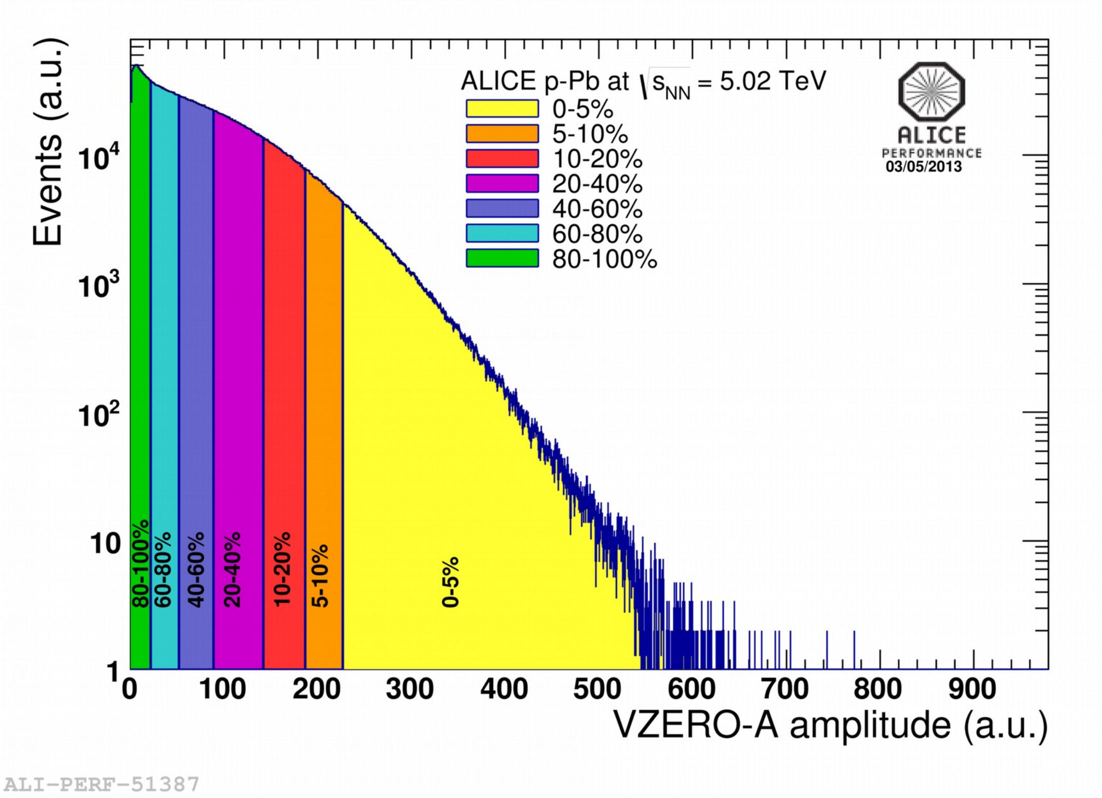

Central collision

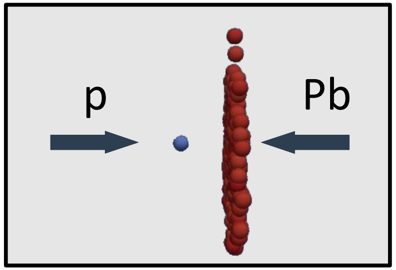

Peripheral collision

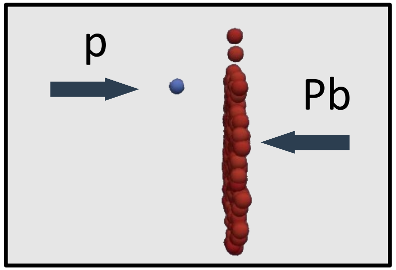

Correlation between impact parameter and multiplicity is not as straight-forward as in Pb-Pb

Outlook – Run 2 data

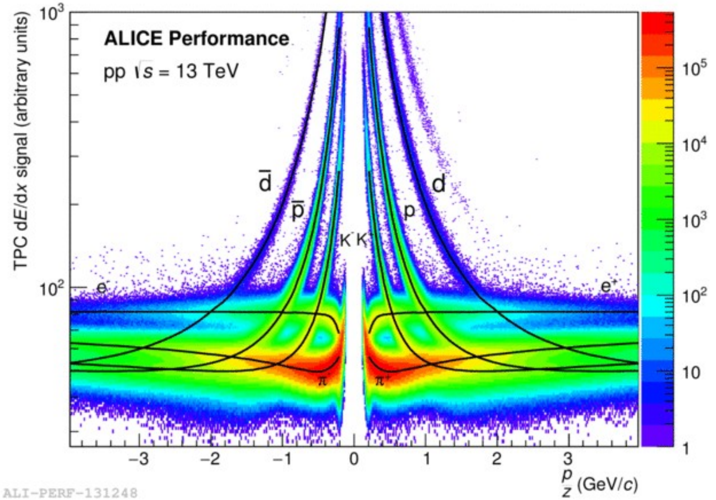

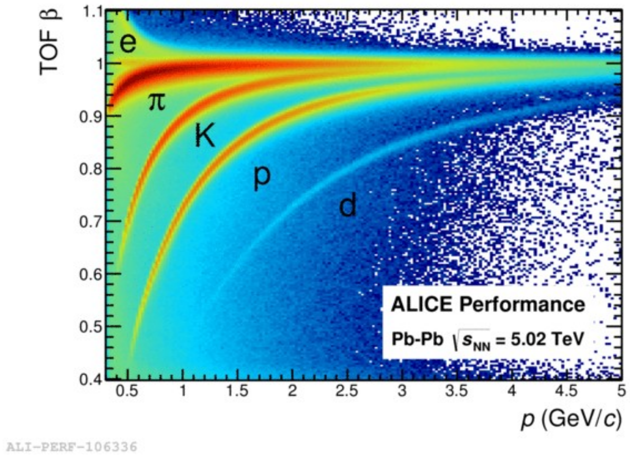

- pp collisions at $\sqrt{s}$ = 13 TeV: new results are expected soon for light (anti-)nuclei production
- p-Pb collisions at $\sqrt{s_{NN}}$ = 5.02 TeV and $\sqrt{s_{NN}}$ = 8 TeV collected at the end of 2016 → will provide new and more precise measurements
- Pb-Pb run at the end of 2018: expected a significant increase of statistics → more precise measurements